Synthetic Rainfall Generation Using Stochastic Downscaling and Atmospheric Circulation Patterns

A Thesis Submitted In Partial Fulfillment of the Requirements

for the Degree of

MASTER OF TECHNOLOGY

by

Antima Jain

to the

DEPARTMENT OF CIVIL ENGINEERING

INDIAN INSTITUTE OF TECHNOLOGY, KANPUR

JULY, 2004

CERTIFICATE

It is certified that the work contained in the thesis entitled "Synthetic Rainfa Generation Using Stochastic Downscaling and Atmospheric Circulation Patterns" by Antima Jain (Roll No. Y210305) has been carried out under our supervision and that this work has not been submitted elsewhere for any degree.

for

Professor Dr.-Ing. Gerd Schmitz
Professor
Institute of Hydrology and Meteorology,
Technical University of Dresden, Germany

Dr. Ashu Jain
Assistant Professor
Indian Institute of Technology
Kanpur, India

August 11, 2004

Abstract

The point rainfall values at different locations in a large catchment are key inputs to many important water resources management activities. Historically observed rainfalls are normally not available for sufficient lengths or are available at coarse resolutions both in space and time. This has led the scientists and researchers around the world to explore the possibilities of synthetically generating rainfall that are similar to the historical rainfall in statistical character in a catchment using various techniques, such as stochastic or conceptual. In the present study, an attempt has been made to use stochastic approaches for the purpose of synthetically generating rainfall data.

A Stochastic Downscaling Model (SDM), proposed by Stehlik and Bardossy (2002), has been employed in this study to generate synthetic rainfall in the Freiberger Mulde catchment, Germany. The data employed include daily Rainfall data in 1/10(in mm), Pressure data, and Discharge data (m^3/s). An important input to the SDM is the classification of the circulation patterns (CPs) in the area. An automated objective classification method based on the concepts of fuzzy sets has been employed in this study to classify the daily CPs. The validation of the classification method has been carried out using the optimization technique of simulated annealing. Once the CPs have been classified, they were used as inputs to generate daily synthetic rainfall values at 32 different stations scattered throughout the (Frieberger Mulde) catchment, Germany. The synthetic rainfalls generated from the SDM model were compared to the historically observed rainfall at these 32 stations using statistical and graphical techniques. The synthetic rainfall series generated at these 32 stations were then interpolated at each node point of a dense grid of the catchment. The size for each grid

was 2.5 x 2.5 km^2 and the total number of nodes in the catchment was 1574. The interpolation of both synthetic and historical rainfall data was carried out using two different Kriging tools, Ordinary Kriging and Kriging with External Drift. A comparison of the interpolated values of the synthetic and historical rainfall was also carried out. The results obtained in this study indicate a very good agreement between the synthetic and historical rainfall values in terms of the various statistical parameters considered in this study for both generated and interpolated rainfalls.

Acknowledgement

I take this opportunity to express my deep sense of gratitude to ***Dr. Ashu Jain*** *for his constant inspiration, incomparable support and encouragement given to me from time to time. His guidance, cooperation, meticulous scientific attitude inspired and immensely benefited me for the completion of this work. I am very much grateful to him to give me the opportunity to do my M. Tech. thesis under IIT-DAAD Masters Sandwich Programme.*

I am thankful to Professor Dr.-Ing. Gerd Schmitz, Institute of Hydrology and Meteorology, Technical University of Dresden, German for guiding me for my work. I would like to express my special gratitude to Professor Andras Bardossy, Institute of Hydrology in Stuttgart, Germany. At this point of time, I can only thank him for all the favours he has done to me. I am finding myself speechless in thanking him for guiding me for my work and providing me a very friendly and cooperative working environment during one week stay in Stuttgart, Germany, which gave me mental strength to complete the work successfully.

I pay my sincere gratitude to Dr. Gangadharaiyah, Dr. Rajesh Srivastava, Professor Bithin Datta and Dr. Pranab Mahapatra for their encouragement and affection throughout my stay in IIT Kanpur.

I thank gratefully to DAAD (Deutscher Akademischer Austausdienst) for awarding me the IIT-DAAD Masters Sandwich scholarship.

My acknowledgement cannot be completed without my friends, seniors and juniors in Hydraulics and Water Resources Engineering group, IIT Kanpur. I would like to thank all the lab members. I would like to thank for their timely help during my work.

I would like to express my deepest gratitude to my parents for their love, care, blessings, throughout and unconditional support in my whole academic career and above all believe in me, which helped me always, especially to adjust in an entirely new environment in Germany, without deviating from the true path showed by them. I can hardly pay off their sacrifice. I would also thank to all my relatives for their love and care.

I cannot forget to express my thankfulness to my friends in IIT Kanpur for their throughout support and encouragement in my work. Special thanks to my friends in Dresden, Sonia, Brajesh, Ranjana, Aswini and Vinod who made my stay very comfortable and

memorable. Thanks to all people who have helped me directly or indirectly throughout the project work and have helped me in completing the job successfully.

August 11, 2004 **ANTIMA JAIN**

CONTENTS

LIST OF FIGURES

LIST OF TABLES

DEDICATED

TO

MY PARENTS

Chapter-1

Introduction

1.1 General

Weather variations on the daily time scale exert important influences on the courses of many natural processes. Rainfall is the major component of weather variations. Long-term historical records of rainfall form the basis of planning and design of major water resources projects. However, in most instances such historical records are often unavailable, and in situations where they are available the records are too short to give any statistically significant meaning.

One approach adopted to overcome this difficulty is to synthetically generate long-term rainfall series. Hence, the simulation of rainfall time series is important not only from the pure scientific point of view but it also has a lot of practical consequences in hydrology. The generated synthetic rainfall series can be used for making predictions of recurrence interval of various extremes like dry periods or extreme rainfall events. Another important need of generating synthetic rainfall series insists in the fact that the observed series are very often too short or not enough spatially resoluted for the purpose of hydrological modeling (Bardossy et al., 2002). Using the generated extreme rainfall events as input in hydrological models enables one to asses their hydrological influence.

There is a close relationship between atmospheric circulation and climatic variables (i.e. rainfall). This has been investigated by a large number of authors since middle of the 20th century. For example Burger (1958) and Lamb (1977) stated that even the highly varying rainfall is strongly linked to the atmospheric circulation that means that changes in atmospheric circulation affect rainfall.

Especially because of the need to deal with the future climate scenarios much attention has been given to downscaling of surface weather variable (precipitation) from large-scale atmospheric circulation. Downscaling is the term given to the process of deriving finer resolution data (e.g., for a particular site) from coarser resolution Global Circulation model (GCM) data. Most researchers feel that the horizontal resolution of most GCMs is generally too coarse to be used in impact models (The impact model is a global, three-dimensional coupled dynamics, radiation and chemistry model of the troposphere and middle atmosphere having GCM based dynamics component) in its original format. A lot of useful information can be derived from GCMs without the need for downscaling to be undertaken, but it is recognized that sometimes it is necessary to try and add value to a scenario by making it more applicable for finer resolution studies. Downscaling is nothing but the transformation from a large-scale feature to a small-scale one, not necessarily of the same kind. A downscaled forecast is one that has been defined in more detail for a particular location from a forecast for a larger area.

Due to the high non-linearity and influence of local factors like latitudes, prevailing winds, altitudes, topography (especially in mountain range), distance from the ocean, and ocean

currents, present in the atmospheric system, it is sometimes difficult to describe the relationship between atmospheric circulation and rainfall using a deterministic approach. Therefore, the downscaling method is generally adopted by using stochastic models, with parameters depending on circulation pattern (CP) types. The advantage of conditioning the downscaling on CPs is that the CPs characterize the atmospheric circulation on a large (continental) scale.

CPs can be determined using classification techniques. The classification can be one of the two kinds: subjective and objective. The advantage of subjective method is that the knowledge and experience of meteorologists is fully used in the classification. Major disadvantages are that the results cannot be reproduced and that this method can only be applied for certain geographical regions. The second type of classification method is presented by objective techniques. They are based on the automated algorithms operating on selected datasets, and they allow fast classification, which is necessary especially for climate change scenarios. Fuzzy classification method, based on subjectively defined rules (Bardossy et al., 1995) is one of the objective classifications. The advantage of this classification technique is the fact that in contrast to common CP classifications, its objective is to explain the variability of local rainfall. It means that, the CPs explain the relationship between large-scale atmospheric circulation and rainfall.

Many hydrological models require synthetic rainfall series in higher resolution as an input. Now a days various Kriging methods are widely adopted for generating Rainfall data series at required resolution. Kriging provides a means of interpolating values for points not

physically sampled using knowledge about the underlying spatial relationships in a data set to do so.

1.2 Objective of the Thesis

This research effort is aimed at generating synthetic rainfall data in a watershed using empirical or statistical approaches. Since the high resolution rainfall is needed each grid points in space, some Kriging tools will be explored for interpolation or the generated point synthetic rainfalls. Specially, followings are the objectives of this study.

1. Generate daily rainfall series using stochastic downscaling model. Besides this, in order to get weather conditions leading to flood events, rainfall will be generated as stochastic downscaling process coupled with atmospheric circulation pattern.
2. This will require developing daily-classified Circulation Patterns for downscaling of rainfall. In this study, new fuzzy rule based method (Bardossy et al., 2002) will be employed.
3. In order to achieve synthetic rainfall series at higher resolution in space, interpolation of observed and synthetic rainfall series will be carried out using Kriging tools. Ordinary kriging and external drift kriging will be employed.
4. Finally Comparison of mean seasonal cycles, mean values and deviations of yearly totals and other diagnostics will be carried out to evaluate the synthetic rainfall series with historically observed series.

The proposed methodologies will be tested using the data from River Freiberger Mulde catchment. The daily rainfall data set for 20 years (1971-1990) over thirty-two stations

spread over the whole catchment will be employed. For the CP classification discharge data and Sea Level Pressure (SLP) data have been used. Discharge data from Freiberger Mulde river catchment for the period of 20 years (1971-1990) are employed. The SLP data obtained from the National Meteorological Center (NMC) at grid point set for different windows over whole Europe with a grid resolution of $5^{\circ} \times 5^{\circ}$ will be employed.

1.3 Organization of the Thesis

The structure of thesis is as follows: chapter 1 provides general introduction to the topic, objectives of the thesis and organization of the work. Chapter 2 reviews the literature available in the area of the present study. Chapter 3 describes the model development with methodology and results of SDM and automated classification of circulation patterns. Geostatistical Kriging is described in chapter 4 along with the results. In chapter 5, concluding remarks have been made. References and appendices have been provided at the end.

Chapter 2

Literature Review

This chapter discusses the review of literature in the area of present study and closely related areas. The review of literature has been divided into four parts. The first section describes the literature on rainfall modeling. The second section describes the literature on the technique of stochastic downscaling. The review of literature on Atmospheric circulation is taken up in the third section and last section describes literature available for interpolation of hydrologic variables.

2.1 Rainfall Modeling

The earlier attempts for rainfall modeling employed time series technique of simple autoregressive moving average (ARMA) models for annual precipitation totals. Also the monthly totals can be modeled with the help of appropriate transformations. In case of daily rainfall, the problem of time intermittence occurs which cannot be solved by classical time series models because these assume continuous and mostly normal distribution of variables.

Some studies have been reported that Markov models and Markov renewal models can be applied for modeling of rainfall occurrence and duration (Foufoula-Georgiou and Lettenmaier, 1987). These models belong to the class of Markov renewal processes and, are, in general, a nonrenewal clustered (over-dispersed relative to the independent Bernoulli) process. In the model proposed by Foufoula-Georgiou and Lettenmaier (1987), the sequence of times between events is formed through sampling from two geometric distributions

according to transition probabilities specified by a Markov chain. As a special case, the proposed model includes a renewal process with a mixture distribution for the interarrival times. The model was fitted to daily rainfall occurrences for five seasons at Snoqualmie Falls, Washington. The adequacy of the model fit was confirmed by comparing the empirical normalized spectrum of counts, log-survivor function, and variance time curve, with their fitted counterparts. Another example of stochastic model for rainfall occurrence and amount, named 'chain-dependent stochastic daily precipitation model' was developed by Wilks (1989). These were conditional on the monthly total rainfall (i.e., separately for subsets of the climatological record). Ten thousands months of daily data for each month and each of the parameter sets were generated. Each month of synthetic data was initialized separately, so that each realization was independent. These models had been shown to be capable of synthetically generating daily rainfall data, which also reproduce certain aspects of longer-period rainfall variations. A commonly used alternative, unconditionally derived daily stochastic rainfall model, may seriously distort such characteristics.

A Semi-Markov chain model was developed by Bardossy and Plate (1991) for atmospheric circulation pattern (CP). Local rainfall was linked with the help of conditional probabilities. These conditional probabilities were variable in space and had to be estimated from local rainfall data. An advantage of the model was that a simultaneous simulation at different locations could be done much easier as the CP remains the same for a big region (for Europe). This ensured a natural correlation between independently simulated series.

locations could be done much easier as the CP remains the same for a big region (for Europe). This ensured a natural correlation between independently simulated series.

Hay, Wolock, Ayers (1991) developed a model for rainfall simulation that incorporates climatological information. A markovian-based model was used to generate temporal sequences of six daily weather types. Rainfall values were assigned to individual days by using observed statistical relation between weather types and rainfall characteristics. The strength of this weather type rainfall model was that it models rainfall as a function of weather type. The accuracy of this model was evaluated by Monte Carlo simulation runs. The Monte Carlo simulation runs reproduced daily weather types and rainfall sequence similar to those of observed record.

2.2 Stochastic Downscaling

Downscaling of rainfall under climate change conditions is an important issue to be understood by hydrologists and has been explored widely by many researchers. The General Circulation Model (GCM) developed by the Goddard Institute for Space Studies (GISS) in New York City, is the main tool used by scientists to understand the interplay between the factors that make up climate, and to predict the climate change caused by emissions of greenhouse gases (GHGs). GCMs provide quantitative estimates of potential climate change by "modeling" the physical climate system. To date, GCMs are the best available tools to estimate future global climate changes. However, their spatial resolution is currently in the range of 200-500 km. This resolution is too coarse to study the changing climate and its impact on the environment on regional and local scales, essential for many applications in

e.g. agriculture, forestry or civil engineering. Therefore, Global circulation model (GCM) could not provide realistic rainfall series even for the present climate scenarios. Even if it would be the case, it would not be possible to generate rainfall time series for smaller regions or selected locations because of their course space resolution (Bardossy et al., 2002). Besides this, it is possible to downscale rainfall behavior from the GCM air pressure or geopotential height outputs. A lot of attention had been paid in the last few years to the problem of statistical downscaling from GCM (Wilby, et al. 1998a).

Bardossy (1992) developed a methodology for downscaling GCM output results to regional scale rainfall using atmospheric circulation patterns. A sequence of observed daily air pressure distribution was used to define CPs. The classification of the CPs was done with the help of a neural network. A multivariate stochastic model described their link to observe daily rainfall amounts at number of selected locations. To assess rainfall under changed climate CPs derived from GCM output, pressure values were used to condition the stochastic rainfall model. This methodology was applied on the selected location (Essen, Germany). They concluded that GCMs couldn't simulate accurate rainfall amounts in the present climate control runs. However, they found that GCM can be more accurate on air pressure. There is a stochastic link between rainfall and CPs. Using this link local rainfall amounts could be simulated corresponding to the GCM output CPs. These amounts were much closer to the observed values than the GCM output rainfall.

Bardossy and Plate (1992) developed a multi-dimensional stochastic downscaling model for space-time distribution of daily rainfall. The rainfall was linked to atmospheric CP using

conditional distributions and conditional spatial covariance functions. The model was a transformed conditional multivariate autoregressive AR(1) model, with parameter depending on the atmospheric CP. The model reproduced both the local rainfall occurrence probabilities and the distribution of the rainfall amounts at given locations, and the spatial dependence described with the help of cross-covariances of the transformed series. Parameter estimation methods based on the moments of the observed data were developed. CPs were generated using the Semi-Markov model described by Bardossy and Plate (1991). The model was applied using the classification scheme of the German Weather Service for the time period 1881–1990. Rainfall data measured at 44 different stations for the time period 1977–1990 in the catchment of the river Ruhr (Germany) were used to demonstrate the model. Both the distribution of duration of wet and dry periods, and the autocorrelation functions were found to be in good agreement with the observed values. They concluded that the spatial distribution of daily rainfall was strongly linked to the atmospheric circulation and could be modeled as a coupled process. Also, model parameters could be estimated from the probability of rainfall and the daily rainfall amount at a location for given CP. The model was well suited for rainfall simulation, coupled to a deterministic or stochastic atmospheric circulation model.

Katz and Parlange (1993) performed the stochastic modeling of time series of daily rainfall amount conditional on a monthly index of large-scale atmospheric CPs. Conditional chain-dependent processes were fit to time series of daily rainfall amounts given an index of large-scale atmospheric circulation (i.e., either below or above normal monthly mean sea level pressure). Rainfall data for January at several locations in California, USA were analyzed.

The two conditional daily models differ both in terms of the parameters of the occurrence process and of the intensity process. Each of these daily effects contributes to changes in the distribution of monthly total rainfall associated with the circulation index. The process induced by combining the conditional daily models produced a variance for monthly total rainfall much closer to the observed value than that for the corresponding unconditional chain-dependent model.

A two step downscaling method for GCM was developed by Enke and Spekat (1997). The investigation was based on daily upper air geopotential and humidity fields (Atlantic-European sector) and surface observations (52 German climate stations) from 1966 to 1993. In the first step, significant CPs were identified using cluster analysis, which takes advantage of information exclusively from upper airfields. This lead to composite charts which could be readily interpreted synoptically, but which only explained a portion of the variance of the local weather elements. In the second step, a conditional (weather pattern-dependent) stepwise screening regression analysis was performed for each weather element and five German climate regions. A principal finding was that the modeled (downscaled) local climate was in good agreement with observations. An application to a GCM control run was added. It showed that the method was capable of reconstructing interannual variability of local weather elements.

Recently, a space-time model has been developed by Bardossy and Mierlo (2000) for simultaneous regional rainfall and temperature simulation using a classification of special CPs on a daily basis. The model was based on coupled multivariate stochastic processes

between CPs and measured regional rainfall and temperature in a catchment. Applying CPs classified out of GCM outputs (geopotential height based on a GCM grid), the downscaling model simultaneously generated rainfall and temperature time series at several sites in a smaller regional catchment, taking spatial correlation into account. This model was an improvement of the rainfall model developed by Bardossy and Plate (1992).

More recently, Stehlik and Bardossy (2002) developed a multivariate stochastic downscaling model (SDM) for generating daily rainfall series based on atmospheric circulation. This model was an advancement of the rainfall model developed by Bardossy and Plate (1992). That model included only winter and summer seasons, whereas, the new model includes the annual cycle and generates rainfall time series for several sites. For the calibration and validation for this downscaling model, the observed and simulated daily rainfall amounts from eight rainfall stations spread over Germany were used. The model was calibrated using the data for the period 1970–1979, validated using the data for the period 1980–1990, and applied for the whole period 1970–1990. The model was successfully applied in two regions with different climate conditions: Central Europe (Germany) and Eastern Mediterranean (Greece). The rainfall characteristics depend on large-scale atmospheric circulation conditions; the conditional rainfall characteristics for each CP are computed. Fuzzy rules based method of CP classification was used to determine the CPs. It was generally possible to take arbitrary number of rainfall stations into account and therefore the process could be derived as multivariate stochastic one. The seasonal cycle of rainfall was simulated by using Fourier series. The statistical comparison of observed and simulated rainfall series based on standard diagnostic [referred by Wilby et al., (1998)] showed that most features were in good agreement. Several tests like comparison of mean seasonal cycles, comparison of mean

2.3 Atmospheric Circulation

There is a good reason for relating rainfall characteristics to large-scale atmospheric circulation. Several studies proved relationships between CP and climatic variables. Burger (1958) studied the relationship between the atmospheric patterns and mean, maximum, and minimum daily temperatures, rainfall amounts, and cloudiness using the time series from 1890 to 1950 measured at four German cities (Berlin, Bremen, Karlsruhe and Munich). He found a good correspondence between climatic variables and atmospheric circulation.

Lamb (1977) stated that even the highly varying rainfall is strongly linked to the atmospheric circulation of all elements of climate affected by changes in the patterns of flow and intensity of the prevailing atmospheric circulation, none is more obvious than rainfall. The effects are very clearly seen (especially when analyzed in terms of percentage), despite the intricacy of local rainfall distribution owing to its dependence on even small-scale orography.

The daily occurrence of large scale CPs was linked with the partial duration of series of floods in small to moderate sized river basins, using a case study in Central Arizona (USA) by Duckstein et al., (1993). The probabilistic linkage was evaluated by means of two performance indices, relating flood occurrence, observed CP occurrence before flood and purely random count of CPs. Three seasons (Summer, autumn and winter) were distinguished, and CPs were grouped into two flood producing groups year around.

The daily precipitation of Bern, Neuchatel and Payerne in Switzerland was statistically linked by (Brandsma et al., 1997) to atmospheric circulation and temperature. For all three stations, there was a marked increase of the mean precipitation amount with increasing temperature for wet days with temperatures between -5 and 20 °C. The amount of precipitation was also controlled by the direction and strength of the atmospheric flow. To take these dependencies into account, the daily precipitation amounts were modeled as a function of temperature and strength of the flow for three categories of flow direction. The non-linear effects of temperature and strength of the flow on the amount of precipitation were described by natural cubic splines and piecewise linear functions.

Recently, Bardossy et al., (2002) developed an automated objective classification of daily atmospheric CP for rainfall downscaling based on optimized fuzzy rules. The main goal of the method was to provide a basis (Daily classified CPs) for downscaling of rainfall and temperature, which could be done by means of downscaling models with parameters depending upon CP. The CPs were described by fuzzy rules, which indicate the location of the pressure center highs and lows. The fuzzy rules were obtained automatically using an optimization of the performance of the classification. The rules were assessed using a discrete optimization procedure based on simulation annealing. For rainfall, the performance of the classification was measured by rainfall frequencies and rainfall amounts conditioned on the CPs. So the task was to define the wet and dry CPs. The performance of CPs was validated using a split sampling approach. This methodology was applied on the central Europe (Germany) and the eastern Mediterranean (Greece).

More recently, the same classification method of daily CPs was also applied on the catchments the Ardeche in France and the Liobregat in Spain by Bardossy et al., (2003) for identification of flood producing atmospheric CPs based on discharge data set.

2.4 Interpolation of Hydrologic Variables Using Kriging

Most of the methods currently used in hydrosciences for interpolation and spatial averaging fail to quantify the accuracy of the estimates. The theory of regionalized variables enables one to point out the relationship between the spatial correlation of hydro meteorological or hydro-geological fields and the precision of interpolation, or determination of average values, over these fields. A new estimation method called kriging has proven to be quite well adapted to solving water resources problems.

Delhomme (1978) used this method and presented a series of case studies in automatic contouring, data input for numerical models, estimation of average rainfall over a given catchment area, and the design of measurement network.

Ahmed and Marshley (1987) compared Geostatistical methods for estimating transmissivity. Four such methods were compared which were kriging combined with linear regression, co-kriging, external drift kriging and kriging with a guess field. According to referred study, Co-kriging is a geostatistical technique developed to improve the estimation of a variable using the information on other spatially correlated variables, which are generally better sampled. It is the method having the best theoretical foundation, meaning that no assumptions are made on the nature of the correlation between the two variables. External

drift kriging utilizes more than one variable. It consists in having the mean of one variable depend linearly on the other, thus giving rise to a new universality condition in the kriging system. Kriging with guess field can be better applied only if the second variable is available at all the locations where the first variable is measured. It can be extended more than two variables using multiple regressions. They concluded that Co-kriging is the more rigorous method and requires less assumptions. Kriging combined with linear regression can be used only in the case of two variables. Kriging with external drift can be used for an unlimited number of variables.

2.5 Summary

Clearly, many studies have been reported in literature for stochastic downscaling based on atmospheric circulation for generating synthetic rainfall series. Stehlik and Bardossy (2002) developed a model for this purpose in two regions of Central Europe (Germany) for nine stations covering West, North and South part of the Germany and Eastern Mediterranean (Greece). In present study an attempt has been made to test this model in different climatic conditions, by applying over it a larger catchment having higher number of stations spread over the whole catchment to obtain synthetic rainfall series in higher resolution using new interpolation technique of External Drift Kriging.

Chapter 3

Model Development

3.1 Overview of Downscaling

Climatic changes have important impacts on the hydrologic cycle. These influences might manifest themselves at different temporal and spatial scales. The temporal scales might vary from short times to annual balances. Spatially, the effect might be local, regional, or global. Water related projects are often having life times of 50 to 100 years. Thus, the design of these water resources project has to consider possible effects of climate changes. It is widely accepted that General Circulation Models (GCMs) are the best physically based models to describe the effects of the changes in the atmosphere. Unfortunately, these models have a very coarse spatial resolution (typically several hundred km grid meshes). Further, they reproduce the general meteorological features that can be inaccurate on single grid boxes. Thus the useful grid size is even much coarser than the conceptual grid. Rainfall that is the most important input in many hydrological models is not well modeled by theGCMs. Systematic errors in mean and annual cycles of rainfall generally occur. This means the hydrological models cannot use the output of the GCM directly. Therefore, downscaling models are used to provide reasonable small-scale information.

Downscaling is a technique, which might give some hints for future hydrological changes. It is an attempt to give subscale realization from a higher temporal and / or spatial scale.

Downscaling is nothing but the transformation from a large-scale feature to a small-scale one, not necessarily of the same kind. A downscaled forecast is one that has been defined in more detail for a particular location from a forecast for a larger area. There are several possibilities for downscaling, which form two main groups: (a) dynamical downscaling, and empirical downscaling.

In the case of dynamical downscaling, nested regional climate models are used to simulate sub-grid scale features using a higher spatial resolution (15 to 50 km) using the time varying atmospheric conditions obtained form GCM. The advantage of this method is that it delivers meteorologically consistent variables. However, the uncertainty related to this method and the nonuniqueness of the solution are generally not taken into account.

Empirical downscaling methods are based on local observations. These methods can generate a large number of realizations – thus the assessment of the uncertainty of the prediction is possible. Further local details, which cannot be reflected by the dynamical models, are considered in these methods. In principle, there are two methods for empirical downscaling: (a) regression technique and (b) conditional probability approaches. The regression method defines the relations between the large scale and local information by means of an explicit function. The form of the function is usually selected so that the parameters can be estimated without major numerical difficulties. Explanatory variables are often selected using a trial and error procedure. Other empirical techniques use an intermediate step. The large-scale information is first classified using empirical, statistical or other methods. Then, the downscaling is carried out by using stochastic models, with parameter depending upon CP types. In this case, the nonlinearity of the downscaling is

captured by the CPs, each of them having a specific relationship with the surface variables. However, the advantage of conditioning the downscaling on CPs is that the Circulation patterns characterize the CPs on a large (continental) scale.

3.2 Multivariate Stochastic Downscaling Model

The Multivariate Stochastic Downscaling model (MSD) developed by Stehlik and Bardossy (2002) for generating synthetic daily rainfall time series based on atmospheric circulation patterns was used in present study. The rainfall is modeled as a stochastic process coupled with atmospheric circulation. Rainfall is linked to the circulation patterns (CPs) using conditional model parameters. CP classification will be required for this purpose. In this study, new fuzzy rule based method of CP classification has been employed. The details of this classification method are described in a later section in this chapter. The classification can deliver conditional mean rainfall amounts and probability of rainfall occurrence for a specific location. However, the downscaling aims to produce realistic series. This means that the temporal and spatial variability should be reproduced. For this purpose, specific models have been developed. The detailed description of this model is given below.

3.2.1 Mathematical Basis

Both spatial and temporal intermittence causes problems in mathematical modeling of rainfall on daily basis. Usually, the probability of dry days is relatively high and the rainfall amounts on a day with rainfall are described by means of a continuous distribution.

Therefore, random variables with mixed distribution are required to describe daily rainfall. Another problem occurs in clustering of wet and dry day occurrence. This clustering has natural causes and is usually modeled with the help of appropriate distribution. In this time-space model, clustering is the consequence of the persistence of atmospheric circulation patterns.

Let $A = \{ \alpha^1, \ldots\ldots, \alpha^n \}$ be a set of possible atmospheric circulation patterns. Let $\tilde{A}_t$ be the random variable describing the actual atmospheric circulation, taking its value from A. Let the daily rainfall amount at time t and point u in the region U be modeled as a random function $Z(t, u)$, u in U. The distribution of rainfall amounts at a selected location is skewed. In order to relate it to simple normally distributed random function $W(t, u)$ (for any locations $u_1, \ldots, u_n$ the vector $(W(t, u_1), \ldots\ldots, W(t, u_n))$ as a multivariate normal random vector) the following power transformation relationship is introduced:

$$Z(t,u) = \begin{cases} 0 & \text{if } W(t,u) \le 0 \\ W^{\beta}(t,u) & \text{if } W(t,u) > 0 \end{cases} \qquad (3.1)$$

where β is an appropriate positive exponent.

This way, the mixed (Discrete-continuous) distribution of $Z(t, u)$ is related to a normal distribution. As the process $Z(t, u)$ depends on the atmospheric circulation patterns, the same applies to $W(t, u)$. The reason for this transformation is that multivariate processes can be modeled much easier if the process is normal. Further, the problem of intermittence can also be handled this way, as negative values of W are declared as dry days and dry

locations. The exponent β is needed as the distribution of rainfall amounts is usually much more skewed than the truncated normal distribution.

The relationship between W (t, u) and the circulation pattern $\tilde{A}_t$ is obtained through the rainfall process Z (t, u) using Eq. (3.1). The probability of rainfall at time t and location u depends on $\tilde{A}_t$:

$$P[W(t,u)>0 \mid \tilde{A}_t = \alpha_i] = P[Z(t,u)>0 \mid \tilde{A}_t = \alpha_i] = p_i(u) \tag{3.2}$$

The distribution of daily rainfall amount at location u, $F_i(z/u)$, also depends on $\tilde{A}_t$:

$$P[Z(t,u)<z \mid \tilde{A}_t = \alpha_i, Z(t,u)>0] = F_i(z/u) \tag{3.3}$$

Let $f_i(z/u)$ be the density function corresponding to $F_i(z/u)$. The relation between the normal density function of W(t,u) and the probability of rainfall $p_i(u)$ and the density function of $f_i(z/u)$ is explained in Figure 3.1.

For the subsequent development let us introduce the following notation:

$$W(t) = (W(t,u_1),\ldots,W(t,u_n)) \tag{3.4}$$

$$Z(t) = (Z(t,u_1),\ldots,Z(t,u_n)) \tag{3.5}$$

The expectation of W (t, u) for a given CP is:

$$w_i(t^*) = E[W(t^*,u) \mid \tilde{A}_t = \alpha_i] \tag{3.6}$$

Where t* stands for Julian date. It means that the annual cycle of expectation is taken into account. To simplify, the following development the vector of the expectation of W (t, u) is introduced:

$$w_i(t^*)= (w_i (t^*, u_1),....., (w_i (t^*, u_n)) \quad (3.7)$$

The random process describing W (t) is described by using the following equation:

$$W (t) = r (t^*) (W (t-1) - w_i (t^*-1))+ Ci (t^*) \Psi (t) + w_i (t^*) \quad (3.8)$$

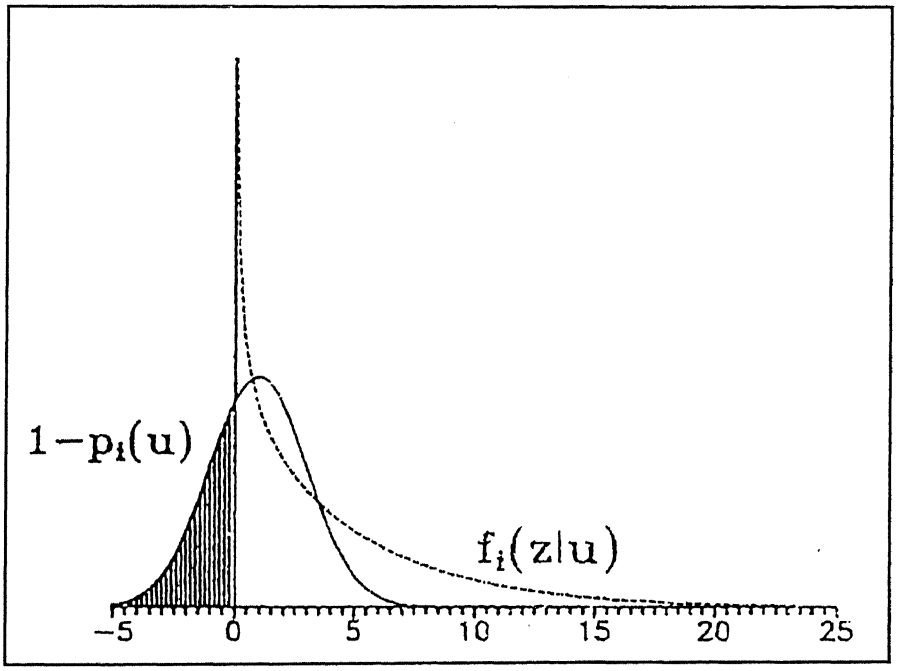

Fig. 3.1: The relationship between the densities of Z(t, u) and W(t, u) and the probability of rainfall $p_i(u)$.

Where

$$\Psi (t) = (\psi (t, u1),....., \psi (t,u_n) \quad (3.9)$$

is a random vector of independent N(0,1) random variables. Again, the symbol t is valid for the day of the simulation; whereas, t* holds for the Julian date corresponding to the actual day t. The symbol i stands for the CP on day t* and the symbol i′ for the previous day t*-1. The r (t*) is autocorrelation of one-day time lag. Lag 1 auto correlation of the daily rainfall does not vary widely in space – the model assumes them to be equal, due to the large scale features causing rainfall. This assumption might not hold for shorter time steps. The auto-correlation is independent of the CP but dependent on an annual cycle, which is approximated by using the Fourier series:

$$r(t^*) = \frac{A_0}{2} + \sum_{k=1}^{K} (A_k \cos(k\omega t^*) + B_k \sin(k\omega t^*)) \qquad (3.10)$$

where the frequency ω is $2\pi/365$. The advantage of Fourier series approximation (instead of simple polynomial fit) is that adding new A_k and B_k parameters do not change the values of former ones. Usually, the first three Fourier parameters are enough to simulate the annual cycle of autocorrelation. The annual cycle of autocorrelation was computed by means of a 30 day moving window.

The proportion of variance accounted for by each harmonic can be computed as follows:

$$R_k^2 = \frac{n/2(a_k^2 + b_k^2)}{(n-1)s^2} \qquad (3.11)$$

where s^2 is sample variance of the series. Since each harmonic provides independent information about the data series, the joint proportion of variance exhibited by a regression equation with only harmonic predictors is the sum of R_k^2 values for each harmonics (for maximum number ($n/2$) of harmonics the sum of R_k^2 is 1).

The $C_i(t^*)$ matrix takes spatial variability of the process into account. This n×n matrix is related to W (t) through the following relation (Bras and Rodriguez-Iturbe, 1985 p.93):

$$\Gamma_{0i}(t^*) = E[(W(t) - w_i(t^*))(W^T(t) - w_i^T(t^*))] \tag{3.12}$$

$$\Gamma_{1i}^T(t^*) = E[(W(t-1) - w_i(t^*-1))(W^T(t) - w_i^T(t^*))] \tag{3.13}$$

$$C_i(t^*)C_i^T(t^*) = \Gamma_{0i}(t^*) - \Gamma_{1i}(t^*)\Gamma_{0i}^{-1}(t^*)\Gamma_{1i}^T(t^*) \tag{3.14}$$

where $\Gamma_{0i}(t^*)$ is the spatial covariance matrix and $\Gamma_{1i}(t^*)$ is the space time covariance matrix for the time lag of one day. Assuming that these two matrices are related to each other through

$$r(t^*)\Gamma_{0i}(t^*) = \Gamma_{1i}(t^*) \tag{3.15}$$

leads to

$$C_i(t^*)C_i^T(t^*) = (1 - r^2(t^*))\Gamma_{0i}(t^*) \tag{3.16}$$

The decomposition of $C_i(t^*)C_i^T(t^*)$ (Bardossy and Plate, 1992) is described in the Appendix.

Another method that could be applied is proposed by Koutsoyiannis (1999). Equation 3.1 establishes the link between W(t) and the rainfall Z(t); thus the multisite process is fully described. Figure 3.2 explain the connection between W(t), the circulation pattern $\tilde{A}_t$, and the rainfall Z(t).

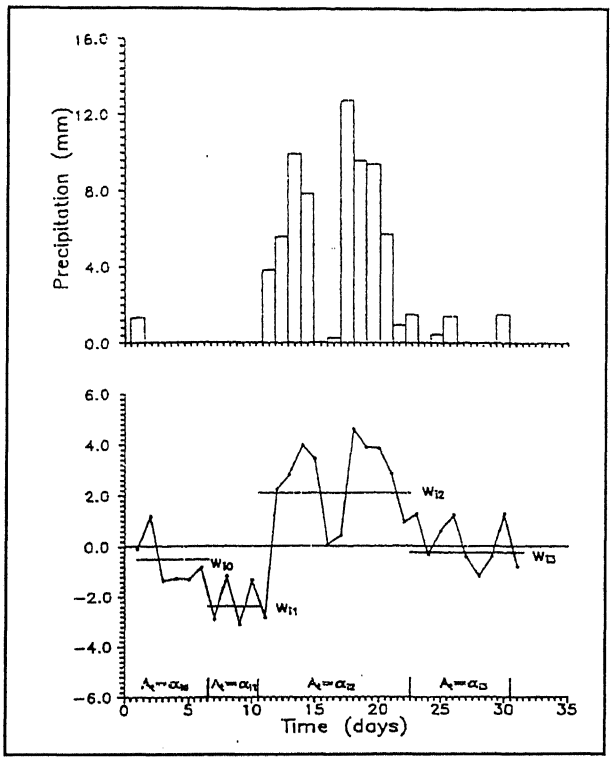

Fig. 3.2: The relationship between the three processes (1) the daily rainfall amount Z(t,u), (2)the normal process W(t,u), and (3) the circulation pattern $\tilde{A}_t$.

The upper half of the figure shows the daily rainfall sequence Z(t, u) and the lower half corresponds to W(t,u). The intervals with constant circulation patterns α_{ij} are marked on the time axis. The value w_{ij} is the mean of W (t, u) corresponding to circulation pattern α_{ij}.

3.2.2 Parameter Estimation

The temporal parameters by MSD model described above were computed by means of maximum likelihood method. Assuming that parameters of the rainfall annual cycle depend on the CP, *i* and the time of the year t* one can obtain:

$$w_i(t^*,u) = \frac{a_0(w_i,u)}{2} + \sum_{k=1}^{K}(a_k(w_i,u)\cos(k\omega t^*) + b_k((w_i,u)\sin(k\omega t^*)) \quad (3.17)$$

$$\sigma_i(t^*,u) = \frac{c_0(\sigma_i,u)}{2} + \sum_{k=1}^{K}(c_k(\sigma_i,u)\cos(k\omega t^*) + d_k((\sigma_i,u)\sin(k\omega t^*)) \quad (3.18)$$

Where $\sigma_i(t^*,u)$ is the standard deviation of the transformed rainfall amount W(t,u) on Julian date t*, $\sigma_i(t^*,u)$ is connected with $\Gamma_{0i}(t^*)$ as it contains the variances in its main diagonal. Due to this fact, the correlations are used for the estimation of spatial co-variances. The log-likelihood function can be written as follows using the derivation of Henze and Klar (1993)

$$L(w_i(t^*,u),\sigma_i(t^*,u);Z(t,u),t=1.....T) = \sum_{Z(t,u)=0}\log\Phi\left(\frac{-w_i(t^*,u)}{\sigma_i(t^*,u)}\right) + \sum_{Z(t,u)>0} \times\log\left[\frac{Z(t,u)^{(1/\beta)-1}}{\beta\sigma_i(t^*,u)}\phi\left(\frac{Z(t,u)^{1/\beta} - w_i(t^*,u)}{\sigma_i(t^*,u)}\right)\right] \quad (3.19)$$

where ϕ and Φ denote the density function and the cumulative distribution function of the standard normal distribution, respectively. This equation can be simplified as follows:

$$L(.) = \sum_{Z(t,u)=0}\log\Phi\left(\frac{-w_i(t^*,u)}{\sigma_i(t^*,u)}\right) + \sum_{Z(t,u)>0}\log\sigma_i(t^*,u) - \sum_{Z(t,u)>0}\log\beta + \left(\frac{1}{\beta}-1\right)\sum_{Z(t,u)>0}\log Z(t,u)$$

$$-\frac{1}{2}\sum_{Z(t,u)>0}\log(2\pi) + \frac{1}{2}\sum_{Z(t,u)>0}\left(\frac{Z(t,u)^{1/\beta} - w_i(t^*,u)}{\sigma_i(t^*,u)}\right)^2 \quad (3.20)$$

Summing the terms, which do not depend on the Fourier coefficient to K, one has:

$$L(.) = K + \sum_{Z(t,u)=0} \log \Phi\left(\frac{-w_i(t^*,u)}{\sigma_i(t^*,u)}\right) + \sum_{Z(t,u)>0} \log \sigma_i(t^*,u) + \frac{1}{2}\sum_{Z(t,u)>0}\left(\frac{Z(t,u)^{1/\beta} - w_i(t^*,u)}{\sigma_i(t^*,u)}\right)^2 \tag{3.21}$$

The above function has to be maximized as a function of $a_0(w_i,u),....,a_k(w_i,u),b_1(w_i,u),.....,b_k(w_i,u),c_0(\sigma_i,u),.....,c_k(\sigma_i,u),d_0(\sigma_i,u),....,d_k(\sigma_i,u)$. This can be done by numerical optimization using appropriate algorithms. The convergence can be substantially increased by using the first approximation for $w_i(t^*,u)$ and $\sigma_i(t^*,u)$ for a selected set of points (for example 12 mid days of the 12 months) and then fitting initial $a_0(w_i,u),....,a_k(w_i,u),b_1(w_i,u),.....,b_k(w_i,u)$, $c_0(\sigma_i,u),.....,c_k(\sigma_i,u)$ and $d_0(\sigma_i,u),.....,d_k(\sigma_i,u)$. Starting from this point ensures a quick optimization. The optimization of the Fourier parameters of the autocorrelation function described by Eq. (3.10) is done by the same technique. The spatial structure of the rainfall is described using a CP dependent covariance structure of the matrix $\Gamma_{0i}(t^*)$ and $\Gamma_{1i}(t^*)$. The covariance structure is assumed to be translation invariant but time dependent supposing:

$$\mathrm{cov}[Z_x, Z_y]_i(t) = p_i(t^*)e^{-h(x,y)q_i(t^*)} \tag{3.22}$$

Where h is the distance. The parameters p_i and q_i depend on the CP i and the time of the year, and are also modeled by means of Fourier series. Anisotropy is taken into account by introducing coordinate transformation.

$$x' = \lambda(x\cos\gamma + y\sin\gamma) \tag{3.23}$$

$$y' = -x\sin\gamma + y\sin\gamma \tag{3.24}$$

Where (x, y) are the coordinates in the original system and (x', y') in the transformed system. The γ is the rotational angle and the λ is the ratio of two orthogonal ranges representing the highest and the lowest variability. It is supposed that the anisotropy changes with the circulation but for a given CP remains constant during the year (due to flow direction). The parameters of the spatial correlation function including λ and γ were estimated using a least squares approach. The generation of rainfall series is based on Eq. (3.8). The series are generated day by day for a set of points simultaneously. For a given series of CPs, the corresponding rainfall is generated using randomly generated Ψ (t) and the values of the previous day in Eq. (3.8). It is an advantage of presented model that it takes the spatial correlation among rainfall series, into account. Therefore, it is suitable in generating of the areal rainfall.

The presented model is an advancement of the rainfall model developed by Bardossy and plate (1992). That model included winter and summer seasons, whereas the new model includes the annual cycle and generated rainfall time series for several sites. With the help of new model it is possible to simulate the rainfall for a set of points simultaneously. Further, the annual cycle of spatial covariances were introduced and the parameter estimation is improved.

In the present study, rainfall was linked to the CP using conditional model parameters. Therefore, to identify the CPs, new fuzzy rule based method of CP classification was used. Detailed description of this method is given below.

3.3 Automated Objective Classification of Daily Circulation Patterns

There is a close relationship between atmospheric circulation and climatic variables (i.e. rainfall). Downscaling methods for rainfall are based on the fact that the surface weather variables (rainfall) on a given day can be directly linked to the atmospheric CP on the same day. Therefore, to generate realistic rainfall series with downscaling methods, CPs were taken into account. However, the advantage of conditioning the downscaling on CPs is that the CP characterizes the atmospheric circulation on a large (continental) scale.

The generated series takes the daily CP into consideration using conditional probabilities. In this study, a new fuzzy rule based classification of CPs was applied (Bardossy, et. al. 2002). The main goal of this method is to provide a basis for downscaling models with parameters depending on the CP. The advantage of this classification technique is the fact that in contrast to common circulation pattern classifications, its objective is to explain the variability of local rainfall. It means that, the CPs explain the relationship between large-scale atmospheric circulation and surface climate (rainfall). Therefore, the CPs obtained by this classification method are suitable as input for the rainfall downscaling. The classification method used in this study is based on the concept of fuzzy sets (Zadeh, 1965). A brief description of all the terms related to Fuzzy logic is described below.

3.3.1 Overview of Fuzzy Logic

Fuzzy logic is basically a multi-valued logic that allows intermediate values to be defined between conventional evaluations like yes/no, true/false, black/white, etc. Notions like 'rather warm' or 'pretty cold' can be formulated mathematically and processed algorithmically. In this way, an attempt is made to apply a more human-like way of thinking in the programming of computers ("soft" computing). Fuzzy logic systems address the imprecision of the input and output variables by defining fuzzy numbers and fuzzy sets that can be expressed in linguistic variables (e.g. small, medium, and large).

3.3.1.1 Fuzzy Set

The Fuzzy set based on fuzzy logic, which enables one to deal with imprecise statements was developed by Professor Lotfi Zadeh of U.C. Berkeley in 1965, but this method had not gained popularity until recently. A fuzzy set is a set of objects without clear boundaries or without perfectly (precisely) defined characteristics. In contrast with ordinary sets where, for each object, it can be decided whether it belongs to the set or not, a partial membership in a fuzzy set is possible. It is a class of objects with a continuum of grades of membership (characteristic) function, which assigns to each object a grade of membership ranging between zero and one. Formally, a fuzzy set can be defined as follows:

Let X be a space of points (objects), with a generic element of X denoted by x. Thus, X = $\{x\}$. A fuzzy set (class) A in X is characterized by a membership (characteristic) function $\mu_A(x)$ which associates with each point in X through a real number in interval [0,1], with

the value of $\mu_A(x)$ at x representing the grade of membership of x in A. Thus, the nearer the value of $\mu_A(x)$ to unity, the higher the grade of membership of x in A. If [0,1] is replaced by the two-element set {0,1}, then A can be regarded as an ordinary subset of X.

3.3.1.2 Fuzzy Number

Special cases of fuzzy sets are fuzzy numbers, which are simply an ordinary number whose precise value is somewhat uncertain. While Boolean operations such as union, intersection or complement can be performed on general fuzzy sets, arithmetic operations such as addition or multiplication can only be performed on fuzzy defined on the set of real numbers. The simplest generalizations of the real numbers are the fuzzy numbers. Formally, fuzzy number can be defined as follows: A fuzzy subset A of the set of real numbers is called a fuzzy number if there is at least one z such that $\mu_A(z) = 1$ (normality assumption) and for every real numbers a, b, c with $a < c < b$

$$\mu_A(c) \geq \min(\mu_A(a), \mu_A(b)) \tag{3.25}$$

Any real number can be regarded as a fuzzy number with a single point support, and is called a "crisp number" in fuzzy mathematics. The simplest fuzzy numbers are the so-called triangular fuzzy numbers. The membership function of the triangular fuzzy number consists of an increasing and a decreasing linear function - forming a triangle. The formal definition is as follows:

The fuzzy number $A = (a_1, a_2, a_3)_T$ with $a_1 \leq a_2 \leq a_3$ is a triangular fuzzy number if its membership function can be written in the following form:

$$\mu_A(x) = \begin{cases} 0 & \text{if } x \le a \\ \dfrac{x - a_1}{a_2 - a_1} & \text{if } a_1 < x \le a_2 \\ \dfrac{x - a_3}{a_3 - a_2} & \text{if } a_2 < x \le a_3 \\ 0 & \text{if } a_3 < x \end{cases} \tag{3.26}$$

3.3.1.3 Fuzzy Rules

Fuzzy rules are linguistic IF-THEN- constructions that have the general form "IF A THEN B" where A and B are (collections of) propositions containing linguistic variables. A is called the *premise* and B is the *consequence* of the rule. In effect, the use of linguistic variables and fuzzy IF-THEN- rules exploits the tolerance for imprecision and uncertainty. In this respect, fuzzy logic mimics the crucial ability of the human mind to summarize data and focus on decision-relevant information. Mathematical description of these rules is not included here. It is given in Zadeh (1965).

3.3.2 Classification Method

The classification method used in this study is the fuzzy rule based classification. The classification essentially consists of the following three steps: (a) Data transformation; (b) Definition of the fuzzy rules; and (c) Classification of observed data

The basis of the classification in the present study is the sea level pressure (SLP) at the geopotential elevation fields and discharge data. The SLP data are available on a regular

grid at daily resolution. In this classification, fuzzy rules are formulated by low and high-pressure anomalies. That is defined as the departure from the mean. Positive pressure anomaly means value is above the mean pressure and negative pressure anomaly indicates value is below the mean pressure. These normalized anomalies $g\ (i,t)$ are calculated from the gridded SLP data $h(i,t)$ as follows:

$$g(i,t) = \frac{h(i,t) - h(\bar{i},t)}{s(i,t)} \tag{3.27}$$

where i = 1,..., I are the grid points, t = 1,...,T is the time (in days), $h(\bar{i},t)$ is the mean annual cycle (mean over the corresponding Julian date) and $s(i,t)$ is the standard deviation for the given date.

Each CP is defined by a fuzzy rule, which indicates the locations of pressure center as low or high. This means that, to each grid point i a fuzzy set membership function is assigned. Five different possibilities were considered; large positive medium positive, medium negative, large negative and arbitrary. While the first four classes describe the location of pressure centers, the fifth class indicates locations whose anomalies are irrelevant for the CP. These five possible classes of pressure anomalies appear to be adequate to describe the main CP features. Thus, the k-th CP is described with the fuzzy rules k represented by a vector $v(k) = v(1,k),....,v(I,K)$. Here $v(i,k)$ is the index (1 to 5) corresponding to grid point I for CP k. The rule system describing K CPs can be represented by the matrix V as follows:

$$V = \begin{pmatrix} v(1,1) & \cdots & v(I,1) \\ \vdots & & \vdots \\ v(1,K) & \cdots & v(I,K) \end{pmatrix} \tag{3.28}$$

The $v(i,k)$'s are the indices (1,....., 5) of the membership function corresponding to the selected locations. The membership functions were defined as triangular (subscript T) fuzzy numbers: v = 1, very low: $(-\infty, -1, 0.2)_T$; v = 2, medium low:$(-1.4, -0.6, 0)_T$; v = 3, medium high: $(0, 0.6, 1.4)_T$; v = 4, very high: $(0.2, 1, +\infty)_T$ and v = 5, the membership function is the constant 1.

The membership function of the triangular fuzzy number $(a,b,c)_T$ is defined as:

$$\mu(g) = \begin{cases} 0 & \text{if } g < a \\ \dfrac{g-a}{b-a} & \text{if } a \le g < b \\ \dfrac{g-c}{b-c} & \text{if } b \le g < c \\ 0 & \text{if } g > c \end{cases} \tag{3.29}$$

The fifth possibility was introduced to allow any possible geopotential height anomalies for those locations that have no influence on the CP. The location and number of such grid points depend on the class to be described. Usually, most grid points belong to this class and only characteristic ones are assigned to other classes. The location of these grid points might vary for different CPs. For the data classification, the membership grades of the normal height anomalies were computed. For a given time t and location *i*, the membership grade corresponding to rule *k* is defined as

$$\mu(i,k) = \mu_{\nu(i)^{(k)}}(g(i,t)) \tag{3.30}$$

The classification of the SLP map of a given day t is done as follows:

1. The daily SLP map is transformed to a daily anomaly map, and
2. For each rule, the degree of fulfillment (DOF) is calculated as follows:

$$\text{DOF}(k,t) = \prod_{I=1}^{4}\left(\frac{1}{N(\nu(i)^{(k)}=1}\sum_{\nu(i)^{(k)}=1}\mu(i,k)^{P_1}\right)^{1/P_1} \tag{3.31}$$

Where N is the number of grid points classified by class I, and $P_1 \geq 1$ is the parameter, which allows one to emphasize the influence of selected classes on the DOF. The k for which DOF (k, t) is maximal is selected as CP for day t.

The problem of this method was how to access the rule vectors. A subjective definition of the rules requires good knowledge of the local meteorological conditions. The expertise is often not available. Another possibility, that was used, is the assessment of the rules using optimization. This classification method is based on the discharge data along with pressure data. The criterion has been taken for the discharge as follows:

3.3.3 Discharge Criterion

Main goal of the classification was aimed at explanation of rainfall behavior variance ability is to define CPs, which bring wet and dry weather into specified region. Discharge data has also been used to identify such CPs along with pressure data. The CPs were

identified using the positive increments of the observed discharge series, which provided a better rainfall behavior. The possible advantage of considering discharge is that it integrates the rainfall falling over a large area, and thus is less influenced by local rainfall variability. In the present study, instead of investigating daily discharge, daily discharge differences $\Delta Q(t)$ were considered because a major problem of linking discharges and atmospheric CP is that a high discharge might correspond not only to a day with heavy rainfall, but also to a dry day following a flood peak, Bardossy and Filiz, (2002). Therefore, a direct link is not possible. So discharge data was used as:

$$\Delta Q(t) = Q(t) - Q(t - \Delta t) \tag{3.32}$$

The time window Δt was taken as one day. Positive increase in discharge is caused by rainfall, therefore, for the analysis of CPs, $\Delta Q(t) > 0$ was important. New function Z(t) was introduced as a positive part of $\Delta Q(t)$ that was as follows:

$$Z(t) = \begin{cases} \Delta Q(t) & \text{if } \Delta Q(t) > 0 \\ 0 & \text{otherwise} \end{cases} \tag{3.33}$$

It was assumed that Z(t) is the additional runoff caused by weather and linked to atmospheric circulation. So the goal was to obtain CPs, which lead the large value of $Z(t)$. The procedure for classifying CPs based on discharge criterion is same as mentioned above.

3.3.4 Performance of Classification

In order to find the best possible rules for the description of local rainfall behavior, the performance of the classification has to be defined. Three types of objective functions were investigated to measure the performance of the classification with regard to surface climate variables (rainfall). The goal of the classification for the description of rainfall was to achieve a set of CPs, which explains the variability of rainfall behavior as much as possible. It was intended to identify both very wet and very dry conditions. Two types of objective functions were defined. Two measure were used, the occurrence of positive increment and a wetness index. The performance regarding the probability of occurrence of a positive increment (a day with increasing discharge) could be measured as:

$$O_1(V) = \sqrt{\frac{1}{T}\sum_{t=1}^{T}(p(z_0(CP(t)=i)) - \overline{p}_{z_0})^2} \qquad (3.34)$$

Here $\overline{p}_{z_0}$ is the probability of an increase of the discharge exceeding a given limit $z_0 \geq 0$ on an arbitrary day; $(p(z_0(CP(t)=i))$ is the probability of an increase of the discharge exceeding a given limit $z_0 \geq 0$ on a day with CP of class i $(CP(t)=i)$; and T is the number of days. The value of O_1 is large, if there are CPs which often lead to higher than z_0 increase of the discharge ($>z_0$) and others which seldom or never lead to a high increase of the discharge. Thus, this measure was related to flood occurrences.

The second measure was to describe the magnitude of an increase:

$$O_2(V) = \frac{1}{T}\sum_{t=i}^{T}\left|\frac{\overline{z(CP(t)=i)}}{\bar{z}} - 1\right| \tag{3.35}$$

Here $\bar{z}$ is the mean increase of the discharge on an arbitrary day with (Z>0); $\overline{z(CP(t)=i)}$ is the mean increase of the discharge on day t with i^{th} CP (CP(t) = i). This objective measured the relative performance of the classification compared to no classification. The value of O_2 is large if there are CP types, which lead regularly to high increase of discharge and others, which do not. This measure is thus related to flood peak and flood volumes.

The objective of the classification was to identify a rule system V that maximizes the above two objective functions. For this purpose, a weighted sum of the two objectives was used as a singe objective function where the weights were defined subjectively assigning higher weight to O_2 since flood peaks and volumes are normally of higher interest than flood occurrences.

$$O(V) = \omega_1 O_1(V) + \omega_2 O_2(V) \tag{3.36}$$

Where ω_1 and ω_2 were weights. The weights were selected in order to express the importance of the different objective functions and to correct for the different ranges of the functions.

The optimization was carried out over the all set of possible rule matrices V. Due to the complexity of the problem; an algorithm based on simulated annealing was used. Details of the simulated annealing algorithm are given below.

3.3.5 Optimization Algorithm

The objective function of optimization procedure was to find such fuzzy rules for which the optimization criterion is maximum. This means that the problem can be defined as combinatorial. Due to a given number of fuzzy rules (CPs), it is necessary to consider that each rule has a given number of terms (grid points), depending on the size of pressure window, and that for each grid point to 1 from 5 states (fuzzy number) can be defined. Because of large number of possible combinations, it is unfortunately not possible to compute the objective functions for each combination systematically. The number of all combinations depend on the size of the pressure window and number of CPs to be optimized. This number was very large; therefore, consideration of all the possibilities to find the best was impossible. A simulated annealing algorithm (Aarts and Korst 1989) was used as an optimization procedure. For the fixed number of rules, the algorithm can be briefly described as follows:

(0) Initialize the rules randomly and evaluate the performance O

(1) Set the initial 'annealing temperature' to q_0

(2) Select a rule k, location i and class v^* randomly

(3) If $v(i)^{(k)} = v^*$ return to step 2

(4) Set $v(i)^{(k)} = v^*$ and perform the classification

(5) Calculate performance O^* for the new rules

(6) If $O^* > O$, then accept the change

(7) If $O^* \leq O$, then with probability $\exp\left(\frac{O-O^*}{q_s}\right)$ accept the change

(8) If the change is accepted, replace O by O^*

(9) Repeat steps 2 to 10 M (given annealing temperature) times

(10) Decrease the 'annealing temperature' by setting $q_{s+1} < q_s$

(11) Repeat steps 2 to 10 until the portion of accepted changes becomes smaller than a pre-defined threshold.

The initial annealing temperature q_0 is selected so that 50% to 80% of the attempted changes are accepted. During the first few iterations, the program adjusts it-self so that the above condition is fulfilled. The reason for this choice is to allow strong departures from the initial rules. The number of attempted changes at a given annealing temperature M should be at least as many as the number of arguments multiplied by the number of rules. The algorithm makes it possible to accept negative changes. The willingness to accept these changes depends on the 'annealing temperature', which is decreased during the optimization procedure. It is worth mentioning that the initial classification does not influence the appearance of the resulting optimized CPs at all. The optimization process adjusts any initial classification to an optimum solution.

3.3.6 Validation of CP Classifications

A split sampling approach was used for the process of CP optimization and validation. The formulae used as optimization criterion can also be applied as measures of the classification quality. However, despite the optimization already carried out, it is still necessary to evaluate the overall quality of the optimization classification, e.g. in comparison to completely different classification techniques. Assessment of a new

classification can either be a comparison to another, for example subjective classification, or an internal classification, with respect to the quality of hydrological conclusions that can be drawn from the membership of one CP within the classification. Parameters to evaluate the performance of precipitation-oriented classifications are based on following quantities: HH (in %) – relative frequency of a CP for a given time period; p(CP(t))(in %) – probability of rainfall on a day with given CP; A/HH – wetness index, the ratio of the percentage of annual rainfall total and the rainfall total of a given CP and its appearance rate (high values indicate 'wet' CPs responsible for flood); mean (in mm) – mean rainfall total on a wet day for a given CP; and Std (in mm) – standard deviation of rainfall total on a wet day for a given CP. Any classification that defines probability p(CP(t)) and, mean z(CP(t)) increase of discharge on a selected station for a single day *t* referring to the classification of the same day can be measured by the indices identical to the objective functions O_1 and O_2 . The results in terms of these indices for the current study are discussed later on.

3.4 Model Application

3.4.1 Study Area and Data

The work carried out in this study concentrates on the catchment of Freiberger Mulde River in the state of Freiberg, Germany. The map of the catchment of Freiberger Mulde River is shown in Fig 3.3. The river Freiberger Mulde is 63-mi- (102 km) long rising from the Ore Mountains. District Freiberg is situated on its banks and it is the largest river of this region, which rises on Czech territory and from there runs northwards.

For the calibration and validation of MSD model, the observed daily rainfallamounts from 32 rainfall stations spread over the catchment (which are marked with dark spot in Fig 3.3) were obtained from German Weather Service (DWD). The daily rainfall data set for 20 years (1971-1990) over thirty-two stations spread over the whole catchment will be employed. Rainfall data was given as an input to the model in 1/10 of the rainfall (in mm). Daily classified CPs were another input to the model.

For classification of CPs, discharge and SLP data were used as an input to the classification method. SLP data used were obtained from National Meteorological Research Center for Atmospheric Research (NCAR, USA) and the National Meteorological Center (NMC). These were available at the grid point data set for different windows over Europe with a grid resolution of $5^{\circ} \times 5^{\circ}$. The daily SLP data set are used for the period of 1899-2002 that were based on 500 geopotential height data in the space windows 35°–65° N, 15° W–30° E. Discharge data were obtained from major tributaries of River Freiberger Mulde for the period of 1971-1990. For the classification based on daily discharge, discharge differences had been taken into consideration. According to Eq. (3.32) Δt =1 day was selected.

3.4.2 Analysis of CPs

MSD model takes the daily classified CPs as an input, therefore CPs were analyzed first. CPs were obtained by the fuzzy rules and these rules were accessed using discrete optimization based on simulated annealing, as described earlier. For the catchment Freiberger Mulde I = 72 grid points in total were used. From the first run K=12 rules

leading to 12 CPs and in second run K= 6 rules leading to 6 CPs were assessed. The CPs obtained by classification are daily CP for the time period from 1899-2002.

Table 3.1 shows the results for the catchment Freiberger Mulde for 12 CPs case. CP 99 is an unclassified pattern. The main goal is to analyze the wet and dry CPs. The frequency of the different CPs, the conditional frequency of discharge increases on days to the given CP, the relative contribution of a CP to the total discharge increases are given in table 3.1.

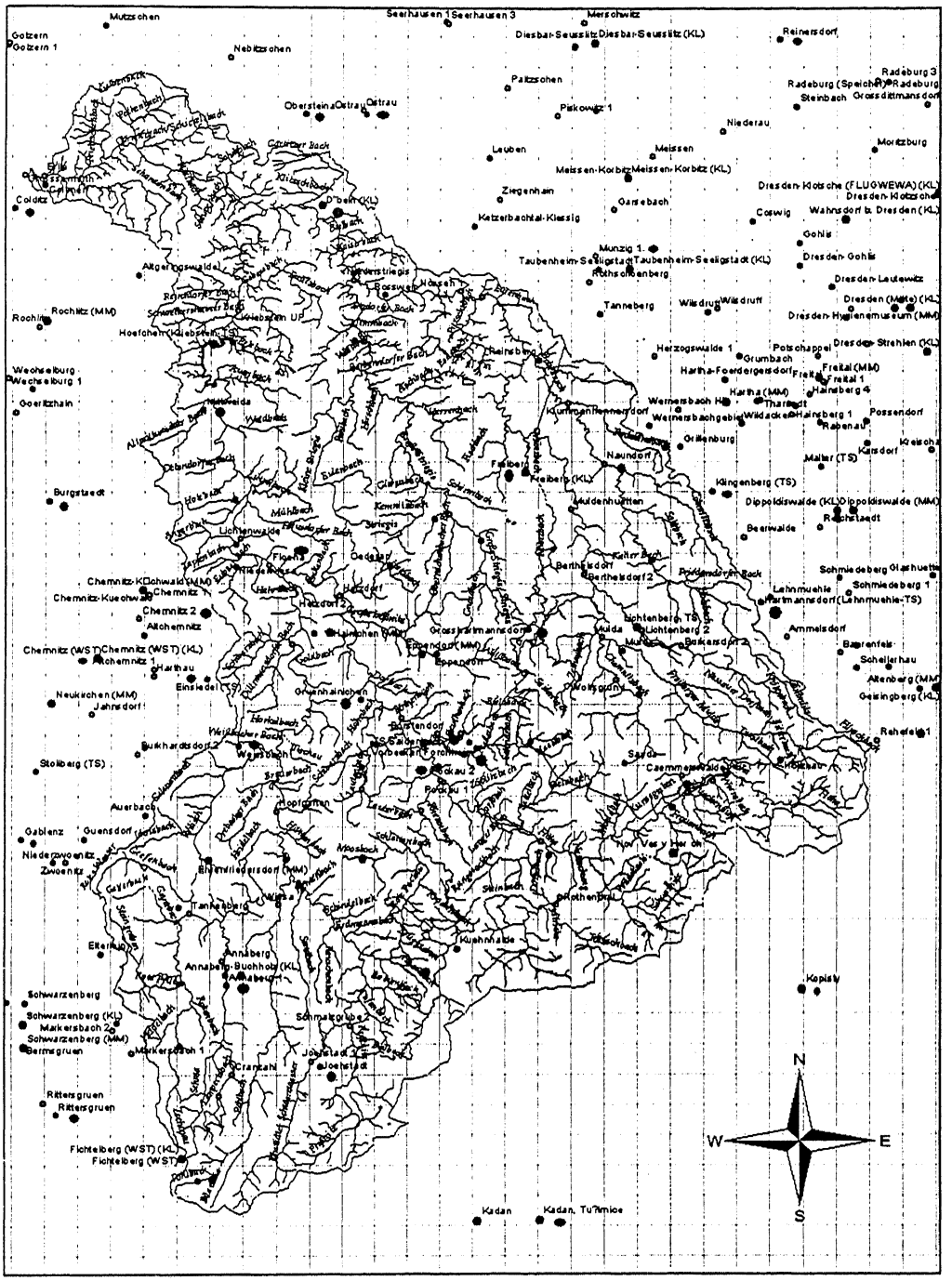

Fig 3.3 Catchment of River Freiberger Mulde

Table 3.1: Statistics of Z(t) [Eq 3.33] for different CPs for Freiberger Mulde Catchment

Freiberger Mulde Catchment				
CP	Frequency [HH] [%]	Probability of Increase [%]	Contribution [A] [%]	Wetness Index [A/HH] [-]
CP01	15.9	60.4	15.2	0.9
CP02	8.4	29.2	3.6	0.4
CP03	3.9	50.6	3.4	0.8
CP04	8.6	73.8	20.7	2.3
CP05	8.0	48.1	8.5	1.0
CP06	6.2	38.4	4.4	0.7
CP07	6.3	68.9	12.7	1.9
CP08	5.5	47.0	5.0	0.9
CP09	14.0	27.8	5.5	0.4
CP10	8.7	46.7	8.8	1.0
CP11	6.9	43.4	3.1	0.4
CP12	9.6	32.0	7.6	0.7
CP99	1.1	38.3	0.8	0.7

The wetness index of a CP is the ratio of the relative contribution of a CP to the increases by the frequency of the CP. The higher this index, the more the increase caused by the CP (wetness index < 1 indicate a dry CP; wetness index = 1 neutral; wetness index > 1 wet CP). According to table 3.1 three CPs, CP04, CP07 and CP01 cause higher increase in discharge than normal having higher probability of increase 73.8%, 68.9%, 60.4% respectively. According to Table 3.1, we can say that CP01 and CP09 are the most frequent CPs. CP09 is having higher frequency but at the same time it is the driest CP with lower increase in the discharge 27.8 % and lowest mean wetness index amount 0.40. The CP04 is an extremely wet CP causing 230% increase compared to a normal day. The CP07 is also considered as a wet CP but less intense than the CP04. The Figures 3.4 & 3.5 show the distribution of the mean (1971-1990) 500 geopotential height anomalies for the all 12

CPs. According to the Fig. 3.5 shows CP09 is characterized by a little negative pressure anomaly north of British Isles and positive pressure anomaly over Eastern Atlantic, which causes a weak air movement and transport of dry air masses from North Atlantic to central Europe (Eastern Germany). The CP04 is a typical wet CP, which has the highest probability of increase (73.8 %), higher contribution 20.7% and higher wetness index 2.3. Figures 3.4 shows, the CP04 is characterized by a typical negative pressure anomaly over the British Isles, which cause the typical west cyclonic transport of wet, ocean air masses from the South Atlantic to the Central Europe (Eastern Germany). The maps of pressure anomaly show that CP04 is the wettest CP and the CP09 is the driest CP among all the CPs.

In order to see the rainfall behavior of the region conditioned on the CPs, the statistics corresponding to all 32 stations used in the Freiberger Mulde catchment were calculated for winter and summer season separately. Table 3.2 and 3.3 show the CP characteristics corresponding to one station Diesbar-Seusslitz for winter and summer season. Other tables showing the CP characteristics corresponding other 31 stations are given in Appendix A. According to Table 3.2 & Table 3.3, both above described CPs, CP04 and CP09 have the same character wet and dry, respectively. In these tables, sum of the precipitation, mean wet day amount (mm), standard deviation (mm) and max precipitation (mm) for a specified CP are also presented. According to the tables, we can say that both the above described CPs have the same character for almost all the stations. Also, in case of other CPs, it holds that wet CPs are wet and dry CPs are dry for almost all the stations simultaneously. Therefore, the maps show that the presented automated classification method produces realistic results.

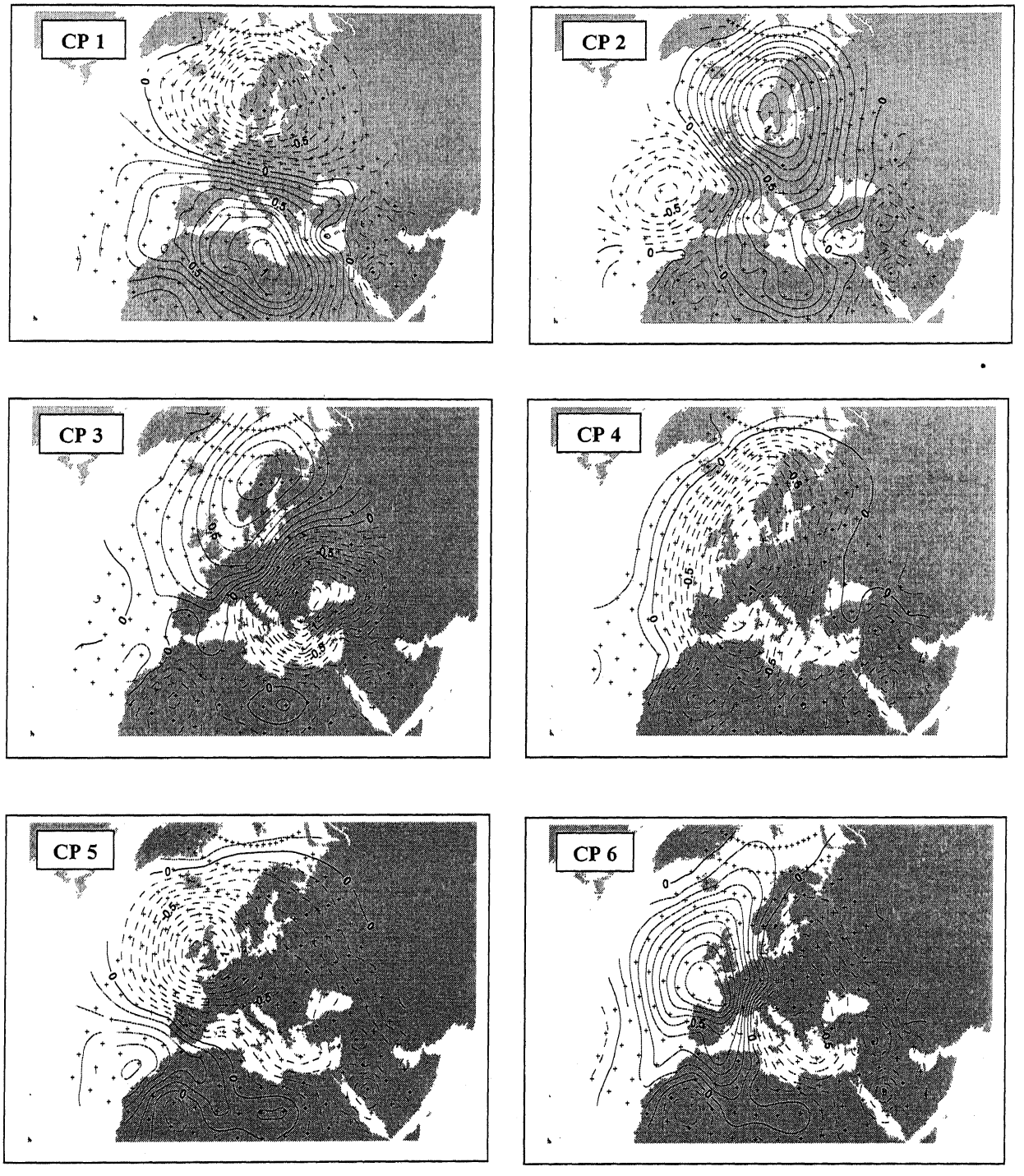

Fig 3.4 Pressure anomaly maps for the period (1971-1990) obtained by optimized Fuzzy rules, CPs 1-6.

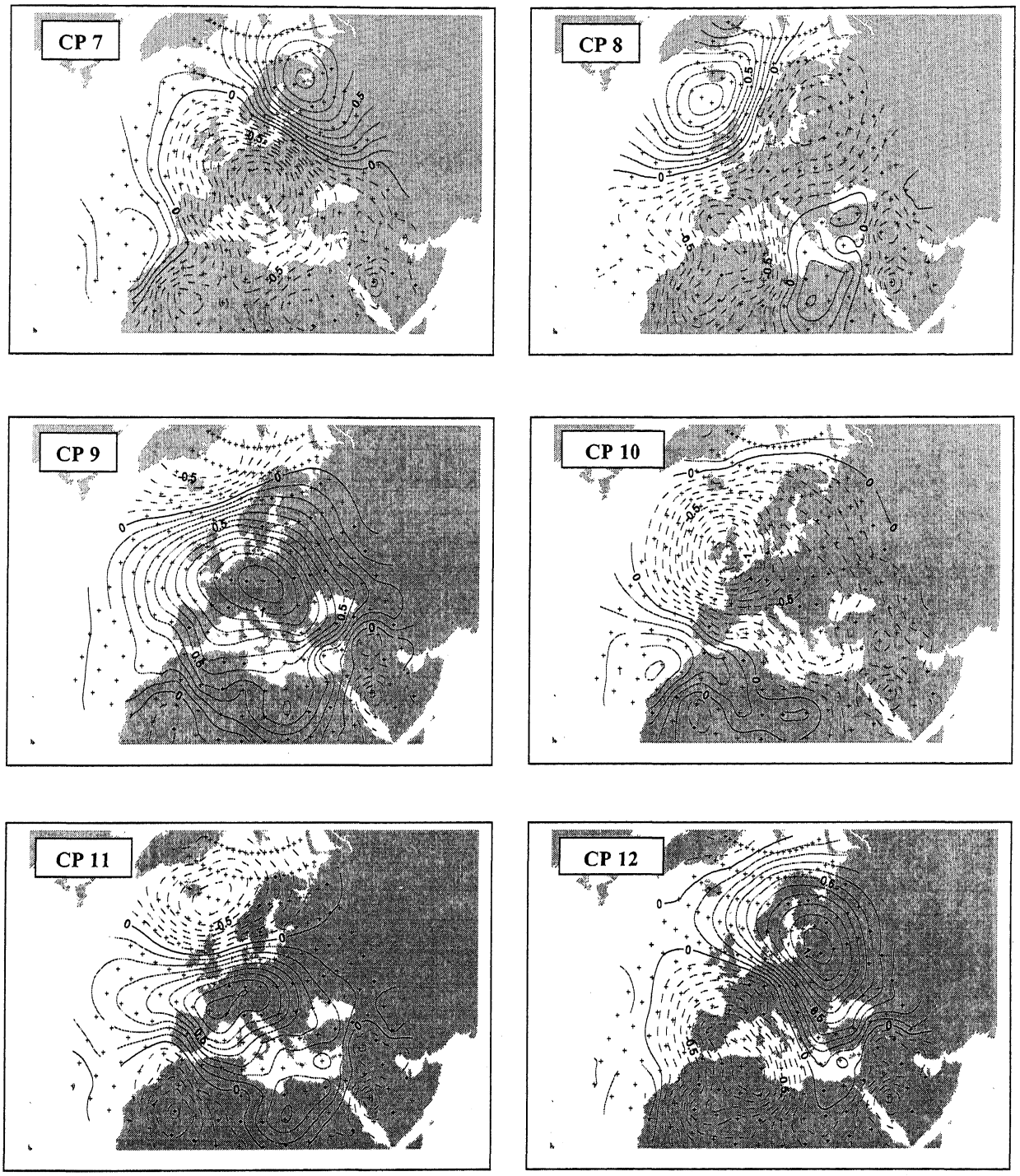

Fig 3.5 Pressure anomaly maps for the period (1971-1990) obtained by optimized Fuzzy rules, CPs 7-12.

Table 3.2 CP and Rainfall Characteristics at Station Diesbar-Seusslitz in Winter

CP	Frequency [HH] (%)	Rainfall Probability (%)	Sum of Precipitation (mm)	Contribution [A] (%)	Wetness Index [A/H]	Mean (mm)	STD* (mm)	Max. (mm)
CP01	16.08	63.98	1330.7	27.67	1.72	3.57	4.56	35.5
CP02	7.50	30.51	141.4	2.94	0.39	1.70	2.35	13.3
CP03	3.48	61.11	144.8	3.01	0.87	1.88	2.51	13.8
CP04	7.59	79.64	758.6	15.78	2.08	3.46	3.85	27.5
CP05	7.37	44.19	259.5	5.40	0.73	2.20	3.35	29.0
CP06	5.79	41.43	124.9	2.60	0.45	1.44	1.96	10.6
CP07	6.23	68.58	641.7	11.35	1.82	4.14	5.64	36.6
CP08	5.13	51.08	218.0	4.53	0.88	2.29	2.38	10.7
CP09	14.90	31.48	267.6	5.57	0.37	1.57	2.07	9.8
CP10	9.13	49.85	472.3	9.82	1.08	2.86	3.38	22.3
CP11	5.85	50.00	159.5	3.32	0.57	1.50	2.02	13.1
CP12	9.66	32.00	242.4	5.04	0.52	2.16	2.60	10.7
CP99	1.30	44.68	47.1	0.98	0.76	2.24	3.33	15.6

*STD = Standard Deviation

Table 3.3 CP and Rainfall Characteristics at Station Diesbar-Seusslitz in Summer

CP	Frequency [HH] (%)	Rainfall Probability (%)	Sum of Precipitation (mm)	Contribution [A] (%)	Wetness Index [A/H]	Mean (mm)	STD (mm)	Max. (mm)
CP01	14.10	58.89	1039.7	16.41	1.16	3.49	4.29	27.7
CP02	9.36	20.54	215.5	3.40	0.36	3.12	4.43	26.2
CP03	3.37	37.19	226.0	3.57	1.06	5.02	10.43	51.8
CP04	9.81	65.34	1206.5	19.05	1.94	5.25	6.78	37.6
CP05	8.19	50.34	611.0	9.65	1.18	4.13	5.38	35.3
CP06	6.55	35.74	321.2	5.07	0.77	3.82	6.51	39.1
CP07	6.47	62.93	793.9	12.45	1.92	5.44	6.33	28.5
CP08	5.32	46.60	367.4	5.80	1.09	4.13	5.23	27.5
CP09	11.76	23.93	352.0	3.56	0.30	3.49	5.66	40.0
CP10	8.22	42.71	482.8	7.62	0.93	3.83	6.76	65.1
CP11	7.27	26.44	143.5	2.27	0.31	2.08	2.59	13.9
CP12	8.64	27.42	528.6	8.34	0.97	6.22	11.06	67.6
CP99	0.92	36.36	46.6	0.74	0.80	3.88	5.44	19.8

3.4.3 Generation of Rainfall Series

Generation of rainfall series has been carried out as a three step process corresponding to the three sub-processes named, Anafour, Korfour and Simfour, in the MSD model. Generation of synthetic series is based on application of these three models in series A-K-S.

Anafour is the model to apply the Fourier series representing the statistic properties conditioned to specific CPs. Rainfall data was given as an input to the model in 1/10 of the rainfall (in mm) for all 32 stations. Another input to this model is daily classified CPs obtained by fuzzy classification. These data are first used to initialize the Fourier series coefficients for the annual cycle of the rainfall model parameters. This model can also analyze the long-term statistics of circulation samples for all the stations. The statistics for station Diesbar-Seusslitz statistics for winter as well as for summer are given in Table 3.4 below. This table represents the wetness index of all optimized CPs. The results of this table are in agreement with the previous results. Therefore, CP04, CP07 and CP01 cause higher increase in probability of rainfall as in case of discharge. The CP04 and CP09 are showing the same characteristics having wetness indices 1.94 and 1.92, respectively. These results verify the statistics of CP and rainfall that was shown in previous section.

The next step in synthetic rainfall generation is the correlation analysis that was carried out using Korfour model. The Korfour calculates the spatial correlation amongst all rainfall stations. The spatial analysis of long-term statistics of circulation samples and rainfall were carried out by this model. Inputs of this model were same as Anafour model but the output of Anafour model was also one of its inputs. In this model, CPs were grouped

corresponding to their characteristics because of less availability of data. CPs with higher wetness index were considered in one group as wet CPs, CPs with lower wetness index were considered in different group as dry CPs, and the remaining CPs were classified into different groups. In presented study eight groups were formed containing CP01, CP04, and CP07 in one group as wet CPs, CP02, CP06, CP09, CP99 in another group as dry CPs and others six CPs were represented as individual group. The output of this model were the spatial correlations for every 30 days. This model also calculated autocorrelation for lag one day. This autocorrelation is independent of CPs but dependent on annual cycle, which was calculated using Anafour model.

The Simfour sub model is developed on the results of the Anafour and Korfour models and simulates daily values of the rainfall continuously and surface covering in connection with circulation samples with space dependent correlation and autocorrelation. Grouping of CPs were the same as in Korfour. Different synthetic series can be generated by this model using different random numbers. In the present study, two different series were developed in 12 CPs case using different random numbers. Generated series was synthetic rainfall values in 1/10 of rainfall (in mm) for the time period for which the CPs were available. In this study CPs were determined for the period of 1899-2002. Therefore synthetic rainfall series was generated for the whole period but the main concern with the period of 1971-1990 for which the observed data were available.

Table 3.4 CPs Statistics with Rainfall Station

Diesbar-Seusslitz				
	Winter		Summer	
CP	Rainfall Probability (%)	Wetness Index	Rainfall Probability (%)	Wetness Index
CP01	63.98	1.72	58.89	1.16
CP02	30.51	0.39	20.54	0.36
CP03	61.11	0.87	37.19	1.06
CP04	79.64	2.08	65.34	1.94
CP05	44.19	0.73	50.34	1.18
CP06	41.43	0.45	35.74	0.77
CP07	68.58	1.82	62.93	1.92
CP08	51.08	0.88	46.60	1.09
CP09	31.48	0.37	23.93	0.30
CP10	49.85	1.08	42.71	0.93
CP11	50.00	0.57	26.44	0.31
CP12	32.00	0.52	27.42	0.97
CP99	44.68	0.76	36.36	0.80

3.5 Results and Discussions

In this section, the results in terms of comparison between observed and simulated daily synthetic rainfall series are presented and discussed. Various criterions like annual rainfall total, mean monthly rainfall, mean values and deviations etc. have been employed comparison of observed and synthetic daily rainfall series for 12 CPs case.

3.5.1 Comparison of Annual Rainfalls

Graphs of annual cycle of rainfall totals for all 32 stations are shown in Figures 3.6, 3.7, 3.8 and 3.9. Because of the statistical character of the modeling, the synthetic annual rainfall often differs from the observed ones and correlations at each site are not too high. Table 3.5 represents the mean and standard deviation of annual rainfall totals. The results are very good in mean and variance point of view, especially for some stations like serial no. 1, 6, 9, 11, 17, 21, 23, 24 and 29. Some stations like no. 4 and 32 showing differences in their mean but deviation is in fair agreement. For some stations e.g. 9, 10 and 15 show that the mean is in good agreement but standard deviation is little bit underestimated. Results are good in terms of coefficient of variation (CV) that are presented in Table 3.6. Coefficient of variation of synthetic annual rainfall for the stations no. 8, 16, 21, 28, 29 and 31 in very good agreement with those from the observed series but for the stations 9- 14, 17, 19, 20, 24, 26 and 27 these appears to be some variation. The remaining stations like 1-7, 15, 18, 22, 23, 25 and 32 are in fair agreement with observed series.

3.5.2 Comparison of Monthly Mean Rainfall

Comparison between mean monthly rainfall between observed and synthetic series has been carried out for all 32 stations. Figures 3.10, 3.11, 3.12 and 3.13 show the comparison graphically. These Figures suggest that these is very good agreement between historical and synthetic monthly average values. Especially, stations e.g. 1, 8, 13, 19 and 30 which have high rainfall in summer show very good agreement. In some cases, the synthetic rainfall totals for December and January are little bit underestimated

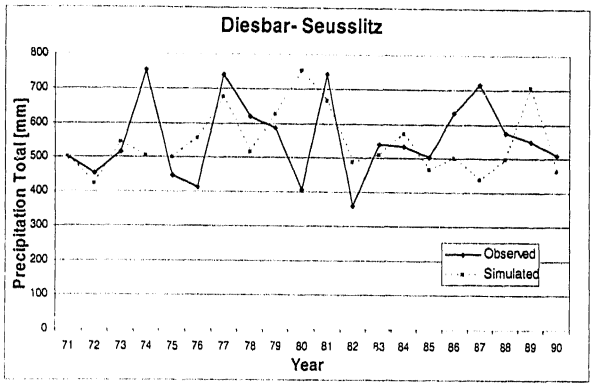

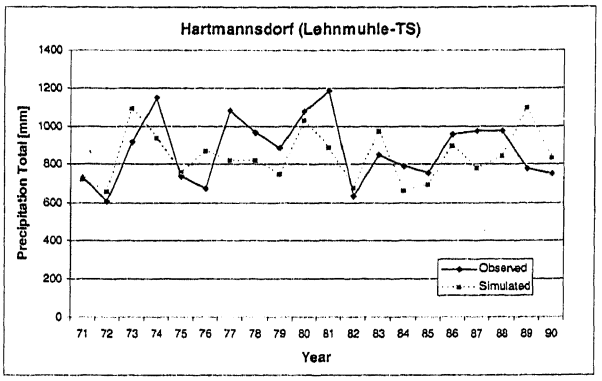

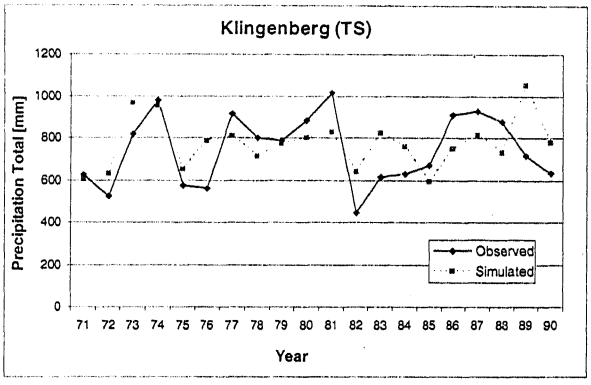

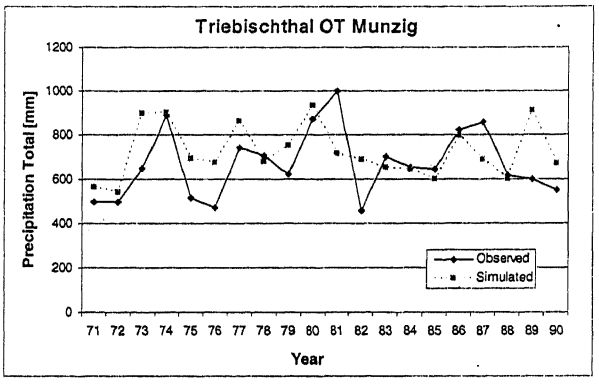

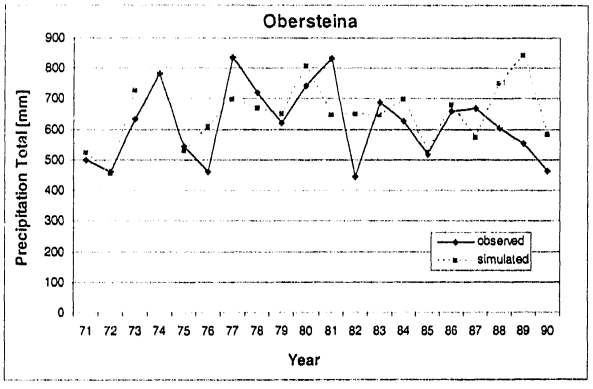

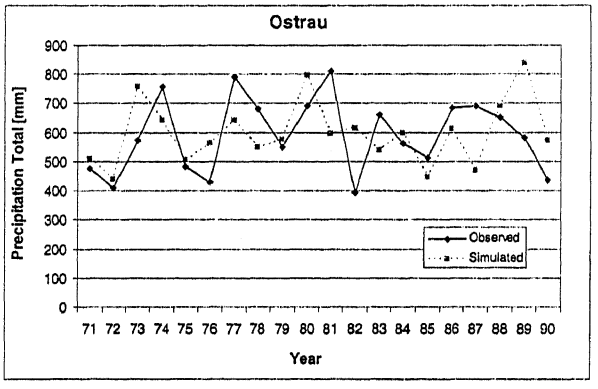

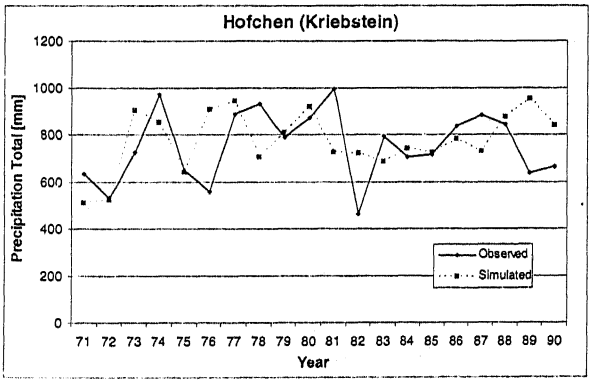

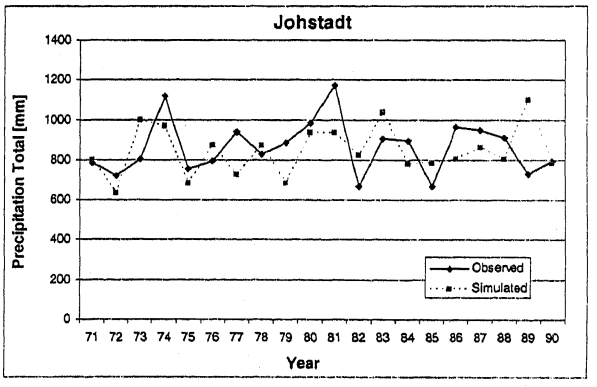

Fig 3.6 Annual Rainfall Totals for Observed and Synthetic Series, Stations 1-8

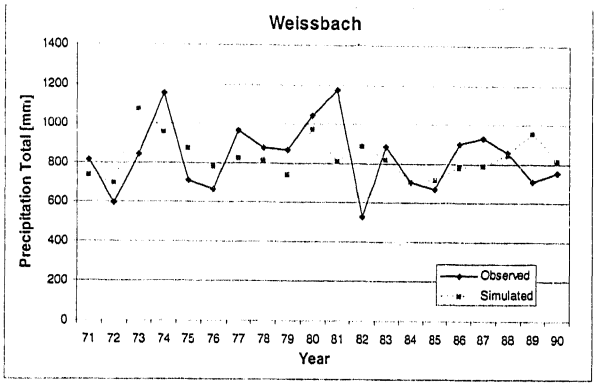

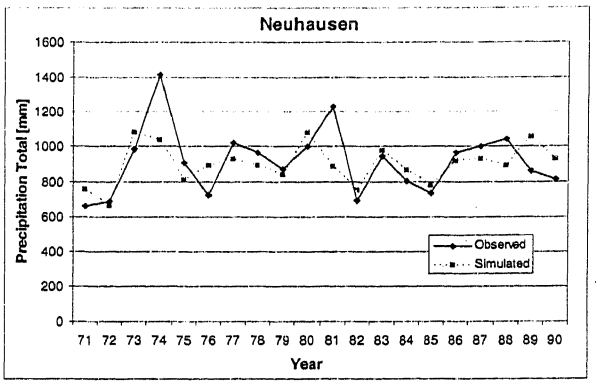

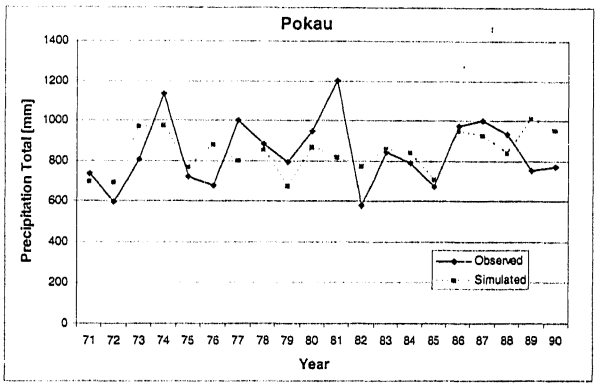

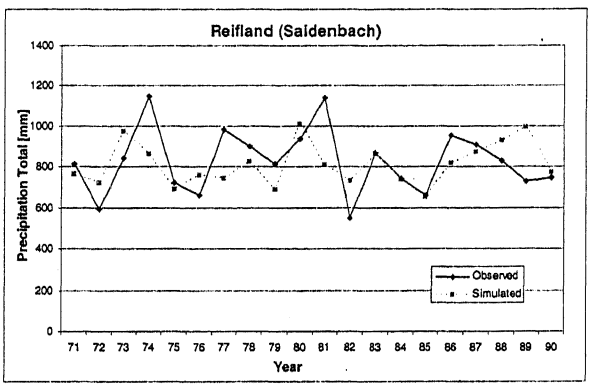

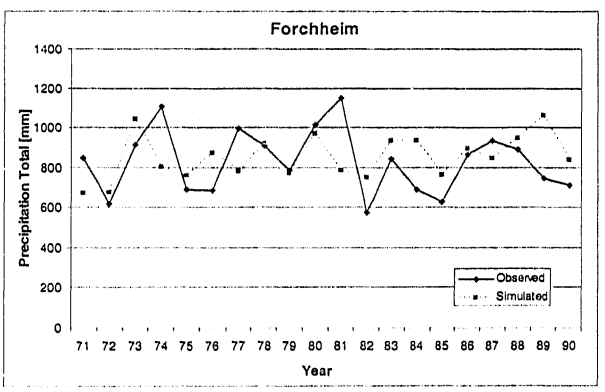

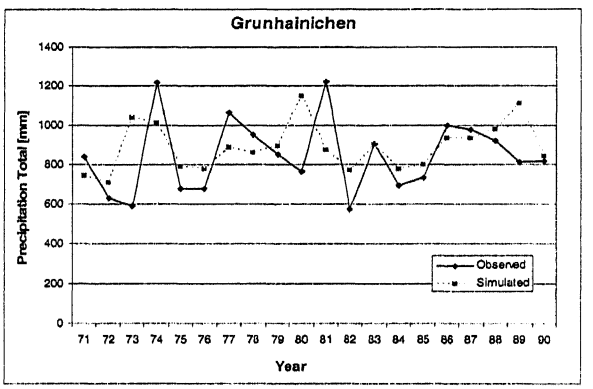

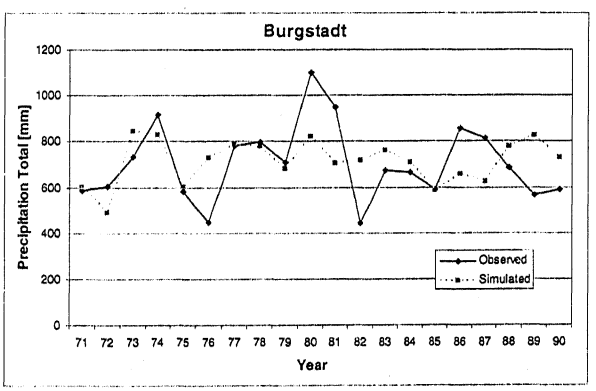

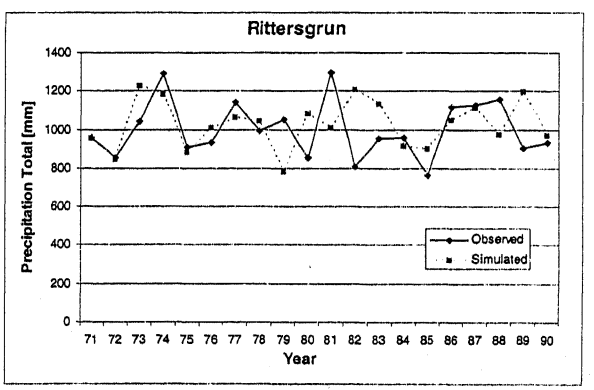

Fig 3.7 Annual Rainfall Totals for Observed and Synthetic Series, Stations 9-16

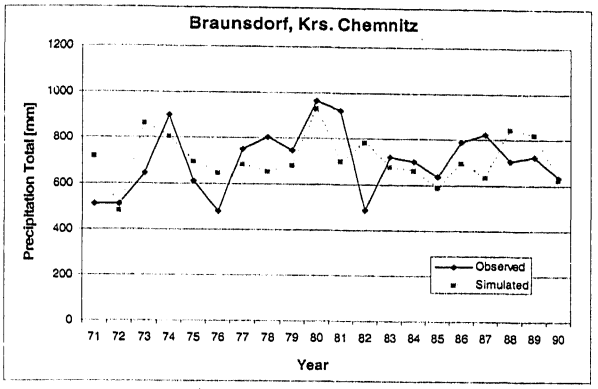

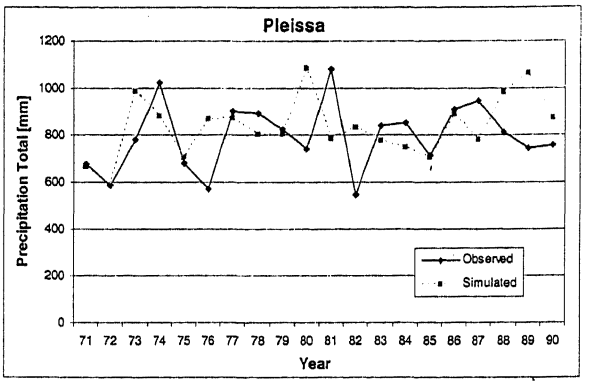

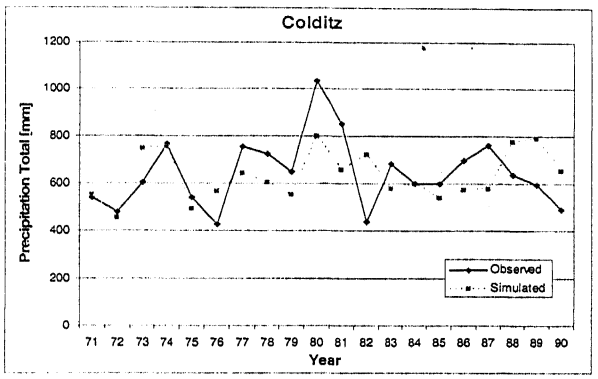

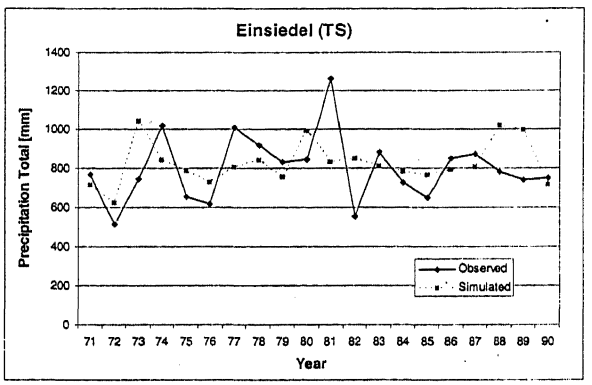

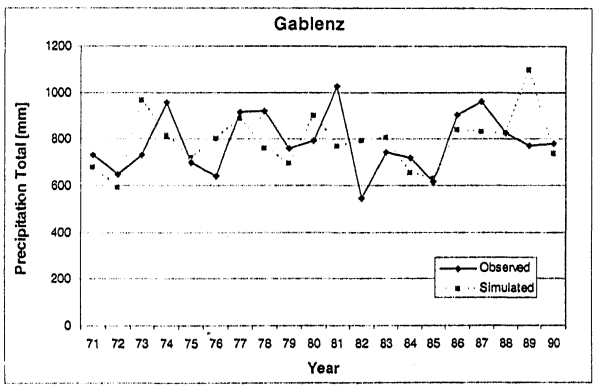

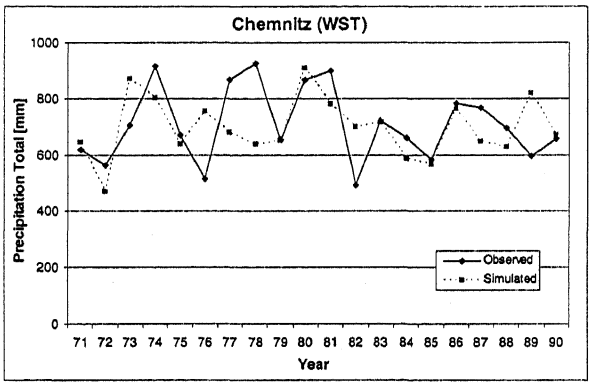

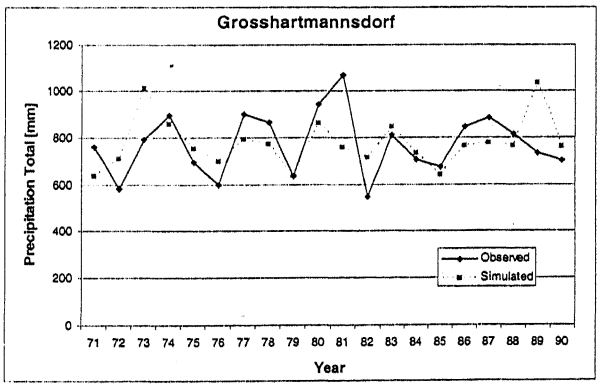

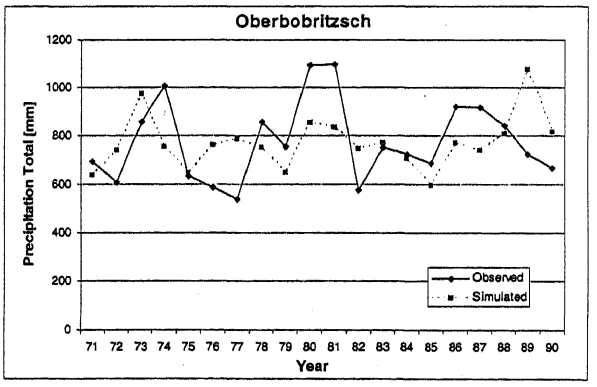

Fig 3.8 Annual Rainfall Totals for Observed and Synthetic Series, Stations 17-24

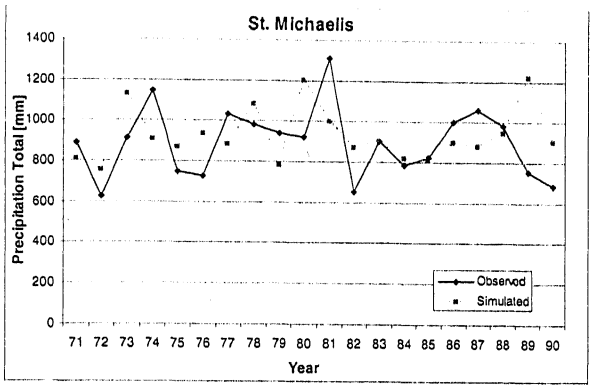

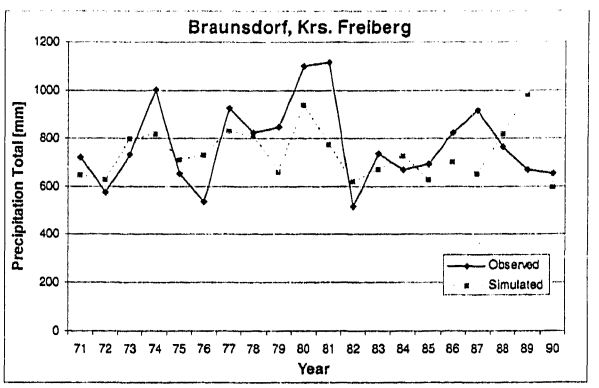

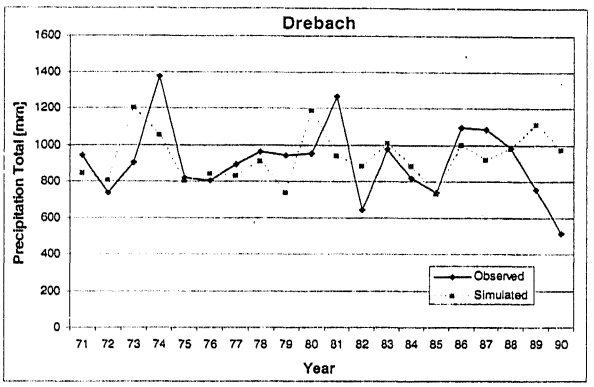

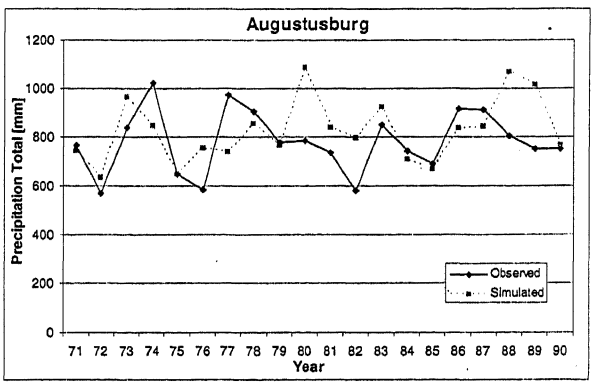

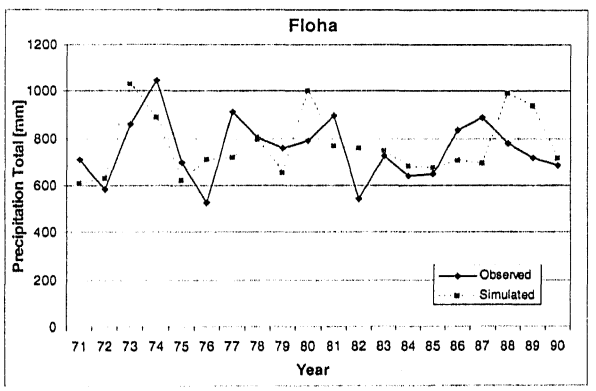

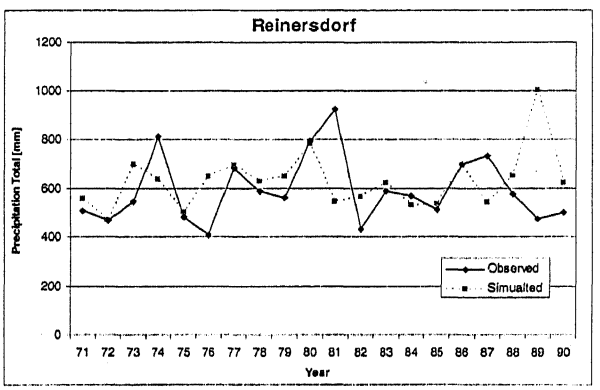

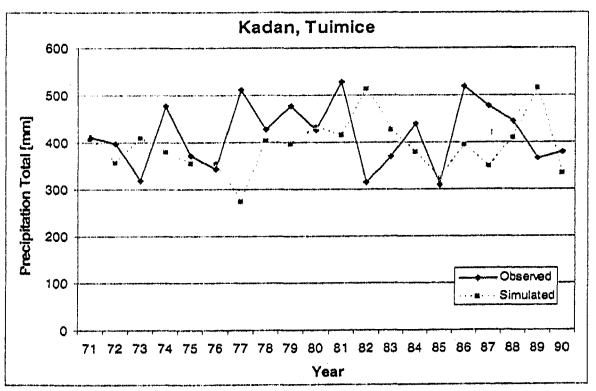

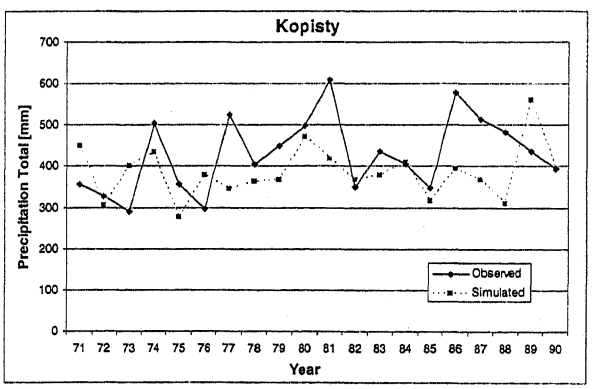

Fig 3.9 Annual Rainfall Totals for Observed and Synthetic Series, Stations 25-32

Table 3.5 Statistics of Observed and Synthetic Annual Totals 1971-1990, 32 Stations in Catchment

Serial No.	Station Name	Mean		Standard Deviation	
		Observed	Synthetic	Observed	Synthetic
1	Diesbar-Seusslitz	554	554	116	93
2	Hartmannsdorf (Lehnmuhle-TS)	874	839	170	135
3	Klingenberg (TS)	745	772	166	120
4	Triebischthal OT Munzig	667	723	155	120
5	Obersteina	618	651	124	101
6	Ostrau	591	598	129	109
7	Hofchen (Kriebstein-TS)	754	774	149	128
8	Johstadt	864	844	135	122
9	Weissbach	832	828	171	98
10	Neuhausen	916	897	187	113
11	Pockau	840	841	167	102
12	Reifland (Saidenbach-TS)	827	811	156	102
13	Forchheim	829	852	162	110
14	Grunhainichen	845	888	187	121
15	Burgstadt	704	713	167	95
16	Rittersgrun	1002	1026	148	126
17	Braunnsdorf, Krs. Chemnitz	703	707	143	105
18	Pleissa	794	835	144	128
19	Colditz	643	630	147	102
20	Einsiedel (TS)	799	824	173	110
21	Gablenz	785	790	128	118
22	Chemnitz (WST)	708	696	133	107
23	Grosshartmannsdorf	772	775	133	106
24	Oberbobritzsch	777	770	166	111
25	St. Michaelis	895	931	173	133
26	Braunsdorf, Krs. Freiberg	774	736	170	106
27	Drebach	910	936	200	133
28	Augustusburg	780	825	127	130
29	Floha	752	765	132	132
30	Reinersdorf	591	627	138	117
31	Kadan, Tuimice	415	391	68	57
32	Kopisty	428	385	91	64

Table 3.6 Coefficient of Variation for Annual Rainfall Total (12CPs), 32 Stations

Serial No.	Stations	Coefficient of variation	
		Observed	Simulated
1	Diesbar-Seusslitz	0.21	0.17
2	Hartmannsdorf (Lehnmuhle-TS)	0.19	0.16
3	Klingenberg (TS)	0.22	0.15
4	Triebischthal OT Munzig	0.23	0.16
5	Obersteina	0.20	0.15
6	Ostrau	0.22	0.18
7	Hofchen (Kriebstein-TS)	0.19	0.16
8	Johstadt	0.15	0.14
9	Weissbach	0.20	0.12
10	Neuhausen	0.20	0.13
11	Pockau	0.19	0.12
12	Reifland (Saidenbach-TS)	0.19	0.13
13	Forchheim	0.19	0.13
14	Grunhainichen	0.22	0.14
15	Burgstadt	0.23	0.13
16	Rittersgrun	0.14	0.12
17	Braunnsdorf, Krs. Chemnitz	0.20	0.15
18	Pleissa	0.18	0.15
19	Colditz	0.22	0.16
20	Einsiedel (TS)	0.21	0.13
21	Gablenz	0.16	0.15
22	Chemnitz (WST)	0.18	0.15
23	Grosshartmannsdorf	0.17	0.14
24	Oberbobritzsch	0.21	0.14
25	St. Michaelis	0.19	0.14
26	Braunsdorf, Krs. Freiberg	0.22	0.14
27	Drebach	0.22	0.14
28	Augustusburg	0.16	0.16
29	Floha	0.17	0.17
30	Reinersdorf	0.23	0.19
31	Kadan, Tuimice	0.16	0.14
32	Kopisty	0.21	0.16

e.g. for stations 9, 11, 16, 26, 27 and 32. The correlations at each station are reported in table 3.7. They are generally higher for the stations with pronounced cycle (having more variation in rainfall) for example, stations 1, 13, 19, 30 and 31. They are generally showing lower values for stations having more smooth cycle (having less variation in rainfall) like 6 and 18. Correlation coefficient is lower for the stations 6, 9, 14, 18, 20, 21, 23, 24, 28 and 29 having an average values 0.7. However, the correlation coefficient results also suggest that the synthetic rainfall generated in this study represents the observed rainfall in statistical sense.

3.5.3 Comparison of Cumulative Distribution Functions (CDFs)

Figures 3.14, 3.15, 3.16 and 3.17 shows the CDF for all 32 stations. The CDFs from synthetics rainfall from only very few stations are in good agreement with those from the observed ones e.g. 3, 4, 7, 11, 18 and 21. For other stations, CDF for synthetic rainfall series are over estimated like 8, 9, 16, 19, 22, 25, 27, 29, 31 and 32. For some other stations like 2, 5, 10, 12, 13, 14, 15, 17, 20, 23, 24, 26, 28, 30 the CDFs are underestimated at some part and overestimated in the other part. However, the departures between cumulative probabilities from synthetic and observed rainfalls are small in both under and over estimation. This indicates that the uncertainty information in the historically observed rainfall is characterized well by those in the synthetic rainfalls generated in this study.

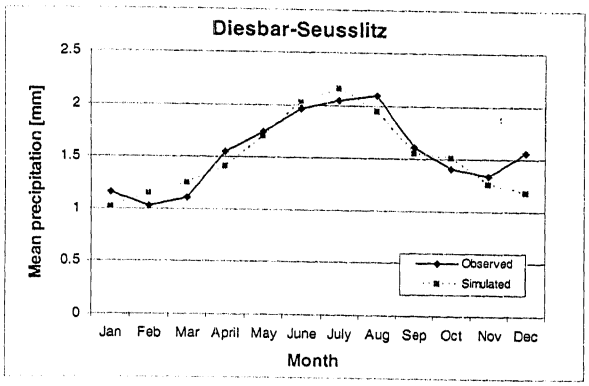

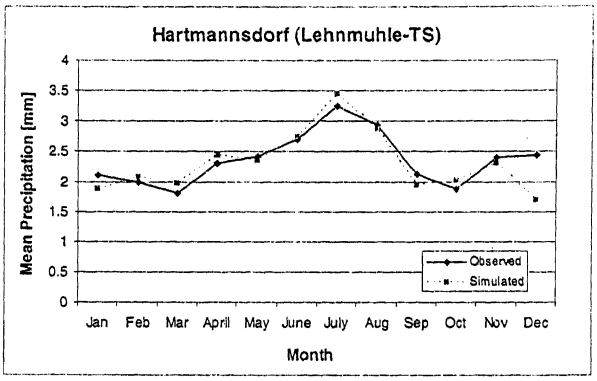

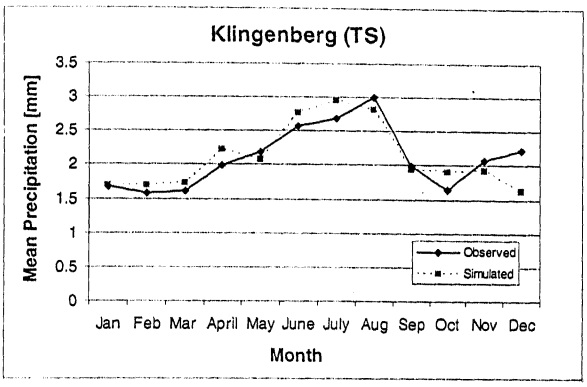

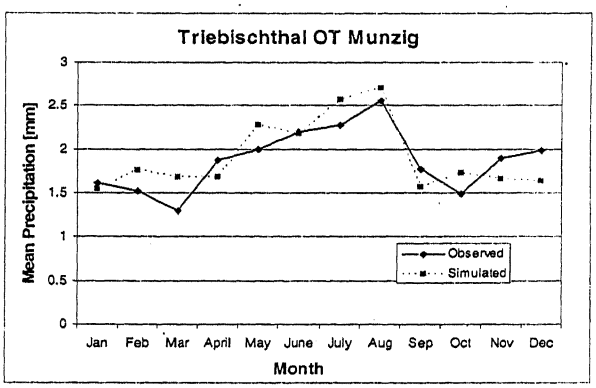

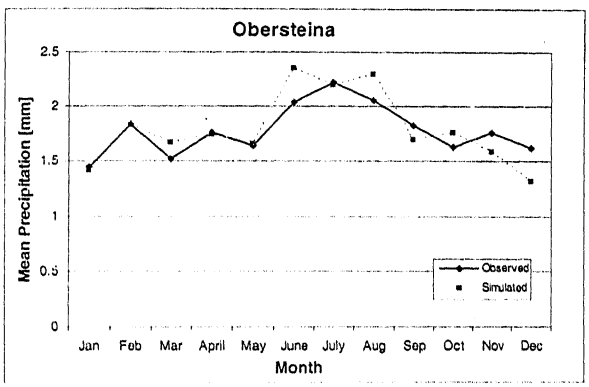

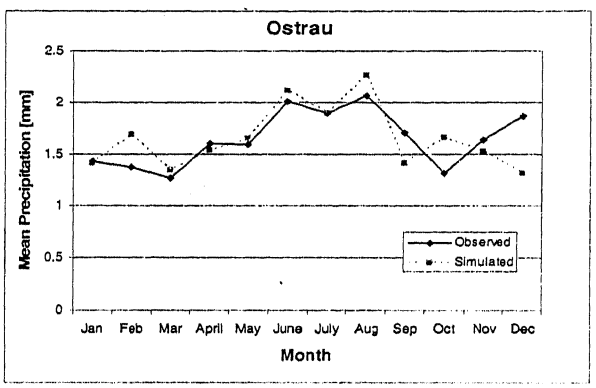

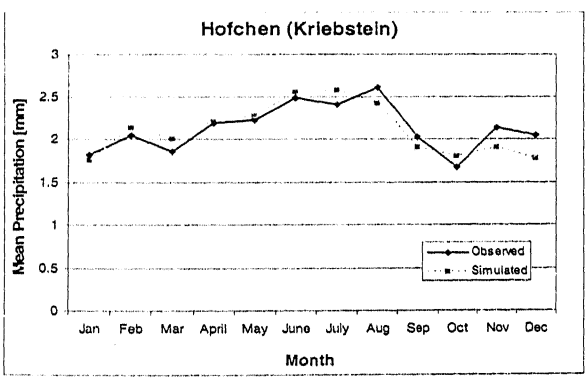

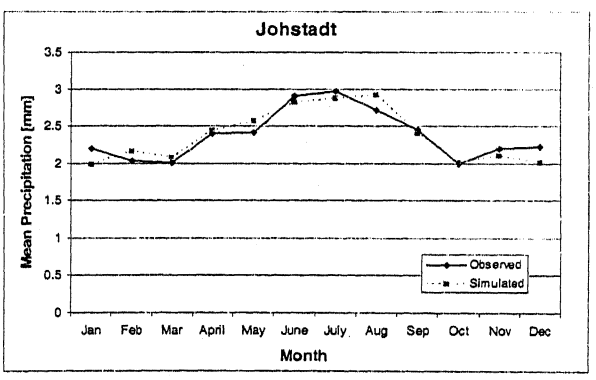

Fig 3.10 Mean Monthly Rainfall for Observed and Synthetic Series at Stations 1-8

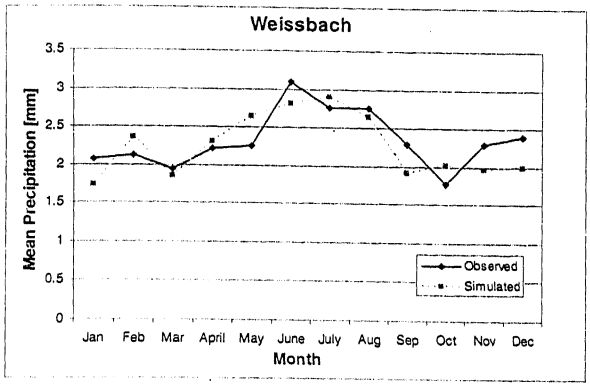

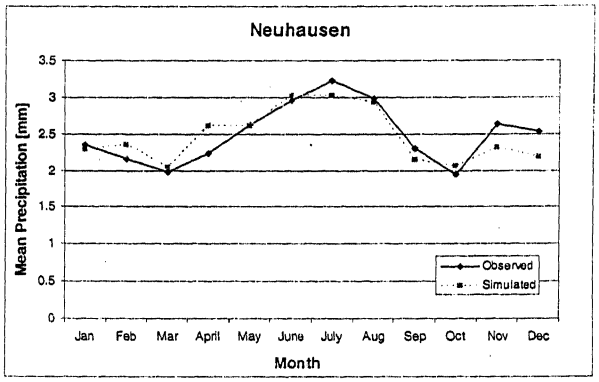

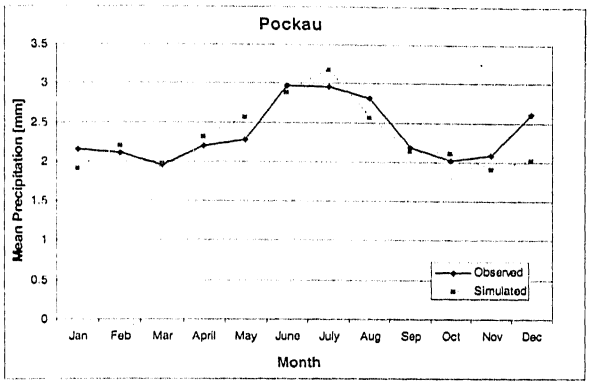

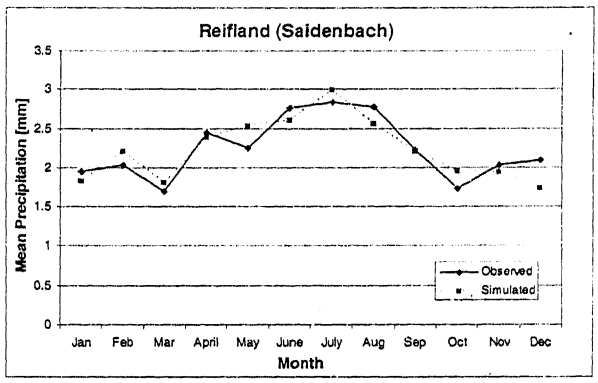

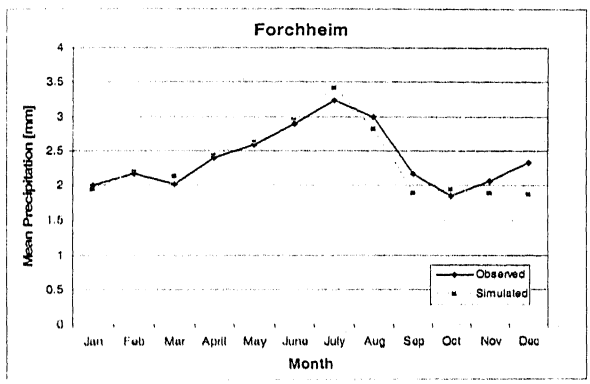

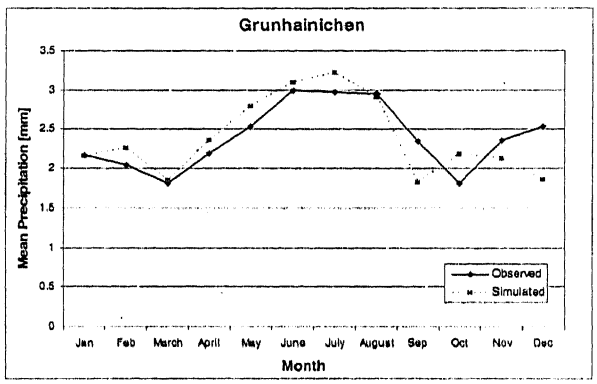

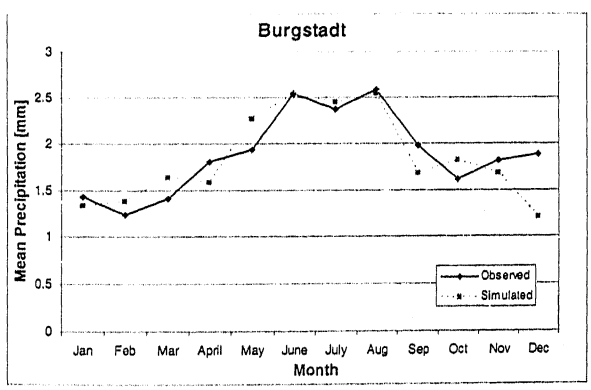

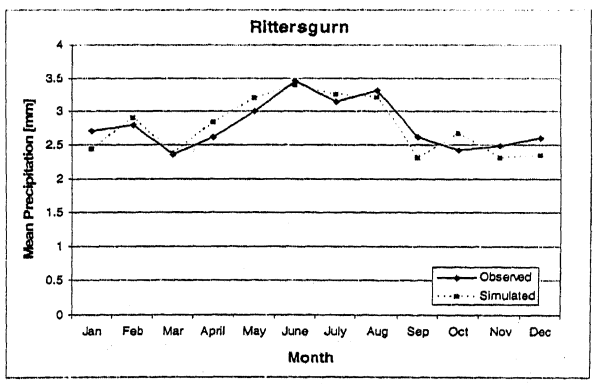

Fig 3.11 Mean Monthly Rainfall for Observed and Synthetic Series at Stations 9-16

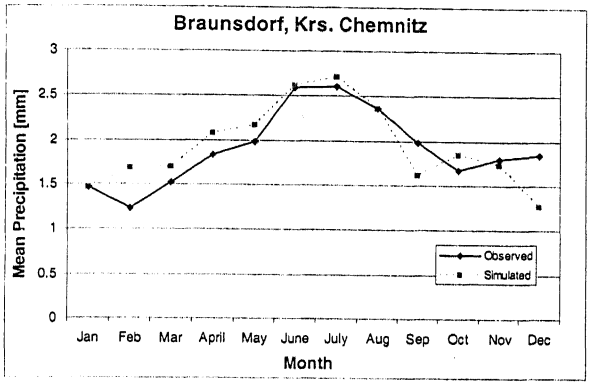

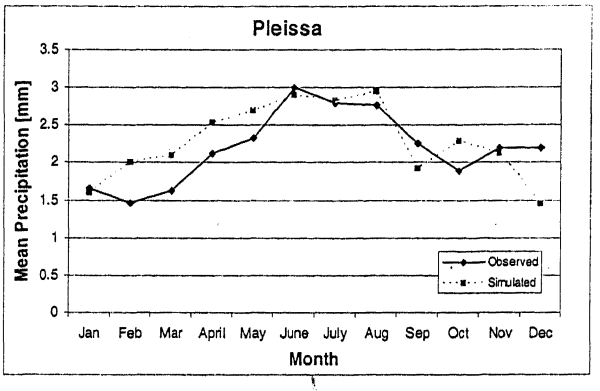

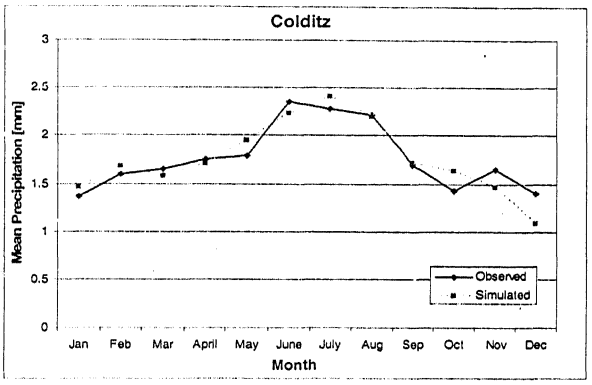

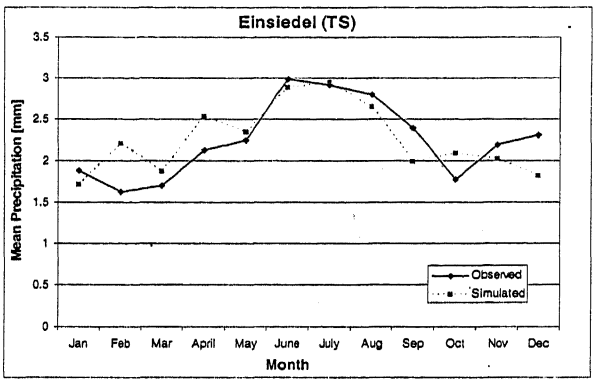

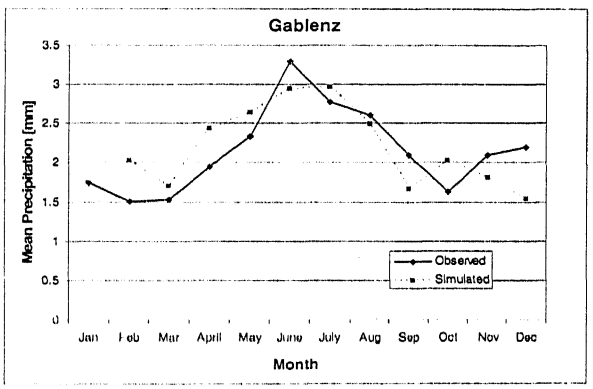

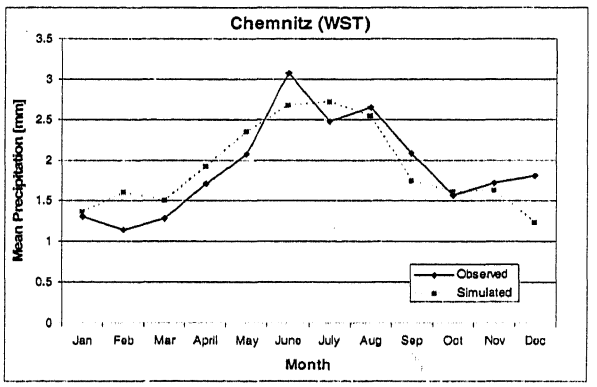

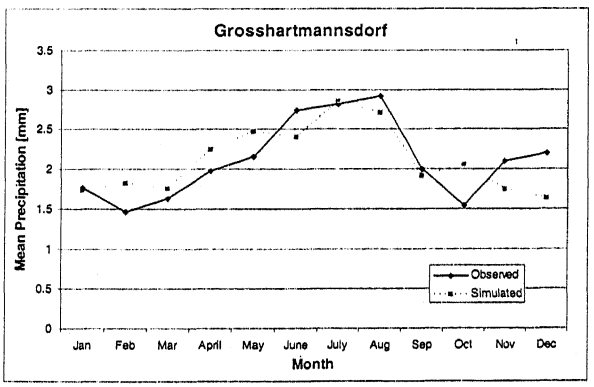

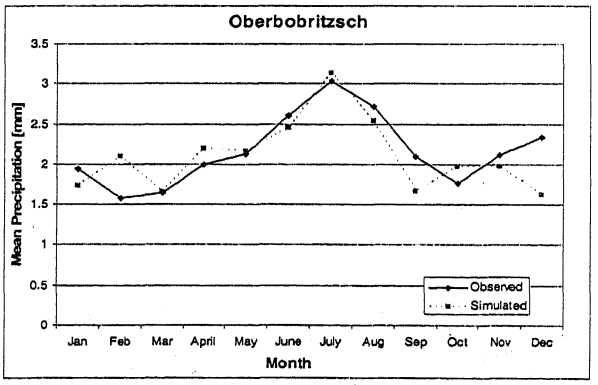

Fig 3.12 Mean Monthly Rainfall for Observed and Synthetic Series at Stations 17-24

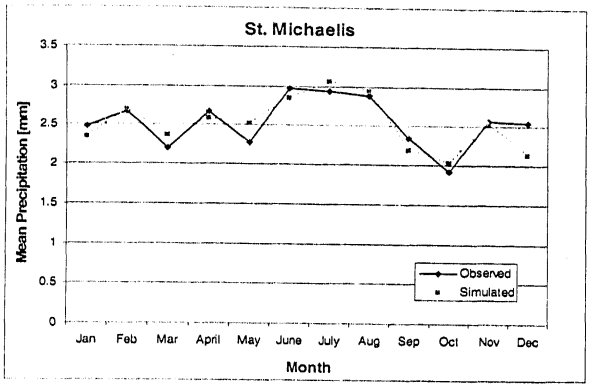

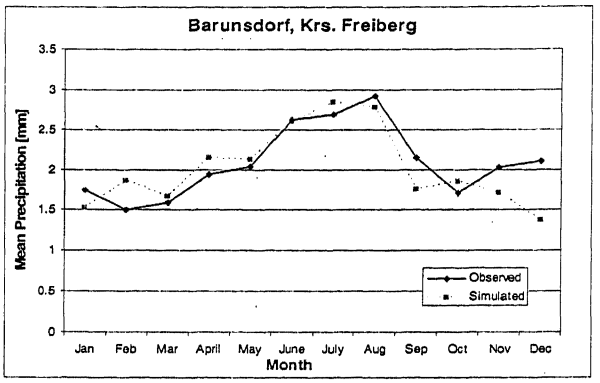

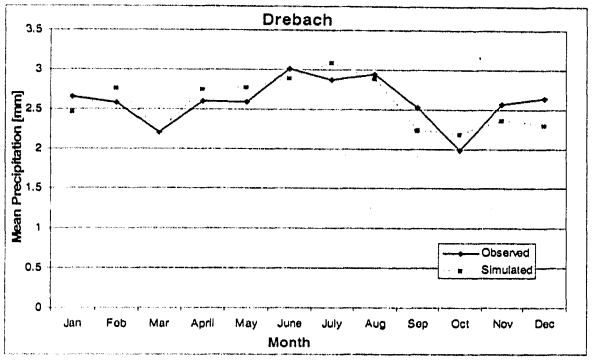

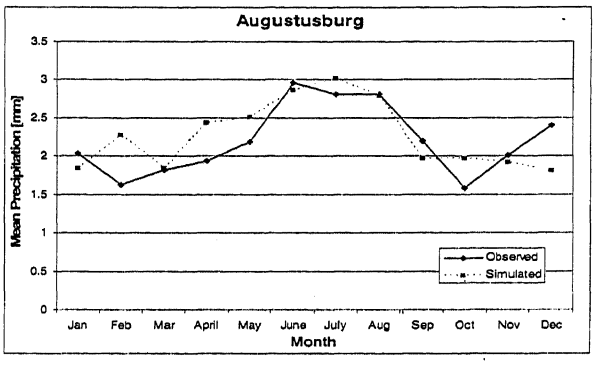

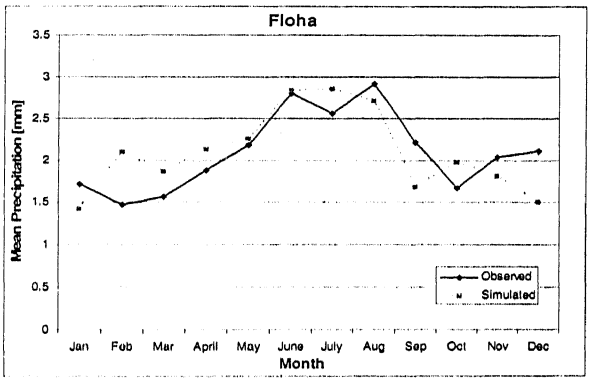

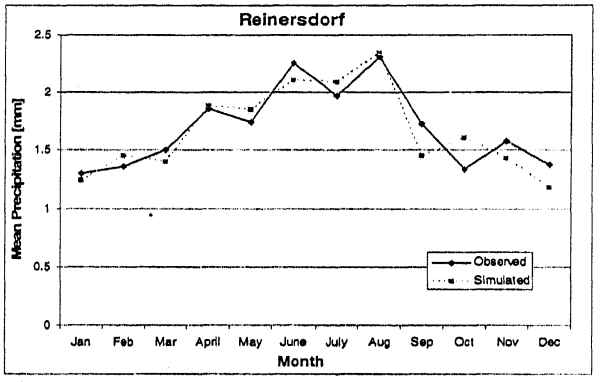

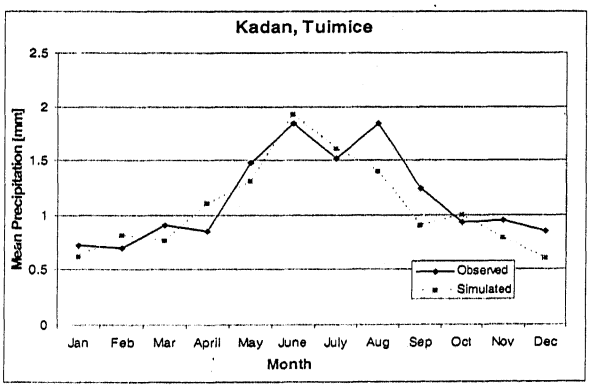

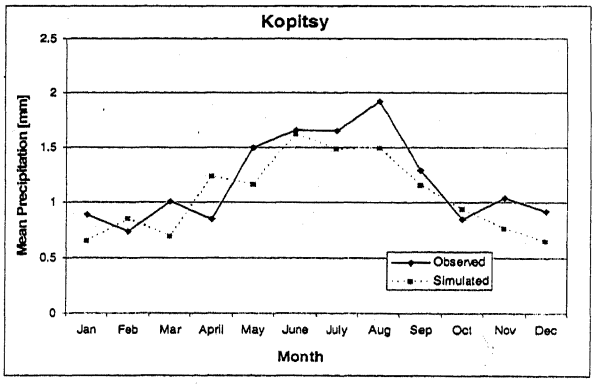

Fig 3.13 Mean Monthly Rainfall for Observed and Synthetic Series at Stations 25-32

Table 3.7: Correlation between Observed and Synthetic Mean Monthly Rainfall

Serial No.	Station	Correlation (r)
1	Diesbar-Seusslitz	0.91
2	Hartmannsdorf (LehnmühleTS)	0.85
3	Klingenberg (TS)	0.86
4	Triebischthal OT Munzig	0.79
5	Obersteina	0.86
6	Ostrau	0.62
7	Höfchen (Kriebstein-TS)	0.86
8	Jöhstadt	0.92
9	Weissbach	0.74
10	Neuhausen	0.86
11	Pockau	0.81
12	Reifland (Saidenbach-TS)	0.87
13	Forchheim	0.93
14	Grünhainichen	0.76
15	Burgstädt	0.83
16	Rittersgrün	0.87
17	Bräunsdorf, Krs. Chemnitz	0.80
18	Pleissa	0.71
19	Colditz	0.92
20	Einsiedel (TS)	0.75
21	Gablenz	0.73
22	Chemnitz (WST)	0.85
23	Grosshartmannsdorf	0.75
24	Oberbobritzsch	0.74
25	St. Michaelis	0.84
26	Bräunsdorf, Krs. Freiberg	0.79
27	Drebach	0.77
28	Augustusburg	0.70
29	Flöha	0.69
30	Reinersdorf	0.91
31	Kadan, Tuimice	0.88
32	Kopisty	0.81

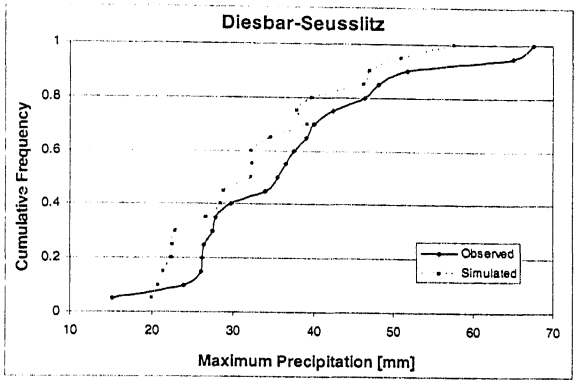

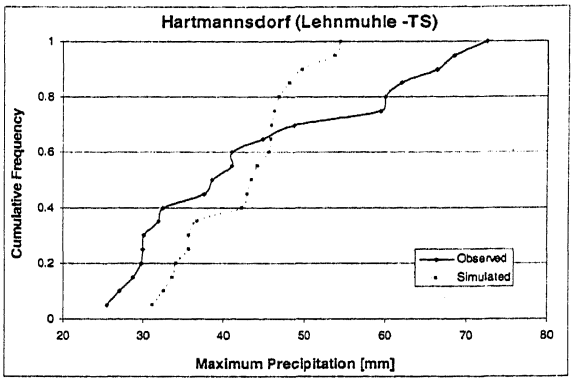

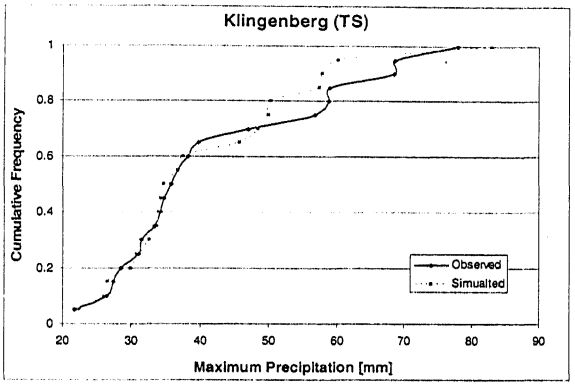

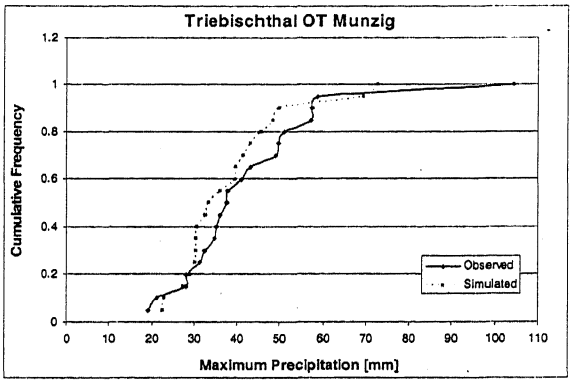

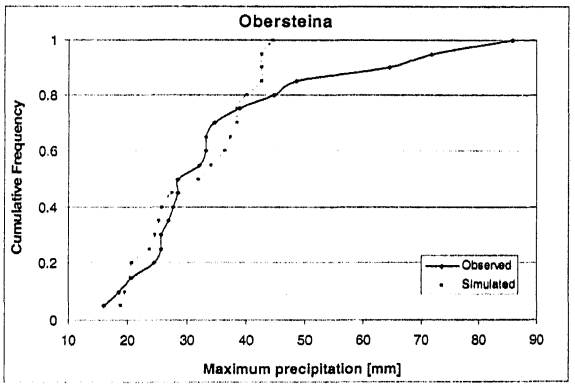

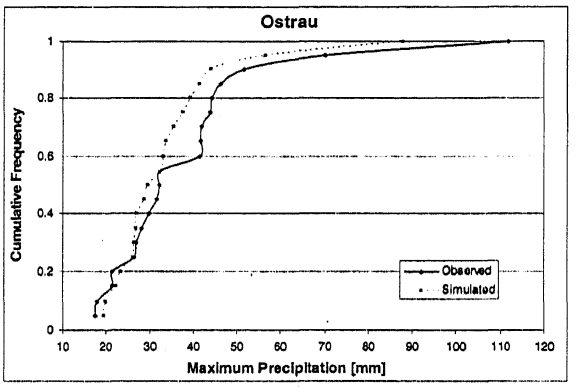

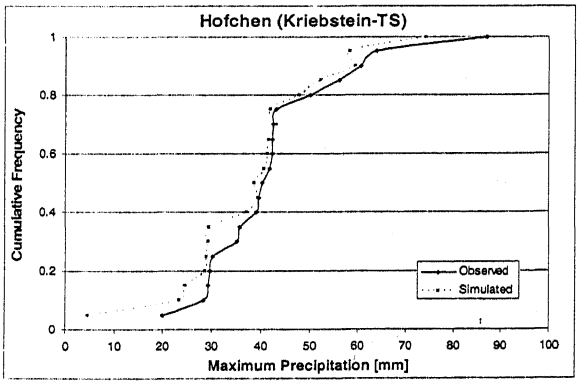

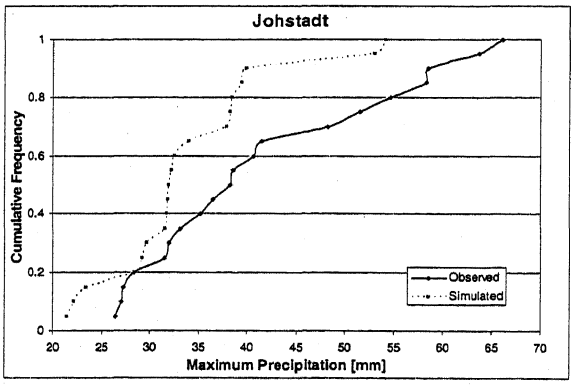

Fig 3.14 Cumulative Distribution Function for Observed and Synthetic series at stations 1-8 (1971-90)

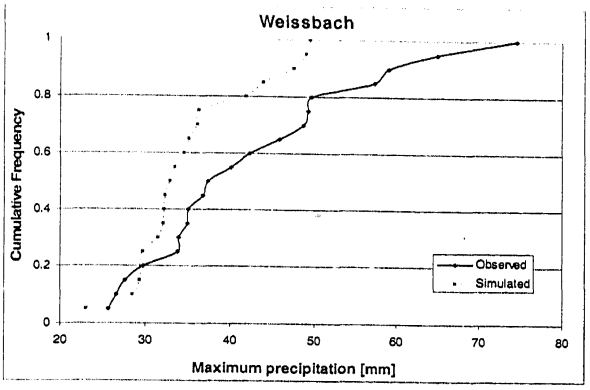

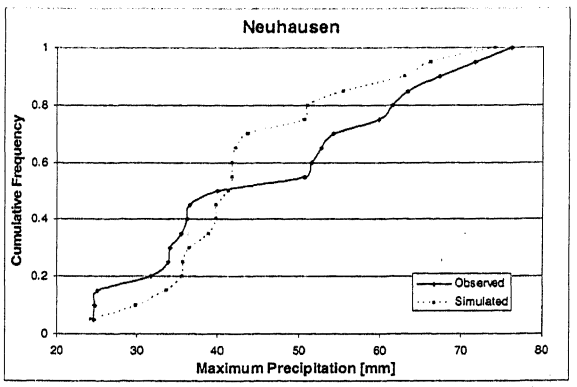

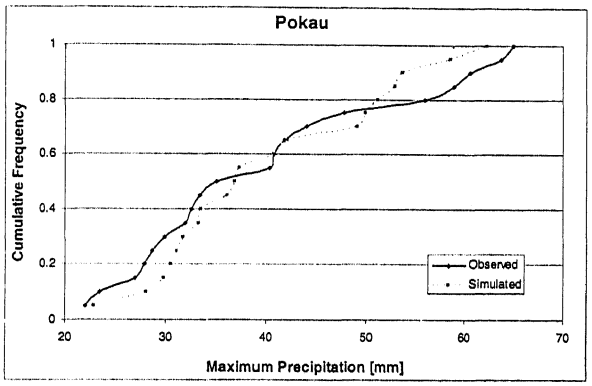

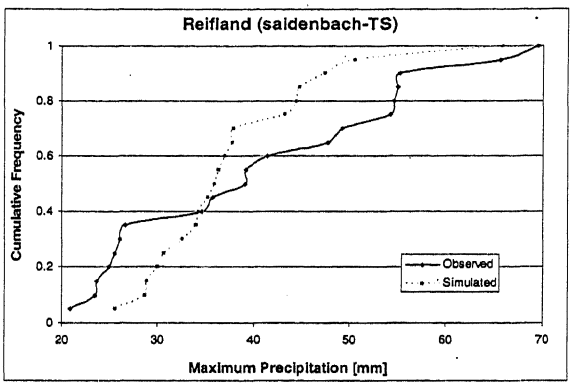

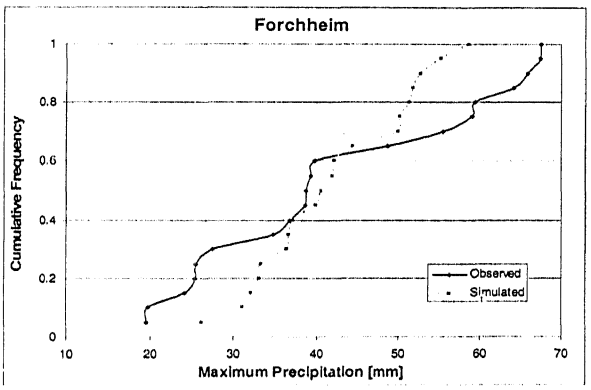

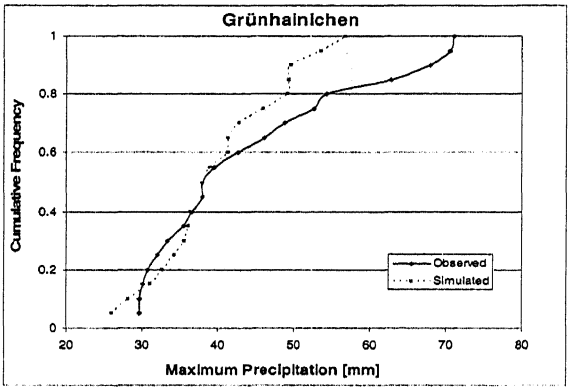

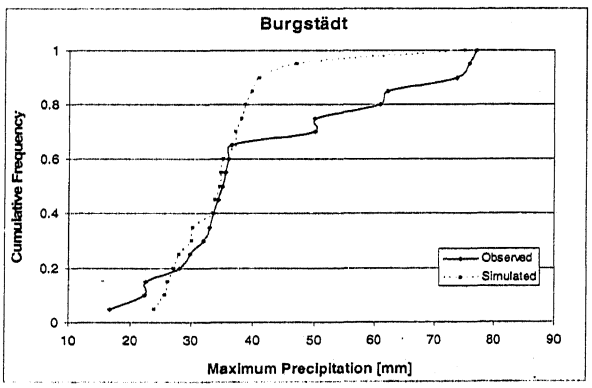

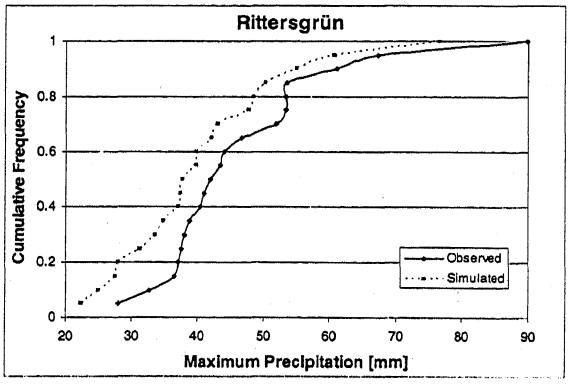

Fig 3.15 Cumulative Distribution Function for Observed and Synthetic Series at stations 9- 16 (1971-90)

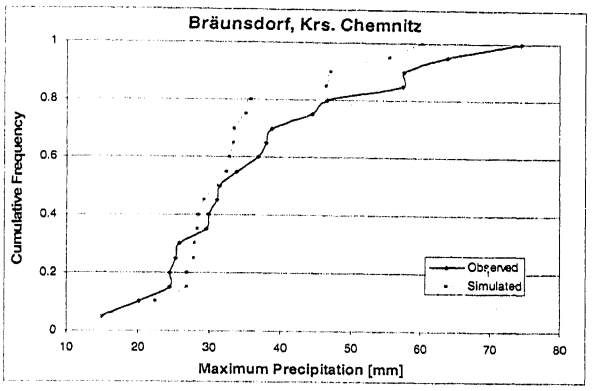

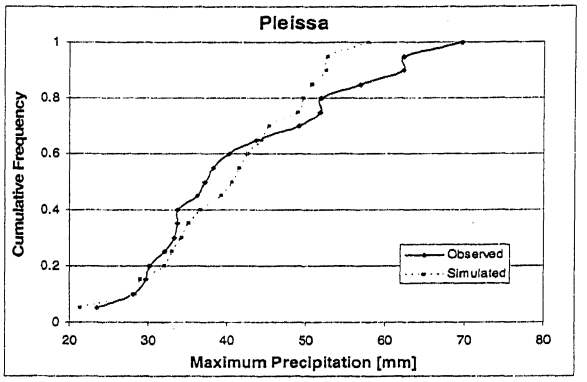

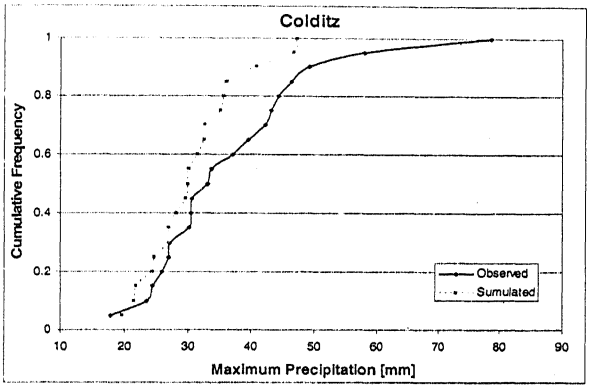

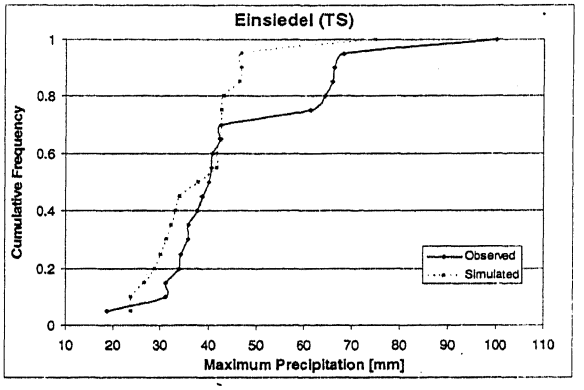

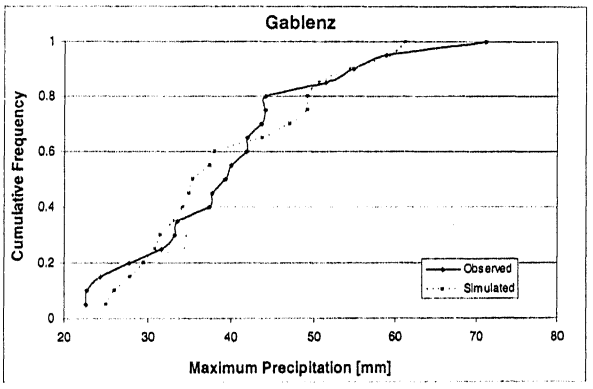

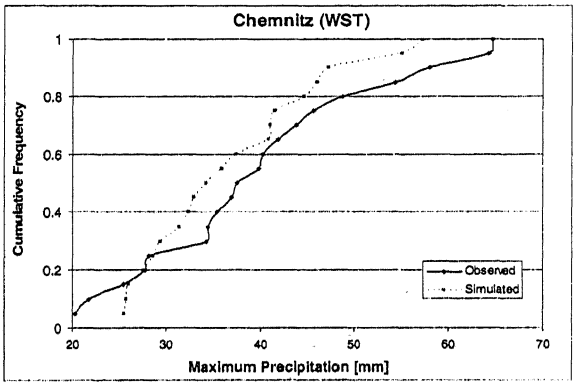

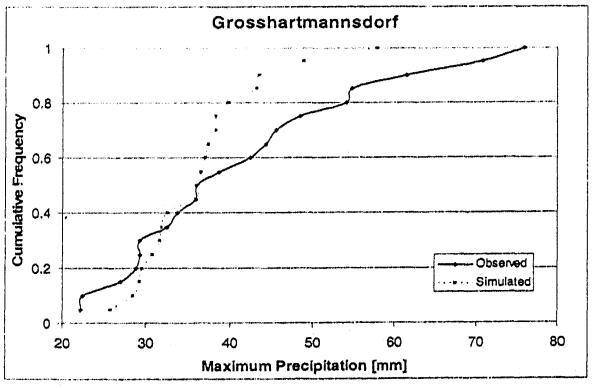

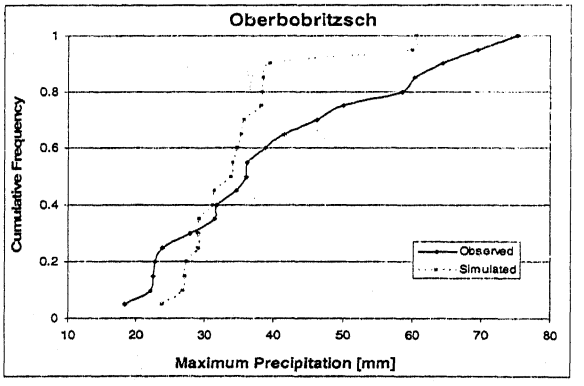

Fig 3.16 Cumulative Distribution Function for Observed and Synthetic Series, stations 17 -24 (1971-90)

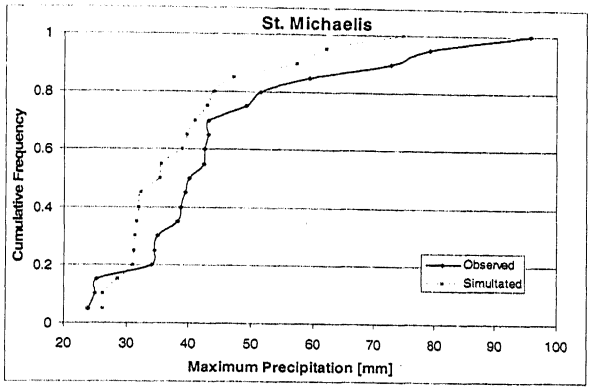

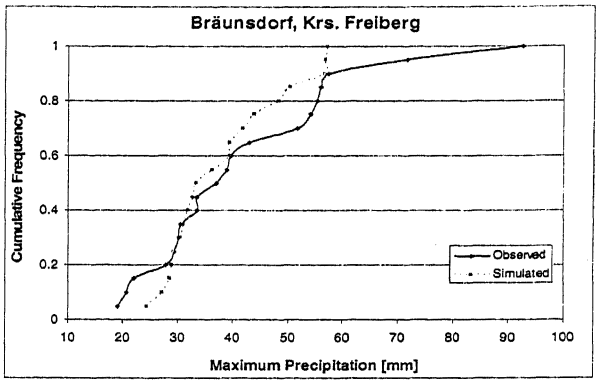

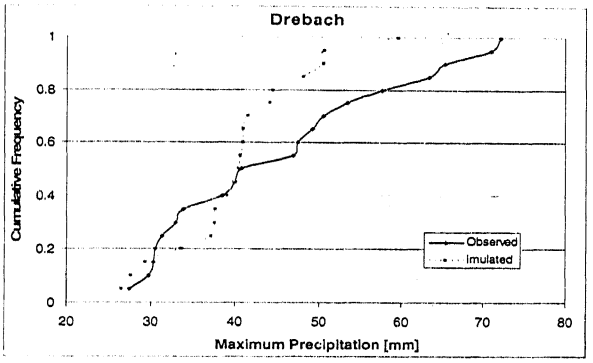

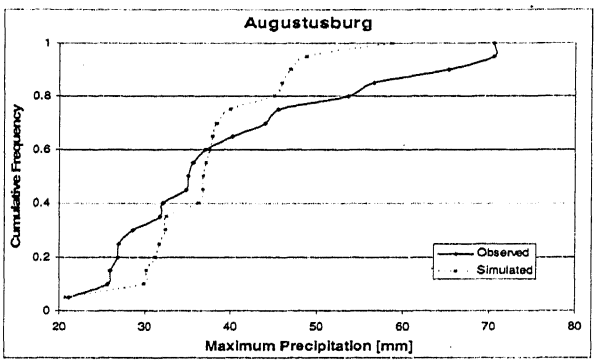

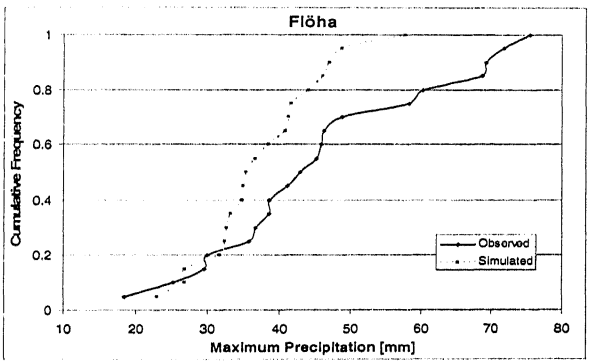

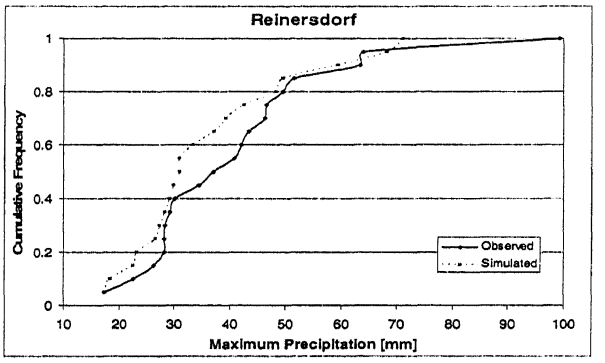

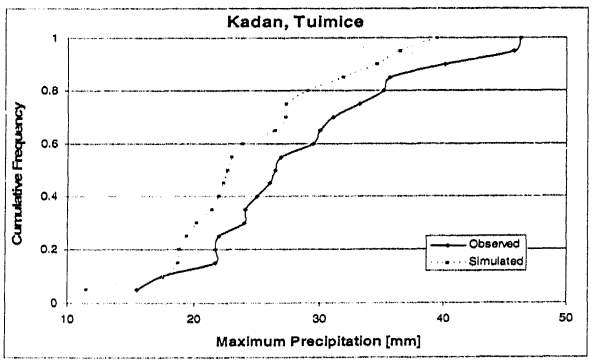

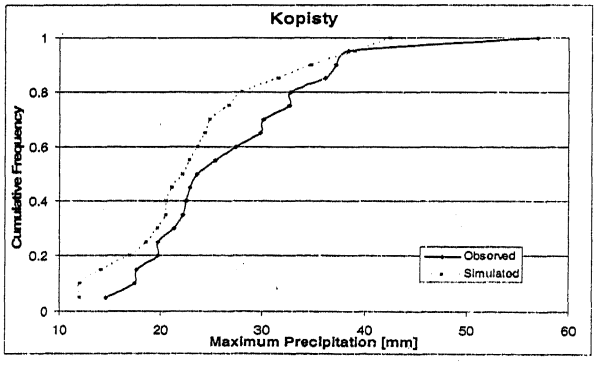

Fig 3.17 Cumulative Distribution Function for Observed and Synthetic Series, stations 25-32 (1971-90)

3.5.4 Comparison of other Simulated Series

Another synthetic rainfall series was simulated using different random number. Comparison of this simulated series was carried out with mean monthly historical rainfall. This comparison has been carried out for the first eight stations. Figure 3.18 shows that very good agreement was achieved for all eight stations. Correlation for all the stations are presented in Table 3.8, they are higher for all eight stations in comparison with previous series. Correlation for all the eight stations close to 90%. These results indicate that it is possible to generate synthetic rainfall series from the model proposed in this study that in good agreement with the historical values.

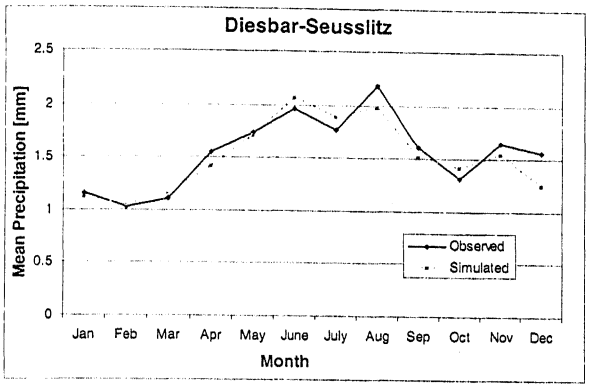

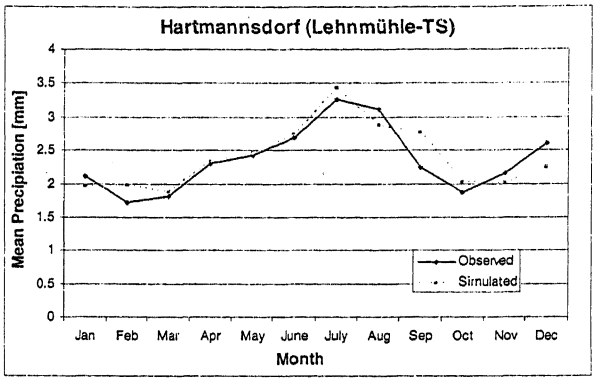

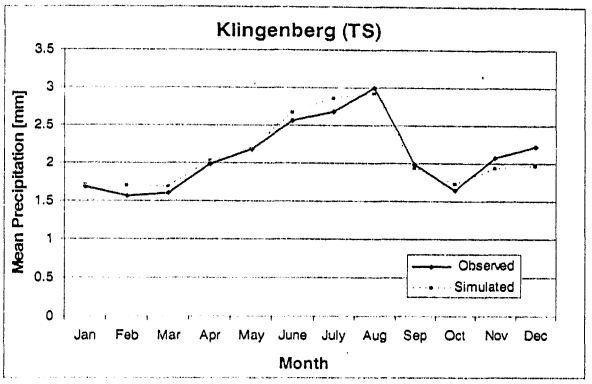

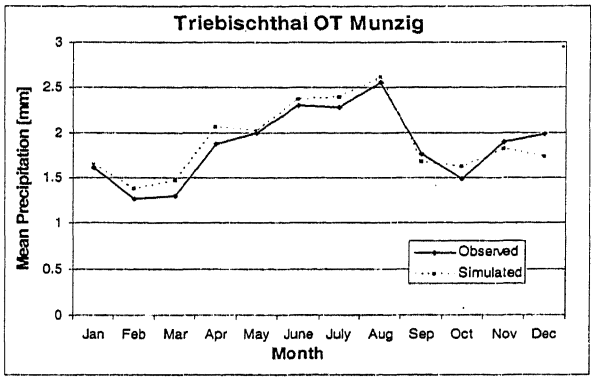

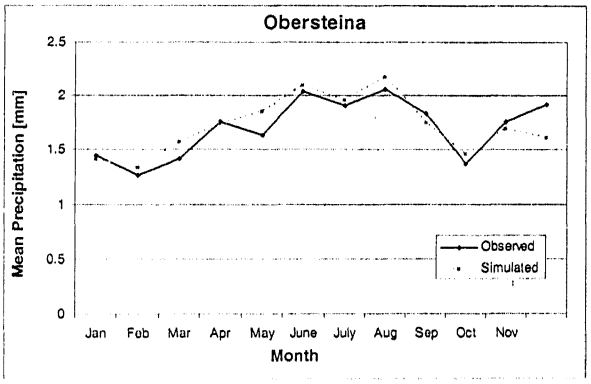

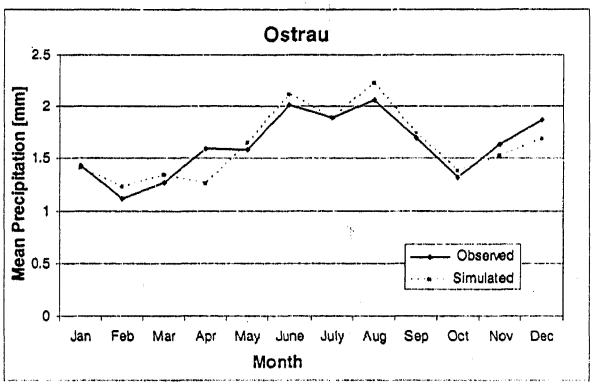

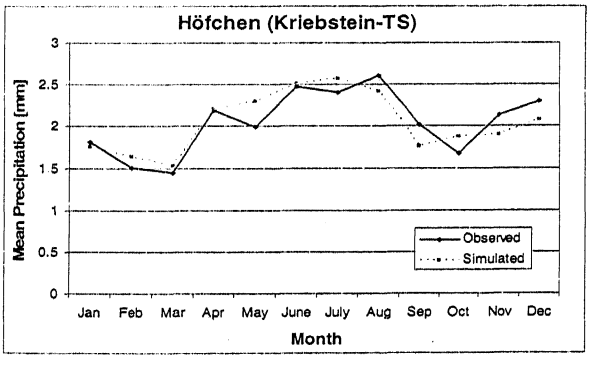

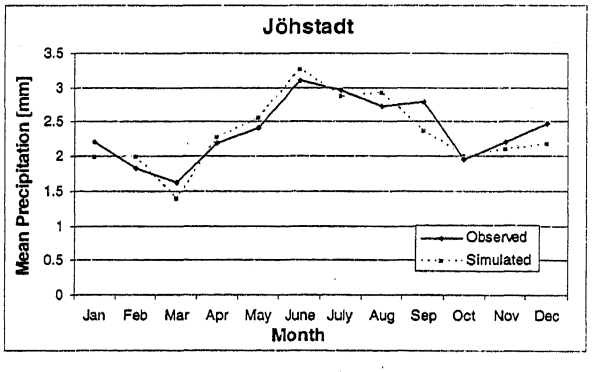

Fig 3.18 Mean Monthly Rainfall for Observed and Synthetic Series at Stations 1-8

Table 3.8: Correlation between Observed and Synthetic Mean Monthly Rainfall

Serial No.	Station	Correlation
1	Diesbar-Seusslitz	0.93
2	Hartmannsdorf (Lehnmühle-TS)	0.88
3	Klingenberg (TS)	0.96
4	Triebischthal OT Munzig	0.95
5	Obersteina	0.87
6	Ostrau	0.89
7	Höfchen (Kriebstein-TS)	0.86
8	Jöhstadt	0.91

3.5.5 Comparison of Simulated Series for 6 CPs Case

Comparison with simulated series obtained in 6 CPs case has been carried out with annual rainfall totals. Graphs of annual total rainfall are shown with Figures 3.19, 3.20, 3.21 and 3.22 and the mean and standard deviation are presented in table 3.9.The graphical results indicate that the agreement in synthetic and historical rainfalls in good but not as good as that for 12 CPs case. It can be observed from the Table 3.9 that the results are very good in terms of mean and variance but not so good as compared to the 12 CPs case. Therefore, it is difficult to say by these results that how many CPs should be taken into consideration. Using too many CPs result in very low occurrence frequencies, which makes positive investigation more difficult. On the other hand considering too few CPs may leads to a loss of information, since their behavior only represents averaged weather conditions. Therefore, a optimal station need to be found depending upon the practical consideration and in a particular catchment.

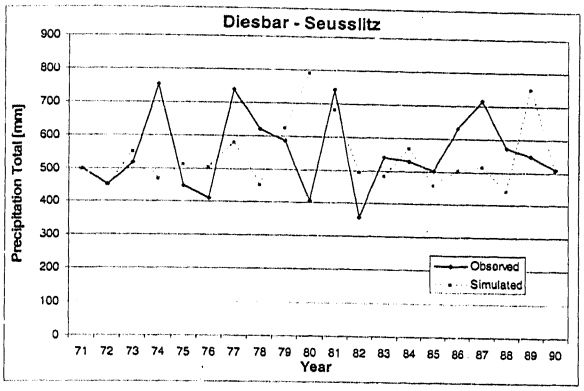

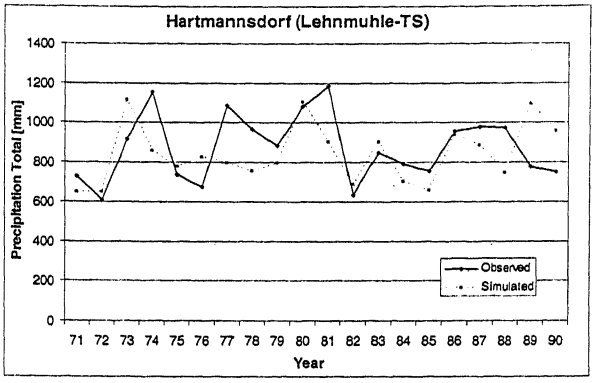

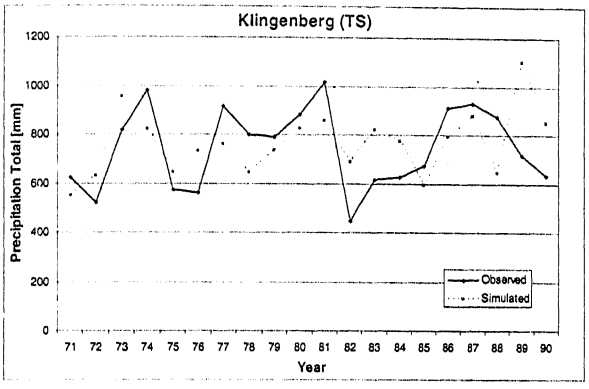

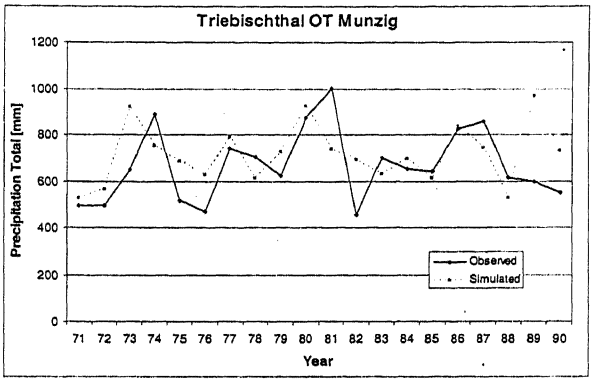

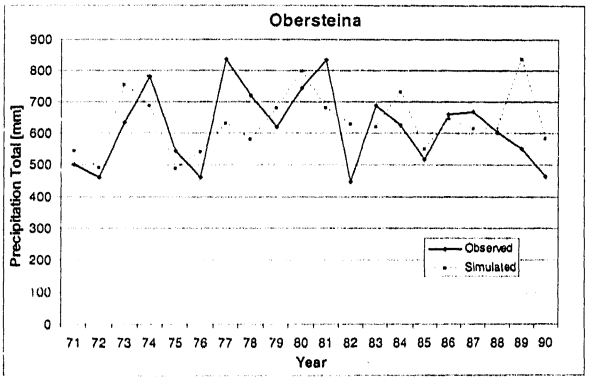

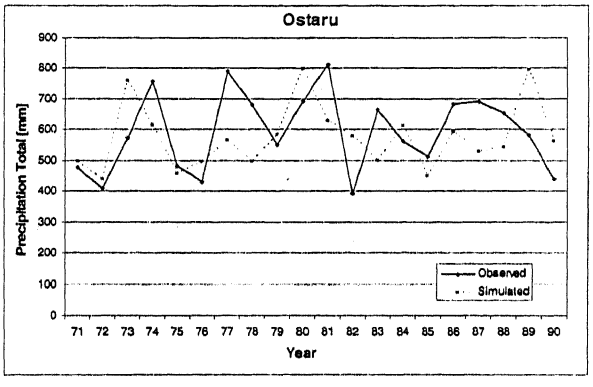

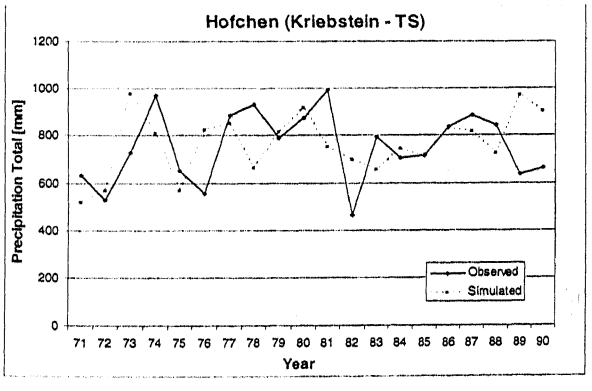

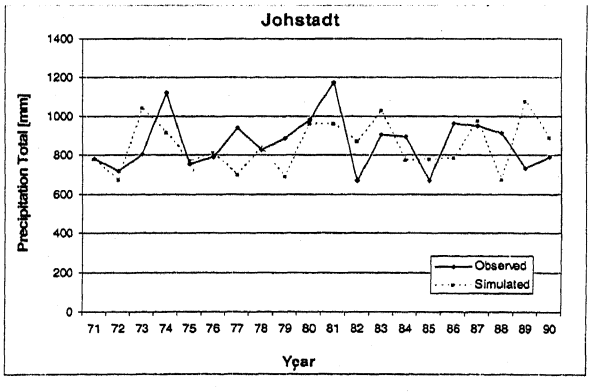

Fig 3.19 Annual Rainfall totals for Observed and Synthetic series, Stations 1-8 (6 CPs)

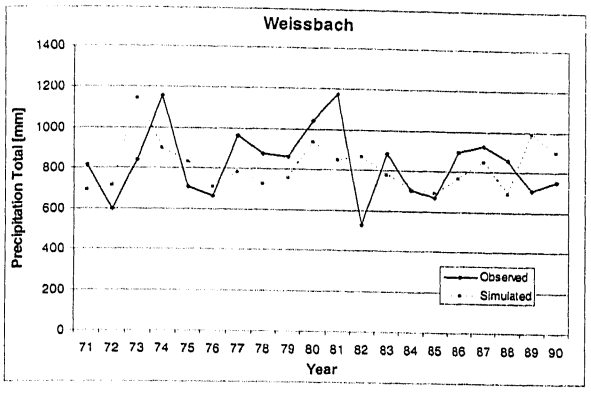

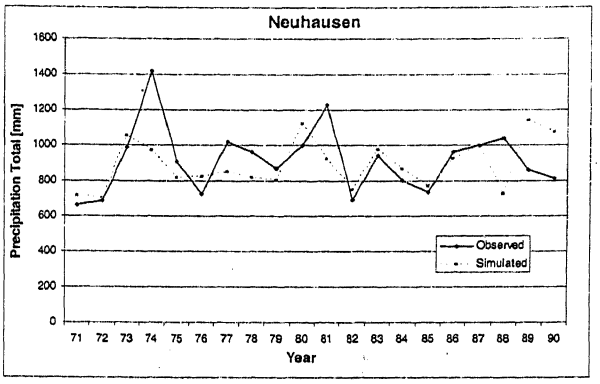

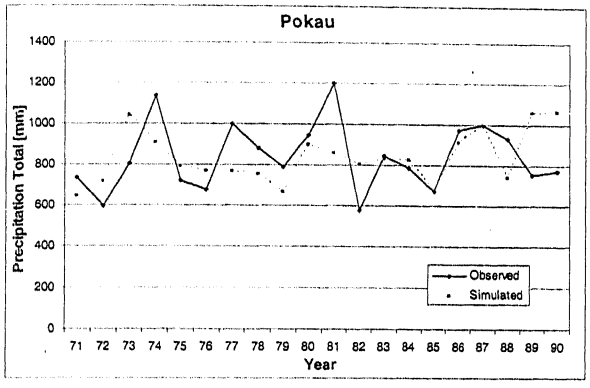

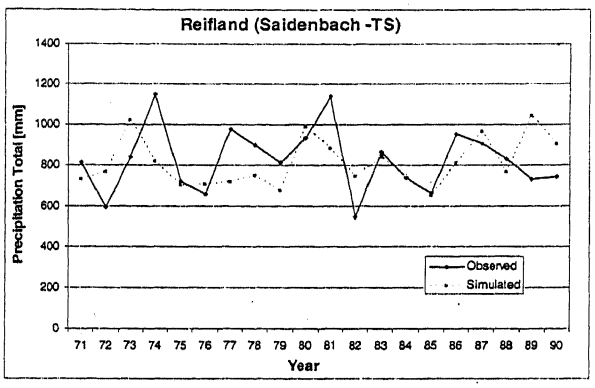

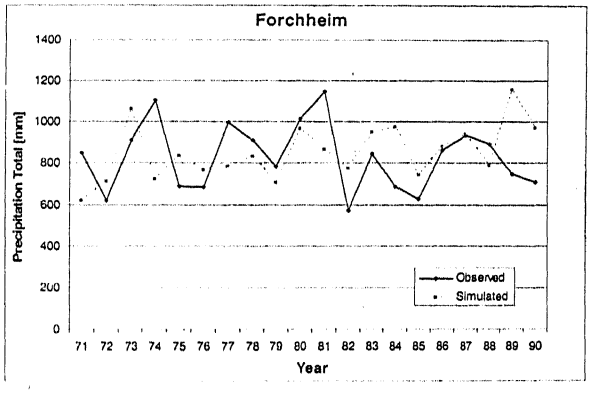

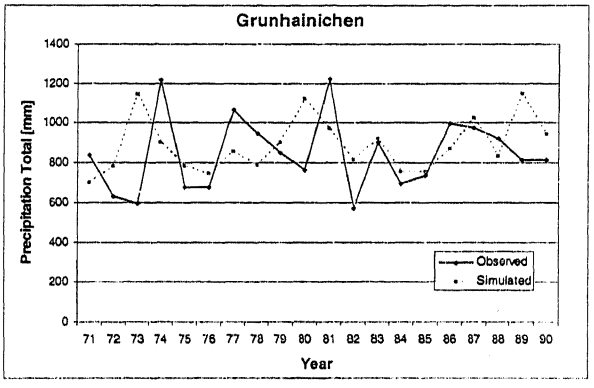

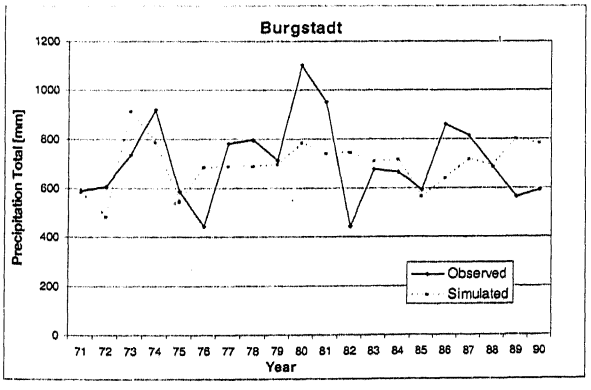

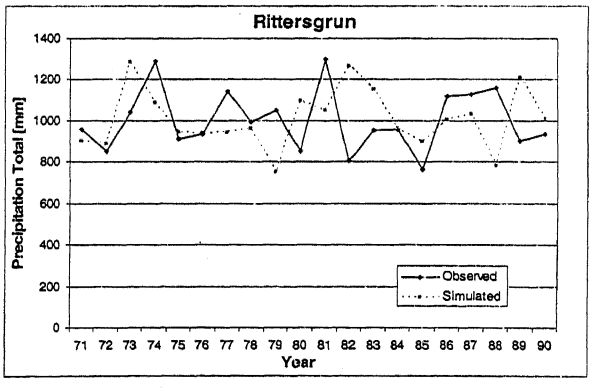

Fig 3.20 Annual Rainfall Totals for Observed and Synthetic series, Stations 9-16

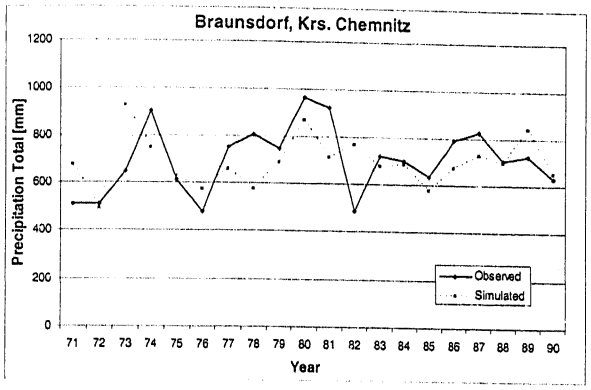

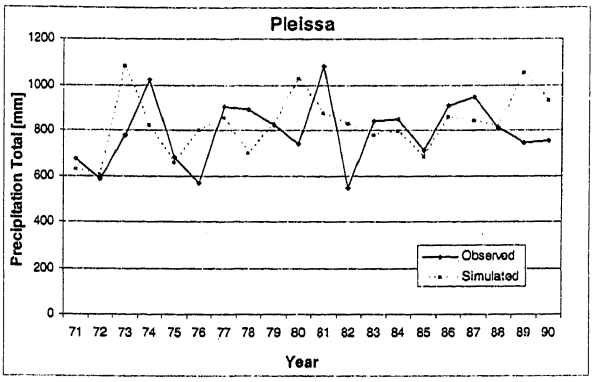

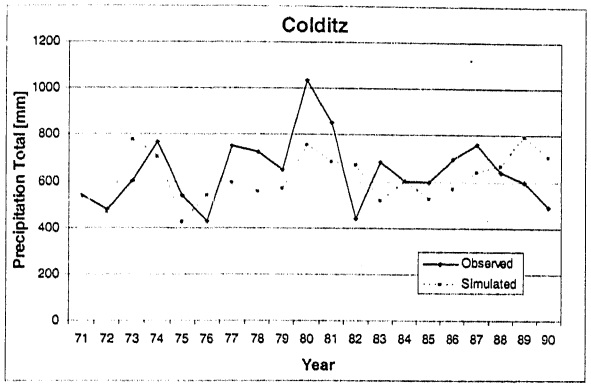

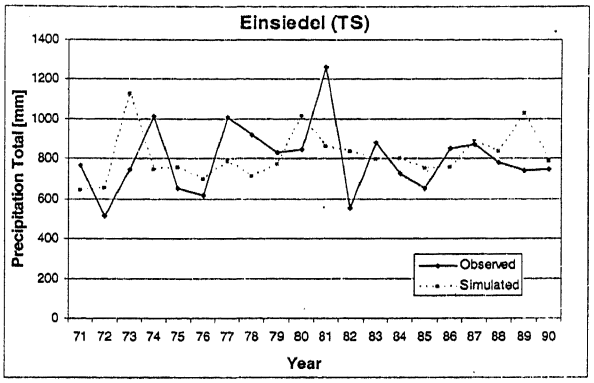

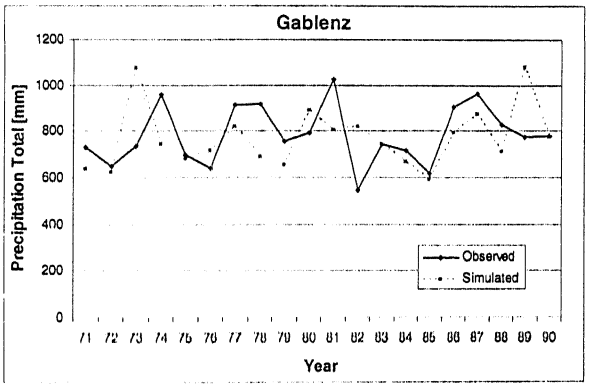

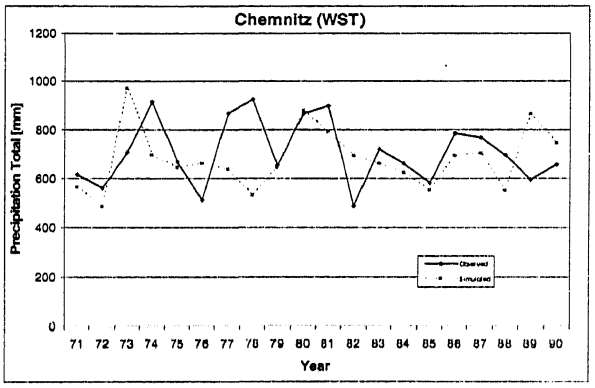

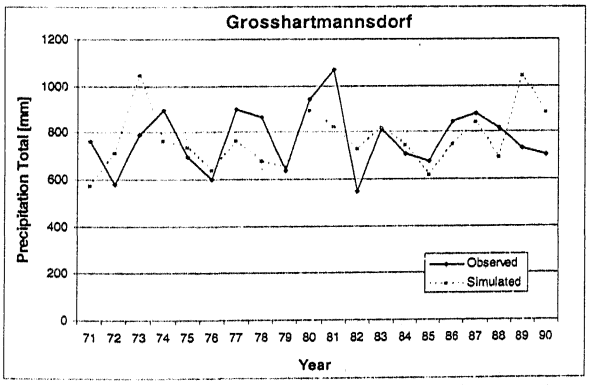

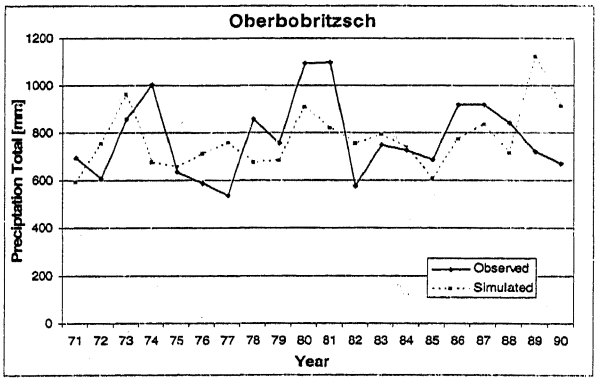

Fig 3.21 Annual Rainfall Totals for Observed and Synthetic series, Stations 17-24

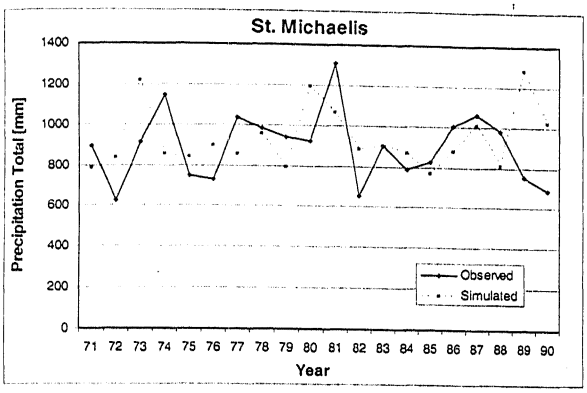

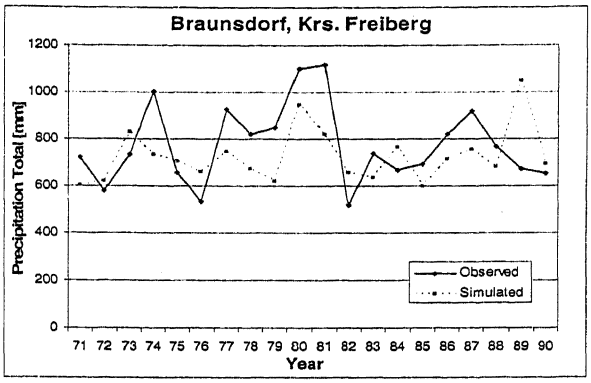

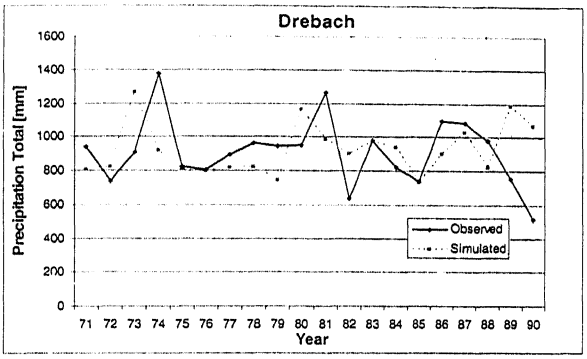

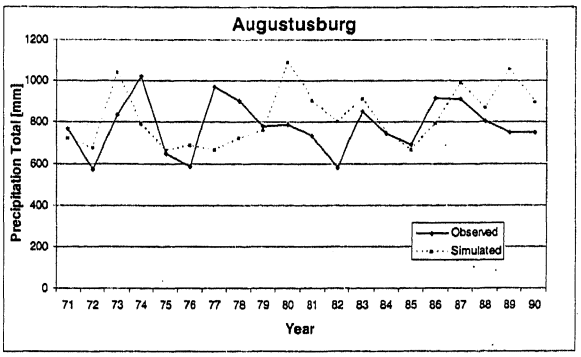

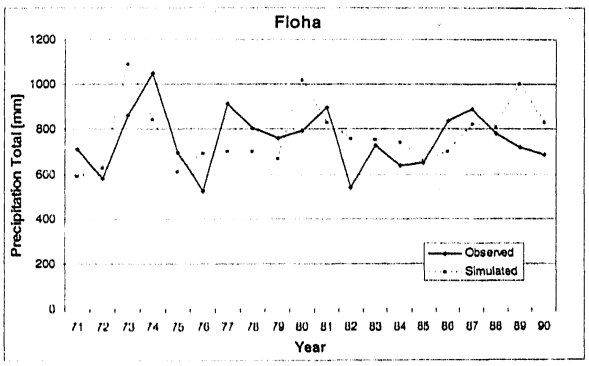

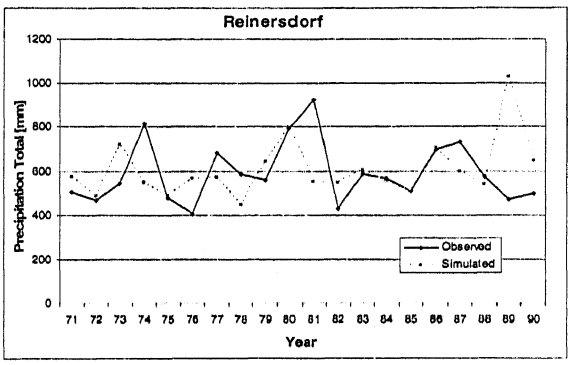

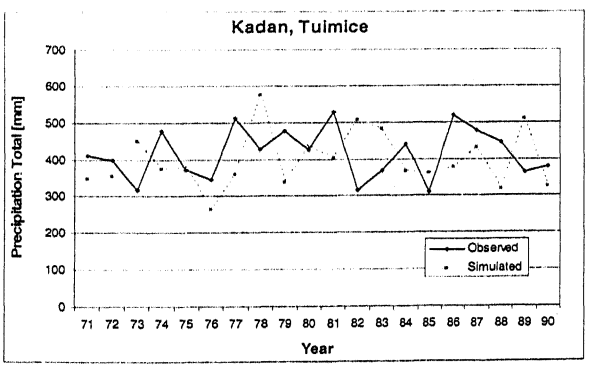

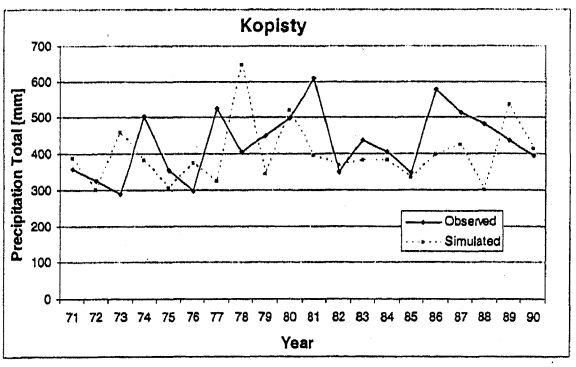

Fig 3.22 Annual Rainfall Totals for Observed and Synthetic series, Stations 25-32

Table 3.9 Statistics of Observed and Synthetic Annual Totals 1971-1990, 32 Stations in Catchment (6CPs)

Serial No.	Stations	Mean		Standard Deviation	
	Name	Observed	Synthetic	Observed	Synthetic
1	Diesbar-Seusslitz	554	540	116	98
2	Hartmannsdorf (Lehnmuhle-TS)	874	840	170	148
3	Klingenberg (TS)	745	765	166	132
4	Triebischthal OT Munzig	667	715	155	126
5	Obersteina	618	634	124	94
6	Ostrau	591	575	129	105
7	Hofchen (Kriebstein-TS)	754	765	149	129
8	Johstadt	864	848	135	126
9	Weissbach	832	814	171	119
10	Neuhausen	916	891	187	138
11	Pockau	840	836	167	129
12	Reifland (Saidenbach-TS)	827	812	156	118
13	Forchheim	829	852	162	134
14	Grunhainichen	845	887	187	136
15	Burgstadt	704	695	167	99
16	Rittersgrun	1002	1008	148	143
17	Braunnsdorf, Krs. Chemnitz	703	692	143	104
18	Pleissa	794	823	144	132
19	Colditz	643	614	147	102
20	Einsiedel (TS)	799	812	173	123
21	Gablenz	785	769	128	133
22	Chemnitz (WST)	708	679	133	123
23	Grosshartmannsdorf	772	768	133	126
24	Oberbobritzsch	777	770	166	128
25	St. Michaelis	895	935	173	149
26	Braunsdorf, Krs. Freiberg	774	725	170	115
27	Drebach	910	924	200	152
28	Augustusburg	780	821	127	139
29	Floha	752	770	132	136
30	Reinersdorf	591	607	138	129
31	Kadan, Tuimice	415	397	68	76
32	Kopisty	428	398	91	87

Chapter 4

Interpolation of Rainfall using Geostatistical Kriging

4.1 General

In real world, it is impossible to get exhaustive values of data at every desired point because of practical constraints. This is particularly true for hydrological variables such as rainfall. Rainfall is measured at a limited number of point raingauge locations in a catchment. However, rainfall data are routinely required at fine grid points in a catchment while developing distributed rainfall-runoff models. There are many methods of interpolation of rainfall data at finer resolution form a coarse spatial resolution kriging is one of them.

The word "Kriging" is synonymous with "optimal prediction". It was named after D. G. Krige from South Africa in 1950s. Kriging is the estimation procedure used in geostatistics using known values in space at coarse resolution and a variogram to determine the unknown values at finer resolution. It is a method of interpolation, which predicts unknown values from data observed at known locations. This method uses variogram to express the spatial variation, and it minimizes the error of predicted values, which are estimated by spatial distribution of the predicted values. It is a stochastic interpolation technique based on the assumption that the rainfall being interpolated can be treated as a regionalized variable. A regionalized variable is intermediate between a truly random variable and a completely deterministic variable. It varies in a continuous manner from one location to the next and therefore points that are near each other have a certain degree of spatial correlation, but points that are

widely separated are statistically independent. Kriging is often used in obtaining estimates of surface elevation using known elevation at specific points, however, the technique can be applied to any phenomenon where an interpolated surface needs to be created from known point data at few location. Kriging is based on regionalized variable theory and is superior to other means of interpolation because it provides an optimal interpolation estimate for a given coordinate location, as well as a variance estimate for the interpolation value.

4.2 Geostatistics

Time series analysis is one of the first fields where variability has been considered and described with stochastic methods. In kriging these methods are extended and further developed to analyze spatial variability. These spatial methods form the discipline called geostatistics. The word 'geostatistics' is formed from the two parts 'geo' and 'statistics' similarly to geophysics or geochemistry. It is used with two different meanings: as a collection of all statistical and probabilistic methods applied in geosciences and as an other name for the theory of regionalized variables.

A unique aspect of geostatistics is the use of regionalized variables. Regionalized variables describe phenomena with geographical distribution (e.g. elevation of ground surface). In the 1960s, the French Mathematician G. Matheron gave theoretical foundations to the above methods. Geostatistics was first used by the mining industry, as high costs of drillings made the analysis of the data extremely important. Books and publications on geostatistics are mostly oriented to mining problems. As the computers got cheaper and cheaper, the computationally expensive methods could also be used in other topics. Applications of geostatistics can be found in many different disciplines

ranging from the classical fields of mining and geology to soil science, hydrology, meteorology, environmental sciences, agriculture, even structural engineering.

4.3 Kriging Methods

Various types of Kriging methods are available used in Geostatistics. These are: Simple Kriging, Ordinary Kriging, Co-Kriging, Indicator Kriging, Universal Kriging and External Drift Kriging. The detail of these methods can be found in Delhomme (1978).

In present study, Ordinary kriging (OK) and External drift kriging have been used as an interpolation method. External drift Kriging (EDK) is an extension of most widely used method known as Ordinary Kriging. Initially an attempt had been made to check the suitability of ordinary kriging and external drift kriging using cross validation approach (that is described in next section) in order to see the performance of both of these methods in interpolating the rainfall data. Detailed description of these two methods is given below.

4.4 Ordinary Kriging

Ordinary Kriging is the most widely used Kriging method. It is used to estimate a value at a point of a region for which the variogram is known, without the prior knowledge about the mean. Therefore, variogram plays an important role in kriging methods. Before going into detail about OK the method, brief description of the variogram is given below.

4.4.1 Variogram

Variogram characterizes the spatial continuity in a data set. It is a plot of the variances (one-half the mean squared difference) of paired sample as a function of distance (and optionally of the direction) between the samples. Typically, all possible sample pairs are examined, and grouped into classes (lags) of approximately equal distance and direction. Variograms provide a means of quantifying the commonly observed relationship that samples close together will tend to have more similar values than samples far apart. The variogram is, however, calculated based on a less restrictive hypothesis and hence is applicable for most of the hydro-geological parameters. The analytical equation to compute a variogram from the field data of any variable (say Z) is as follows:

$$\gamma(h) = \frac{1}{2} E[z(u+h) - z(u)]^2 \tag{4.1}$$

where the function $\gamma(h)$ is the variogram (also called semi-variogram) between the two points, h distance apart; $z(u)$ and $z(u+h)$ are the pair of field values of the parameter Z at location u and $u+h$ respectively. E represents the expected value. The variogram is also calculated in different directions by taking the pairs in that particular direction only. However, in practice the variograms can be calculated using the following formula (Ahmed et al., 1987).

$$\gamma(\hat{h},\hat{\theta}) = \frac{1}{2N(h)} \sum_{i=1}^{N(h)} [z(u_i + h,\hat{\theta}) - z(u_i,\hat{\theta})]^2 \tag{4.2}$$

with

$$h - \Delta h \le \hat{h} \le h + \Delta h, \theta - \Delta\theta \le \hat{\theta} \le \theta + \Delta\theta \tag{4.3}$$

and

$$\bar{h} = \frac{1}{N(h)} \sum_{i=1}^{N(h)} \hat{h}_i, \quad \bar{\theta} = \frac{1}{N(h)} \sum_{i=1}^{N(h)} \hat{\theta}_i \tag{4.4}$$

where d and γ are the chosen lag and direction of the variogram, respectively; Δh and $\Delta\theta$ are tolerance on lag and direction, respectively; $\bar{h}$ and $\bar{\theta}$ are the actual lag and direction for the corresponding calculated variogram; and $N(h)$ is the number of pairs for a particular lag and direction. The variogram calculations were carried out in this study, which were used in both Kriging methods for the purpose of interpolating rainfall values. The calculation of Variogram for an example problem is presented in Appendix- B.

4.4.2 Theory of Ordinary Kriging

Ordinary Kriging is the most commonly used method for interpolating spatially varying variables at finer resolution. It is a variety of kriging, which assumes that local means are not necessarily closely related to the population mean, and which, therefore, uses only the samples in the local neighborhood for the estimate.

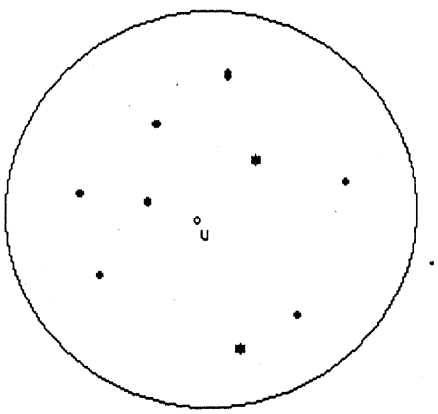

Figure 4.1 Data Points used for Ordinary Kriging

Suppose one wishes to estimate the value at point using the n data points as in the Figure 4.1. Combining the data points linearly with weights λ; we get the weighted average of the variance Z as follows:

$$Z^*(u) = \sum_{i=1}^{n} \lambda_i Z(u_i) \tag{4.5}$$

The weights should be constrained to add up to one. The data are assumed to be part of a realization of an intrinsic random function $Z(u)$ with the variogram $\gamma(h)$. The unbiasedness is assured with unit sum of the weights

$$\sum_{i}^{n} \lambda_i \mathrm{E}[Z(u_i) - Z(u)] = 0 \tag{4.6}$$

The estimation variance is given by

$$\sigma^2(u) = Var[Z(u) - Z^*(u)] = E\left[\left(Z(u) - \sum_{i=1}^{n} \lambda_i Z(u_i)\right)^2\right] \tag{4.7}$$

$$\sigma^2(u) = \gamma(u-u) + \sum_{i=1}^{n}\sum_{j=1}^{n} \lambda_i \lambda_j \gamma(u_i - u_j) - 2\sum_{i=1}^{n} \lambda_i \gamma(u_i - u) \tag{4.8}$$

The ordinary kriging system is obtained by minimizing the estimation variance with the constraint on weights as follows:

$$\begin{bmatrix} \gamma(u_1-u_1) & \cdots & \gamma(u_1-u_n) & 1 \\ \vdots & \ddots & \vdots & \vdots \\ \gamma(u_n-u_1) & \cdots & \gamma(u_n-u_n) & 1 \\ 1 & \cdots & 1 & 0 \end{bmatrix} \begin{bmatrix} \lambda_1 \\ \vdots \\ \lambda_n \\ \mu \end{bmatrix} = \begin{bmatrix} \gamma(u_1-u) \\ \vdots \\ \gamma(u_n-u) \\ 1 \end{bmatrix} \tag{4.9}$$

The left hand side describes the dissimilarities among the data points while the right hand side describes the dissimilarities between the data points and the estimated points.

Performing the matrix multiplication, the OK system can be rewritten in the forms that are called Kriging equations:

$$\begin{cases} \sum_{j=1}^{n} \lambda_j \gamma(u_i - u_j) + \mu = \gamma(u_i - u) \\ \sum_{j=1}^{n} \lambda_j = 1 \end{cases} \qquad i = 1,\ldots,n \qquad (4.10)$$

The minimal estimation variance can be obtained by substituting the kriging weights into (4.8). This variance is called kriging variance $\sigma^2(u)$. It can be proved that:

$$\sigma^2(u) = \sum_{i=1}^{n} \lambda_i \gamma(u_i - u) + \mu \qquad (4.11)$$

OK is an exact interpolator, in other words, at the point of the known data, the estimated value is equal to the data value. If all data are used for each estimation point, only the RHS vector is modified, while the matrix remains unchanged. However, it is generally not necessary to use all the data points while estimating the value at a point. Instead, only the closest data are used, since further data will be assigned a very low weight, diminishing its contribution to the estimated value. Example calculations to estimate an interpolation value using Ordinary Kriging are presented in Appendix-B.

4.5 External Drift Kriging

External Drift Kriging is a new technique that is dependent on an external regionalized variable. This new technique of utilizing more than one variable developed by G. Matheron's Group in Fontainebleau, France is not so much widely used as compare to other Kriging methods.

External knowledge in the form of other physical variables is incorporated into the system with the EDK (Ahmed and Marşily 1987). Here, it is assumed that an additional variable $Y(u)$ that is linearly related to the $Z(u)$ exists. The assumption of the constant expected value is thus replaced by:

$$E[Z(u) \mid Y(u)] = a+bY(u) \tag{4.12}$$

where a and b are unknown constants. The linear estimator should be unbiased for any a and b values. The linear estimator considered can be written as follows:

$$Z*(u) = \sum_{i=1}^{n} \lambda_i Z(u_i) \tag{4.13}$$

Where n is the number of data available for Z, the condition of unbiased estimation is

$$E(\sum_{i=1}^{n} \lambda_i Z(u_i) - Z(u) / Y(u), Y(u_i), i = 1,.....,n) = 0 \tag{4.14}$$

Using Eq. 4.12,the following is obtained

$$a\left[\sum_{i=1}^{n} \lambda_i Y(u_i) - Y(u)\right] + b\left[\sum_{i=1}^{n} \lambda_i - 1\right] = 0 \quad \forall i \tag{4.15}$$

For a and b to be constant for all points u and nonzero, two conditions a re needed:

$$\sum_{j=1}^{I}\lambda_j = 1 \tag{4.16}$$

$$\sum_{j=1}^{I}\lambda_j Y(u_j) = Y(u) \tag{4.17}$$

The Eq. (4.17) represents the new condition of unbiased estimations, which depends on the secondary variable, while the first is identical to the usual kriging condition of unbiased estimations. The condition of optimality of estimations is, as usual, to minimize the variance of the estimation error:

$$E[(Z^*(u) - Z(u))^2 / Y(u), Y(u_i), i = 1,\ldots\ldots,n] \tag{4.18}$$

while at the same time imposing the two conditions in Eq. (4.16) & 4.17. To this end, two Lagrange multipliers (μ_1, μ_2) can be used to add constraints to the variance:

$$\begin{aligned} &E[(Z^*(u) - Z(u))^2 / Y(u), Y(u), i = 1,\ldots\ldots,n] + \\ &-2\mu_1\left[\sum_{i=1}^{n}\lambda_i - 1\right] - 2\mu_2\left[\sum_{i=1}^{n}\lambda_i Y(u_i - Y(u)\right] \end{aligned} \tag{4.19}$$

Minimizing the estimation variance under the above assumption leads to the linear equation system:

$$\sum_{j=1}^{I}\lambda_j\gamma(u_i - u_j) + \mu_1 + \mu_2 Y(u_i) = \gamma(u_i - u) \quad i = 1, \ldots, I \tag{4.20a}$$

$$\sum_{j=1}^{I}\lambda_j = 1 \tag{4.20b}$$

$$\sum_{j=1}^{I}\lambda_j Y(u_j) = Y(u) \tag{4.20c}$$

where $\mu 1$ and $\mu 2$ are Lagrange-multipliers. The variogramm used in these Eqs. is the time invariant curve, as also used in OK. Note that the variable Y has to be known at the location u, to perform estimation. The estimator thus depends on the additional variable $Y(u)$. EDK can be taken if the secondary information $Y(u)$ is available at a high spatial resolution, preferably regular grid. Example calculations for EDK are presented in Appendix-B.

4.6 Properties of Kriging

Kriging is an interpolation (and extrapolation) technique. Important properties of the kriging as an interpolator are as follows:

1. For each observation point u_i, $Z(u_i) = Z^*(u_i)$, and the corresponding estimation variance is zero. This is because taking $\lambda i = 1$ and $\lambda j = 0$ if $i \neq j$ the kriging equations are satisfied.

2. Kriging weights are calculated with the help of the variogram and the locations of the measurement points and the point to be estimated. Not only distances between measurement points and the point to be estimated are considered but also the relative position of the measurement points.

4. Kriging weights are not influenced by the measurement values. If the same configuration appears at two different locations, the kriging weights will be the same, independently from the measured values. The measured values influence the variogram, which is the basis for the calculation of the kriging weights.

5. Kriging weights show a screening effect, distant points receive lower weights if closer measurements are available.

4.7 Results and Discussions

In the present work interpolation has been carried out using ordinary and External Drift Kriging for observed and synthetic series for the catchment Freiberger Mulde, Germany. The methodology for both the Kriging methods is described above. Once the interpolated values of rainfall were computed, Cross Validation is carried out to check the performance of the Interpolation between Ordinary Kriging and External drift Kriging.

4.7.1 Data Employed

The interpolation has been done to achieve the generated synthetic series in higher resolution in space using External Drift Kriging. That has been done over the Grid created by German Weather Service (DWD). This Grid has been created for whole catchment of River Freiberger Mulde that is having 1574 grid points. Each Grid Point is having the resolution of $2.5^{\circ} \times 2.5^{\circ}$. The input data has been used for this study for 20 years daily rainfall data of period from 1971- 1990 for 32 stations for both observed as well as simulated series. Grid file has been created with coordinate location and elevation of each Grid point as an other input for EDK. Table 4.1 represents the example of created grid file for few grids.

Table 4.1 Grid File for Interpolation for Few Grid Points

Grid Point ID	X-Coordinate	Y-Coordinate	Elevation
3740	4548380	5683750	149.20
4037	4630880	5676250	179.80
4560	4618380	5661250	109.51
4820	4608380	5653750	303.58
5059	4545880	5646250	241.29
5499	4545880	5633750	322.08
5973	4630880	5621250	269.60
6036	4568380	5618750	503.09
6149	4630880	5616250	552.22
6310	4593380	5611250	652.22
6571	4585880	5603750	745.91
6916	4568380	5593750	751.95
7024	4618380	5591250	0.00
7381	4630880	5581250	282.22
7524	4548380	5576250	485.18
7644	4628380	5573750	0.00

4.7.2 Interpolation

In the External drift Kriging, many variables can be used as an external variable like Elevation, Exposition and Square root of Elevation etc. In present study, Square Root of Elevation has been used as an external variable. With the help of Kriging tools interpolated daily Rainfall values for each Grid Point have been estimated.

Interpolation with external drift kriging has been done over the entire grid. Rainfall data for 32 stations for the period of 20 years (1971-1990) and Grid file as given in table 4.1 were the inputs to the Kriging program and the average rainfall value over the center of each grid was the output.

The OK and EDK methods were applied to interpolate rainfall values at each of the 1574 points in Freiberger Mulde river basin Germany. Due to the high volume, the results for only selected grid stations have been presented here. The comparison of the observed and synthetic rainfall values interpolated from external drift Kriging in terms of mean, standard deviation, and coefficient of variation is presented in Table 4.2. It has been done for the selected stations (IDs given in the first column of Table 4.2), for which the rainfall amounts were on the higher side. It can be observed that the mean, standard deviation, and the coefficient of variation from the observed and synthetic rainfall series match very well. It can be noted that the comparison of the interpolated values has not been done at the known 32 rain gauge locations due to the fact that Kriging is an exact interpolator. Comparison between interpolating rainfall values over the 16 Grid, points (having heavy rainfall due to higher number of grid points) for Observed and Synthetic series has been presented and discussed here. The results are not so good incase of stations with IDs 7024 and 7644. In case of these two stations, the interpolated values are little bit underestimated both for mean and standard deviation. Coefficient of variation is also higher for simulated series at IDs 7024 & 7644 having 0.9 & 0.9 for observed and 1.08 & 1.07 for simulated rainfall series respectively. The reason may be that these grid points are having 0 elevation, so the effect of external variable is negligible in this case. The results are found to be satisfactory for other grid points. Therefore, results show the suitability of external drift kriging method as an interpolation method for the catchment. However, the real validation of interpolation can only be done by employing the interpolated values in distributed rainfall-runoff modeling and assessing the performance of the models in accurately predicting stream flow.

Table 4.2 Comparison between Observed and Simulated Interpolated Values

Grid Points	Mean (mm)		**Standard Deviation** (mm)		Coefficient of Variation (Cv)	
ID	Observed	Simulated	Observed	Simulated	Observed	Simulated
3740	12.6	10.9	14.1	12.0	0.8	0.9
4037	69.0	57.9	73.2	67.8	0.9	0.8
4560	75.7	71.3	82.8	79.4	0.9	0.8
4820	27.3	28.9	24.4	31.8	1.1	0.9
5059	6.3	5.0	6.80	5.2	0.9	0.9
5499	65.4	59.5	67.1	62.9	0.9	0.9
5973	33.4	34.0	30.2	34.9	1.1	0.9
6036	30.0	29.8	32.3	39.2	0.9	0.7
6149	50.8	56.1	54.5	58.6	0.9	0.9
6310	10.9	14.0	14.3	16.8	0.7	0.8
6571	40.0	37.5	32.0	33.9	1.2	1.1
6916	32.6	33.0	31.9	33.7	1.0	0.9
7024	79.1	68.6	84.0	63.4	0.9	1.08
7381	46.6	41.8	36.1	36.3	1.2	1.1
7524	52.6	54.8	50.6	52.8	1.0	1.0
7644	72.1	67.4	80.1	62.8	0.9	1.07

4.7.3 Cross Validation

Cross-validation analysis allows evaluating alternative models for kriging. In this method, each measured point in a data set is individually removed from the set and its value is then estimated via kriging as though it were never there. This procedure tests the variogram by a procedure where it is most often used, namely the kriging procedure.

In the present study, the cross validation has been carried to check the performance of the interpolation between ordinary kriging and external drift kriging for the available

data set. It has been done with 20 years data set for 32 stations. Input for cross validation was rainfall data in 1/10 of rainfall (in mm) for all the stations. It gives the value of rainfall over all 32 stations day by day for all 20 years (7305 days) with ordinary kriging as well as external drift kriging. Comparison between ordinary and external drift kriging was done with the help of root mean square error for different rainfall classes with historical rainfall. The results of the interpolation methods, external drift kriging and ordinary kriging are shown in Table 4.3.

According to the result presented in Table 4.3, there is not so much variation in Ordinary Kriging and External Drift Kriging. It can be seen that for initial rainfall classes 0–10 mm, 10–20 mm, error is more in case of External Drift Kriging but for slightly higher rainfall classes like 50–60 mm, 60–70mm, 70–80mm, 80–90 mm, error is less in case of External Drift Kriging, So we can infer that for higher rainfall values it's better to use External Drift Kriging.

Table 4.3 Comparison between Ordinary Kriging and External Drift Kriging

Rainfall Classes (mm)	Root Mean Square Error	
	Ordinary Kriging	External Drift Kriging
0 – 10	0.49	0.51
10 – 20	3.08	3.09
20 – 30	5.65	5.56
30 – 40	8.13	8.34
40 – 50	8.23	8.26
50 – 60	12.09	12.04
60 – 70	15.98	14.98
70 – 80	14.51	14.50
80 – 90	9.07	8.16
90 – 100	28.44	28.64

Chapter 5

Summary and Conclusions

Many hydrological models require synthetic rainfall data at higher resolution. In this research, an attempt has been made to generate synthetic rainfall data in a watershed using downscaling approach. It is an attempt to give subscale realization at a higher spatial scale from coarse resolution. Because of the rainfall characteristics depend on large scale atmospheric circulation conditions, rainfall has been generated as a stochastic process coupled with atmospheric circulation using a multivariate stochastic downscaling model (MSD). Rainfall is linked to circulation pattern using conditional MSD model parameters. A new fuzzy rule based method of CPs classification has been employed in this study. External drift kriging tool has been employed for interpolation at the generated point synthetic rainfalls.

Study has been carried out for the catchment of river Freiberger Mulde, Germany for the period of 20 years data set. Work has been carried out in three parts. Firstly daily classified CPs were determined using fuzzy classification based on pressure data and discharge data. Generation of synthetic rainfall has been carried out with MSD model based on CPs and historical rainfall amounts. External drift kriging has been employed on both observed and synthetic rainfall series using elevation as an external variable in order to get rainfall series at higher resolution. The results obtained in this study can be summarized in the following points:

- According to CP classification three CPs, CP04, CP07 and CP01 cause higher increase in discharge than normal having higher probability of increase. CP01 and CP09 are the most frequent CPs. CP09 is having higher frequency but at the same time it is the driest CP with lower increase in the discharge and lowest mean wetness index amount. The CP04 is an extremely wet CP causing higher increase compared to a normal day. Pressure anomaly maps are also verified these results.

- A model for downscaling daily rainfall series has been successfully applied for a larger catchment Freiberger Mulde, Germany. Comparisons of annual rainfall total, mean monthly rainfall, comparison of mean and deviation, coefficient of correlation showed that most features are in good agreement.

- Mean Monthly synthetic rainfall match more closely to historical monthly as compared to annual. That is because of the statistical character of the modeling, the synthetic annual rainfall often differs from the observed ones.

- The synthetic rainfall generation is a function of the initial random number synthetically generated rainfall using different sets of random numbers were found to be performing differently. Therefore, it is necessary to generate a number of realizations of the synthetic rainfall, and select the one that best matches the historical rainfall at known spatial points.

- The model enables generating long rainfall series which can be used as input to hydrological modeling focused on extremes with long recurrence interval (like flood and drought). In addition to this, rainfall observations in a catchment are often from different length, which means that hydrological simulation are based on rainfall obtained from different observation station configurations. However, long series of rainfall can be generated for a greater number of stations based on much shorter common observation. For higher rainfall amount External drift kriging is better than Ordinary kriging.

- Relatively poor annual total performance of the model (Figs. 3.6, 3.7, 3.8 and 3.9) is caused by the aggregation in time and by the statistical character of CP conditioning. May be additional variables could improve quality of inter annual performance (vertical stability, humidity etc.).

References

Aarts, E., Korst, J., (1989) Simulated annealing and Boltzmann machines: a stochastic approach to combinatorial optimization and neural computing, *John Wiley & Sons, Chichester.*

Ahmed, S. and de Marsily, G., (1987) Comparison of geostatistical methods for estimating transmissivity using data on transmissivity and specific capacity. *Water Resources Research*, **23**(9): 1717-1737.

Ahmed, S., Shankaran, S., Gupta, C., (1995) Variographic Analysis of some Hydrological Parameters: Use of geological soft data, Journal of Environmental Hydrology, **3**(2),

Bardossy, A., Plate, E.J., (1991) Modeling daily rainfall using a semi-Markov representation of circulation pattern occurrence, *Journal of Hydrology*, **122**, 33-47.

Bardossy, A., (1992) Stochastic Downscaling of GCM output results using atmospheric circulation patterns, *Proceedings First UNESCO Gyorgy Kovacs Symposium Paris, France.*

Bárdossy, A., Stochastic Downscaling Methods to Assess the Hydrological Impacts of Climate Change on River Basin Hydrology, Knmi *Workshop. [Key note paper]*

Bardossy, A., Plate, E., (1992) Space-time model for daily rainfall using atmospheric circulation patterns, *Water Resources Research,* **28**, 1247-1259.

Bardossy, A.,(1994) Estimation of extreme regional precipitation under climate change, NATO, *Advanced study Institute, Kluwer, Dordrecht,* 195-205

Bardossy, A., Duckstein, L. and Bogardi, I., (1995) Fuzzy rule-based classification of

atmospheric circulation patterns, *International Journal of Climatology*, **15**, 1087-1097.

Bardossy, A., Mierlo, M., (2000) Regional precipitation and temperature scenarios for climate change, *Hydrological Science Journal*, 45(4), 559-575.

Bardossy, A., Stehlik, J., Caspary, H.-J., (2002) Automated optimized fuzzy rules based circulation pattern classification for precipitation and temperature downscaling, *Climate Research*, **23**, 11-22.

Bardossy, A., Filiz, F., (2002) Identification of Flood Producing Circulation Patterns, Applications in Flood Risk Assessment (Proceedings of the PHEFRA Workshop, Barcelona, 16-19th October, 2002).

Blazvoka, S., Beven, K., (1997) Flood frequency prediction of for data limited in the Czech Republic using rainfall runoff model and Top model, *Journal of Hydrology*, **195**, 256-278

Bogárdi, I., Matyasovszky, I., Bárdossy, A., and Duckstein, L., (1994) A hydro-climatological model of areal drought, *Journal of Hydrology*, **153**, 245-264.

Brandsma, T., and T.A. Buishand, (1997) Statistical linkage of daily precipitation in Switzerland to atmospheric circulation and temperature, *Journal of Hydrology*, **198**, 98-123

Brass, R.-S., Rodriguez-Iturbe, I., (1985) Random function in Hydrology, *Addison-Wesley*,Reading, MA 559 pp.

Buishand, T.A., and T. Brandsma, (1997) Comparison of circulation classification schemes for predicting temperature and precipitation in the Netherlands, International *Journal of Climatology* **17**, 875-889.

Burger, K., (1958) Zur Klimatologie der Grosswetterlagen, Ber. Dtsch. Wetterdiensts, **6**, 45.

Delhomme, J., P., (1978) Kriging in Hydro sciences, *Advance in water resources*, **1**(5), 251-266.

Duckstein, L., A.Bárdossy, Bogárdi,I., (1993) Linkage between the occurrence of daily atmospheric circulation patterns and floods: an Arizona case study, *Journal of Hydrology* **143**, 413-428,.

Enke,W., Spekat, A., (1997) Downscaling climate model outputs into local and regional weather elements by classification and regression, *Climate Research,* **8**, 195-207.

Foufoula, G., Lettenmaier, E., (1987) A Markov renewal model for rainfall occurrences, *Water Resources Research*, **23**,875-884.

Hay, L., G., Wolock, D., Ayers, M.,(1991) Simulation of precipitation by weather type analysis, *Water Resources Research* **27**, 493-501.

Henze, N., Klar, B., (1993) Goodness of fit testing for a space-time model for daily rainfall, *Institute Fur Wissenschaftliches Rechnen und Mathematische Modellbildung, Universitat Karlsruhe*, Preprint No. 93/6,21 pp.

Katz, R.W., Parlange, M.B., (1993) Effects of an index of atmospheric circulation on stochastic properties of precipitation, *Water Resources Research* **29**, 2335-2344.

Koutsoyiannis, D., (1999) Optimal decomposition of covariance matrices for multivariate stochastic model in hydrology, *Water Resources Research* **35** (4), 1219-1229.

Laarhoven P., Aarts, E.,(1989) Simulated Annealing: Theory and Application, *Kluwer Academic Publisher.*

Lamb, H.-H., (1977) Climate, Present, Past and Future, Climatic history and the future, **2**, *Methuen and Co Ltd, London.*

Richardson, C., (1981) Stochastic Simulation of daily precipitation, Temperature, and Solar radiation, *Water Resources Research,* **17**(1), 182-190.

Stehlik, J., Bardossy, A.(2002) Multivariate stochastic downscaling model for generating daily precipitation series based on atmospheric circulation, *Journal of Hydrology*, **256**, 120-141.

Troisi, S., Fallico, C., Straface, S., Migliari, E., (2000) Application of kriging with external drift to estimate hydraulic conductivity from electrical-resistivity data in unconsolidated deposits near Montalto Uffugo, Italy, *Hydrogeology Journal*, **8**, 356–367

Wilby R.L., Wigley M.L., Conway D, Jones P.D., Hewitson B.C., Main J, Wilks D.S., (1998a) Statistical downscaling of general circulation model output: A comparison of methods. *Water Resources Research* **34** (11), 2995-3008,

Wilby R.L., Hassan H, Hanaki K., (1998b) Statistical downscaling of hydrometeorological variables using General Circulation Model output. *Journal of Hydrology*, **205**, 1-19.

Wilby, R.L., Hay, L.E., Leavesley, G.H. (1999) A comparison of downscaled and raw GCM output: implications for climate change scenarios in the San Juan River basin, Colorado, *Journal of Hydrology,* **225**, 67–91

Wilks, D.-S., (1989) Conditioning stochastic daily precipitation models on total monthly precipitation, *Water Resources Research* **25**(6), 1429-1439.

Zadeh, L., King-Sun Fu, Tanaka, K., Shimura, M., (1975) Fuzzy Sets and their Applications to Cognitive Processes, *Academic Press, Inc., New York.*

http://www.brpreiss.com/books/opus5/html/page473.html

http://www.cee.vt.edu/program_areas/environmental/teach/smprimer/kriging/kriging.html

http://pangea.stanford.edu/~baris/professional/theoryok.html

http://uk.geocities.com/drisobelclark/PG1979/index.htm

http://www.cse.dmu.ac.uk/~rij/newrep/node4.html

APPENDIX A

CP AND RAINFALL CHARACTERISRTICS FOR REMANING 31 STATIONS IN WINTER AND SUMMER

Table A-1: CP and Precipitation characteristics at Station Hartmannsdorf (LehnmühleTS) in Summer

CP	Frequency [HH] (%)	Precipitation Probability (%)	Sum of Precipitation (mm)	Contribution [A] (%)	Wetness Index [A/HH]	Mean (mm)	Standard Deviation (mm)	Max (mm
CP01	13.97	62.26	1615.2	16.76	1.20	5.05	5.96	38.6
CP02	9.54	27.07	485.8	5.04	0.53	5.11	9.20	68.5
CP03	3.45	46.46	351.0	3.64	1.06	5.95	10.27	59.4
CP04	9.89	75.27	2133.8	22.15	2.24	7.79	11.02	62.0
CP05	8.29	55.74	722.8	7.50	0.91	4.25	5.28	38.0
CP06	6.41	41.10	465.2	4.83	0.75	4.80	6.85	39.0
CP07	6.49	65.69	1176.0	12.21	1.88	7.49	9.47	65.2
CP08	5.38	49.49	539.5	5.60	1.04	5.51	8.98	66.3
CP09	11.60	28.10	518.4	5.38	0.46	4.32	5.44	29.8
CP10	8.32	45.75	668.2	6.94	0.83	4.77	7.88	72.5
CP11	7.09	37.93	278.3	2.89	0.41	2.81	3.42	19.0
CP12	8.67	30.41	605.4	6.28	0.72	6.24	9.10	60.0
CP99	0.90	42.42	75.0	0.78	0.87	5.36	7.44	31.0

Table A-2: CP and Precipitation characteristics at Station Klingenberg (TS) in Summer

CP	Frequency [HH] (%)	Precipitation Probability (%)	Sum of Precipitation (mm)	Contribution [A] (%)	Wetness Index [A/HH]	Mean (mm)	Standard Deviation (mm)	Max. (mm)
CP01	13.73	62.27	1465.7	17.26	1.26	4.77	5.88	39.7
CP02	9.69	26.44	388.9	4.58	0.47	4.23	6.03	28.0
CP03	3.48	48.00	308.1	3.63	1.04	5.13	10.26	59.0
CP04	10.00	73.82	1898.1	22.36	2.24	7.16	10.39	68.6
CP05	8.44	55.78	712.1	8.39	0.99	4.21	5.78	40.3
CP06	6.43	44.59	441.3	5.20	0.81	4.28	6.84	38.2
CP07	6.38	63.32	945.1	11.13	1.74	6.52	8.36	50.0
CP08	5.38	54.40	490.9	5.78	1.08	4.68	8.33	68.5
CP09	11.50	29.78	441.1	5.20	0.45	3.59	5.18	29.9
CP10	8.22	43.05	562.3	6.62	0.81	4.43	8.26	78.0
CP11	7.16	36.19	259.0	3.05	0.43	2.78	3.10	15.2
CP12	8.72	29.71	522.6	6.15	0.71	5.62	9.02	58.8
CP99	0.86	29.03	55.5	0.65	0.76	6.17	4.36	17.6

Table A-3: CP and Precipitation characteristics at Station Triebischthal OT Munzig in Summer

CP	Frequency [HH] (%)	Precipitation Probability (%)	Sum of Precipitation (mm)	Contribution [A] (%)	Wetness Index [A/HH]	Mean (mm)	Standard Deviation (mm)	Max. (mm)
CP01	13.97	48.05	1251.2	16.59	1.19	5.07	5.34	37.4
CP02	9.54	19.09	348.2	4.62	0.48	5.20	6.17	35.3
CP03	3.45	32.28	250.3	3.32	0.96	6.10	10.66	57.2
CP04	9.89	63.19	1679.9	22.27	2.25	7.30	9.53	57.5
CP05	8.29	40.66	663.5	8.80	1.06	5.35	5.95	40.0
CP06	6.41	30.93	346.8	4.60	0.72	4.75	6.02	35.5
CP07	6.49	54.81	883.8	11.72	1.80	6.75	7.58	40.3
CP08	5.38	43.43	420.3	5.57	1.04	4.89	7.82	49.0
CP09	11.60	20.37	368.6	4.89	0.42	4.24	5.07	28.6
CP10	8.32	33.99	539.4	7.15	0.86	5.19	10.66	104.4
CP11	7.09	21.46	164.0	2.17	0.31	2.93	2.96	12.5
CP12	8.67	23.20	576.2	7.64	0.88	7.79	9.99	58.7
CP99	0.90	36.36	51.8	0.69	0.77	4.32	2.66	9.4

Table A-4: CP and Precipitation characteristics at Station Obersteina in Summer

CP	Frequency [HH] (%)	Precipitation Probability (%)	Sum of Precipitation (mm)	Contribution [A] (%)	Wetness Index [A/HH]	Mean (mm)	Standard Deviation (mm)	Max. (mm)
CP01	13.97	58.17	1138.2	17.05	1.22	3.81	4.22	27.6
CP02	9.54	20.80	248.9	3.73	0.39	3.41	4.48	22.9
CP03	3.45	35.43	254.9	3.82	1.11	5.66	12.49	72.0
CP04	9.89	64.29	1326.1	19.87	2.01	5.67	6.46	46.5
CP05	8.29	48.85	722.6	10.83	1.31	4.85	6.68	44.8
CP06	6.41	33.90	266.4	3.99	0.62	3.33	4.26	24.0
CP07	6.49	60.67	801.9	12.01	1.85	5.53	5.76	29.1
CP08	5.38	44.44	364.5	5.46	1.01	4.14	5.76	39.1
CP09	11.60	19.67	314.8	4.72	0.41	3.75	5.38	33.7
CP10	8.32	44.44	568.6	8.52	1.02	4.18	9.61	85.9
CP11	7.09	23.37	158.7	2.38	0.34	2.60	3.43	16.9
CP12	8.67	28.21	459.5	6.88	0.79	5.11	7.71	47.7
CP99	0.90	27.27	49.6	0.74	0.83	5.51	4.93	13.2

Table A-5: CP and Precipitation characteristics at Station Ostrau in Summer

CP	Frequency [HH] (%)	Precipitation Probability (%)	Sum of Precipitation (mm)	Contribution [A] (%)	Wetness Index [A/HH]	Mean (mm)	Standard Deviation (mm)	Max. (mm)
CP01	13.97	58.17	1381.5	17.04	1.22	4.62	5.26	43.1
CP02	9.54	21.94	312.5	3.86	0.40	4.06	4.82	18.4
CP03	3.45	37.01	330.5	4.08	1.18	7.03	14.81	87.0
CP04	9.89	68.96	1799.9	22.21	2.24	7.17	8.61	50.8
CP05	8.29	49.84	821.9	10.14	1.22	5.41	7.36	60.5
CP06	6.41	33.47	310.8	3.83	0.60	3.93	5.33	33.0
CP07	6.49	59.41	965.5	11.91	1.83	6.8	7.59	46.7
CP08	5.38	45.45	418.4	5.16	0.96	4.65	6.31	40.5
CP09	11.60	23.89	398.7	4.92	0.42	3.91	4.41	21.5
CP10	8.32	43.46	614.2	7.58	0.91	4.62	7.12	63.8
CP11	7.09	27.20	204.1	2.52	0.36	2.87	3.09	14.7
CP12	8.67	28.53	482.2	5.95	0.69	5.30	7.20	31.2
CP99	0.90	30.30	65.3	0.81	0.90	6.53	5.76	18.2

Table A-6: CP and Precipitation characteristics at Station Höfchen (Kriebstein-TS) in Summer

CP	Frequency [HH] (%)	Precipitation Probability (%)	Sum of Precipitation (mm)	Contribution [A] (%)	Wetness Index [A/HH]	Mean (mm)	Standard Deviation (mm)	Max. (mm)
CP01	13.97	56.23	1081.9	16.66	1.19	3.74	4.39	28.2
CP02	9.54	19.94	239.2	3.68	0.39	3.42	4.63	21.5
CP03	3.45	33.07	296.9	4.57	1.33	7.07	18.13	112.0
CP04	9.89	64.29	1309.7	20.17	2.04	5.60	6.88	42.0
CP05	8.29	47.21	710.8	10.95	1.32	4.94	7.63	48.0
CP06	6.41	33.47	248.3	3.82	0.60	3.14	4.27	24.3
CP07	6.49	58.58	765.8	11.80	1.82	5.47	6.58	36.2
CP08	5.38	44.95	345.7	5.32	0.99	3.88	5.43	30.5
CP09	11.60	21.31	340.4	5.24	0.45	3.74	5.94	43.8
CP10	8.32	42.81	531.1	8.18	0.98	4.05	8.22	70.0
CP11	7.09	22.22	137.8	2.12	0.30	2.38	2.98	14.5
CP12	8.67	27.90	442.3	6.81	0.79	4.97	8.27	53.9
CP99	0.90	33.33	42.3	0.65	0.73	3.85	4.17	13.0

Table A-7: CP and Precipitation characteristics at Station Jöhstadt in Summer

CP	Frequency [HH] (%)	Precipitation Probability (%)	Sum of Precipitation (mm)	Contribution [A] (%)	Wetness Index [A/HH]	Mean (mm)	Standard Deviation (mm)	Max. (mm)
CP01	13.97	62.45	1522.6	15.99	1.14	4.74	5.09	27.4
CP02	9.54	27.07	430.6	4.52	0.47	4.53	7.51	58.3
CP03	3.45	45.67	313.6	3.29	0.95	5.41	8.55	46.0
CP04	9.89	77.20	2032.8	21.35	2.16	7.23	9.77	66.1
CP05	8.29	56.39	797.9	8.38	1.01	4.64	6.11	38.6
CP06	6.41	40.25	407.4	4.28	0.67	4.29	6.98	39.5
CP07	6.49	69.87	1161.7	12.20	1.88	6.96	7.85	51.2
CP08	5.38	52.53	553.0	5.81	1.08	5.32	6.94	32.8
CP09	11.60	31.38	503.2	5.28	0.46	3.76	4.88	26.8
CP10	8.32	49.02	746.2	7.84	0.94	4.97	7.92	63.7
CP11	7.09	37.93	360.6	3.79	0.53	3.64	4.99	25.5
CP12	8.67	34.48	629.6	6.61	0.76	5.72	8.14	36.0
CP99	0.90	45.45	62.8	0.66	0.74	4.19	6.19	24.0

Table A-8: CP and Precipitation characteristics at Station Weissbach in Summer

CP	Frequency [HH] (%)	Precipitation Probability (%)	Sum of Precipitation (mm)	Contribution [A] (%)	Wetness Index [A/HH]	Mean (mm)	Standard Deviation (mm)	Max. (mm)
CP01	13.97	62.84	1453.7	15.83	1.13	4.50	5.01	28.4
CP02	9.54	23.36	391.9	4.27	0.45	4.78	7.70	59.0
CP03	3.45	42.52	355.9	3.88	1.12	6.59	12.02	74.5
CP04	9.89	76.65	2071	22.55	2.28	7.42	9.78	65.0
CP05	8.29	56.07	794.0	8.65	1.04	4.64	6.37	37.6
CP06	6.41	40.68	427.4	4.65	0.73	4.45	7.15	40.7
CP07	6.49	65.69	1087.1	11.84	1.82	6.92	8.27	57.3
CP08	5.38	50.00	557.6	6.07	1.13	5.63	7.36	48.8
CP09	11.60	28.81	462.7	5.04	0.43	3.76	5.07	34.6
CP10	8.32	47.39	700.3	7.63	0.92	4.83	7.81	56.0
CP11	7.09	35.63	280.3	3.05	0.43	3.01	3.83	19.3
CP12	8.67	31.97	532.7	5.80	0.67	5.22	7.81	49.4
CP99	0.90	39.39	69.2	0.75	0.84	5.32	6.51	20.6

Table A-9: CP and Precipitation characteristics at Station Neuhausen in Summer

CP	Frequency [HH] (%)	Precipitation Probability (%)	Sum of Precipitation (mm)	Contribution [A] (%)	Wetness Index [A/HH]	Mean (mm)	Standard Deviation (mm)	Max. (mm)
CP01	13.97	66.15	1617.2	16.25	1.16	4.76	5.63	38.7
CP02	9.54	29.06	400.7	4.03	0.42	3.93	6.45	36.2
CP03	3.45	48.82	349.8	3.51	1.02	5.64	10.80	71.7
CP04	9.89	74.73	2152.2	21.62	2.19	7.91	11.12	76.2
CP05	8.29	60.66	855.9	8.60	1.04	4.63	6.24	35.1
CP06	6.41	41.53	499.9	5.02	0.78	5.10	8.07	43.7
CP07	6.49	70.71	1185.7	11.91	1.83	7.02	9.23	67.4
CP08	5.38	51.01	564.5	5.67	1.05	5.59	8.34	52.8
CP09	11.60	31.85	566.6	5.69	0.49	4.17	5.83	32.5
CP10	8.32	51.31	765.5	7.69	0.92	4.88	7.87	59.2
CP11	7.09	37.55	303.0	3.04	0.43	3.09	3.64	19.5
CP12	8.67	32.92	620.3	6.23	0.72	5.91	9.03	61.2
CP99	0.90	42.42	71.7	0.72	0.80	5.12	7.20	29.2

Table A-10: CP and Precipitation characteristics at Station Pockau in Summer

CP	Frequency [HH] (%)	Precipitation Probability (%)	Sum of Precipitation (mm)	Contribution [A] (%)	Wetness Index [A/HH]	Mean (mm)	Standard Deviation (mm)	Max. (mm)
CP01	13.97	62.45	1573	17.30	1.24	4.90	5.48	40.3
CP02	9.54	27.07	321.0	3.53	0.37	3.38	4.37	25.0
CP03	3.45	42.52	326.6	3.59	1.04	6.05	10.66	63.8
CP04	9.89	73.63	1963.7	21.59	2.18	7.33	9.83	60.7
CP05	8.29	56.72	790.7	14.75	1.78	4.57	5.52	31.3
CP06	6.41	38.98	442.6	4.87	0.76	4.81	7.58	47.7
CP07	6.49	64.85	1135.2	12.48	1.92	7.32	8.22	51.8
CP08	5.38	48.48	526.1	5.79	1.08	5.48	7.16	40.8
CP09	11.60	28.10	449.1	4.94	0.43	3.74	5.03	23.4
CP10	8.32	47.06	641.7	7.06	0.85	4.46	7.22	65.0
CP11	7.09	32.95	295.2	3.25	0.46	3.43	3.92	21.0
CP12	8.67	32.29	554.5	6.10	0.70	5.38	8.01	41.8
CP99	0.90	45.45	74.8	0.82	0.92	4.99	6.55	21.9

Table A-11: CP and Precipitation characteristics at Station Reifland (Saidenbach-TS) in Summer

CP	Frequency [HH] (%)	Precipitation Probability (%)	Sum of Precipitation (mm)	Contribution [A] (%)	Wetness Index [A/HH]	Mean (mm)	Standard Deviation (mm)	Max. (mm)
CP01	13.97	64.40	1587.4	17.41	1.25	4.80	5.58	47.7
CP02	9.54	27.92	344.1	3.77	0.40	3.51	4.54	24.6
CP03	3.45	43.31	337.0	3.70	1.07	6.13	10.84	65.7
CP04	9.89	77.47	1970.4	21.61	2.18	6.99	9.55	55.2
CP05	8.29	58.69	779.5	8.55	1.03	4.35	5.37	35.8
CP06	6.41	39.83	436.6	4.79	0.75	4.64	7.29	45.6
CP07	6.49	67.36	1087.9	11.93	1.84	6.76	7.90	50.3
CP08	5.38	53.54	536.3	5.88	1.09	5.06	7.21	41.3
CP09	11.60	29.74	441.3	4.84	0.42	3.47	4.62	23.3
CP10	8.32	48.37	679.7	7.45	0.90	4.59	7.50	69.5
CP11	7.09	38.31	311.9	3.42	0.48	3.12	3.65	22.3
CP12	8.67	33.23	532.0	5.83	0.67	5.02	6.94	39.2
CP99	0.90	36.36	75.2	0.82	0.92	6.27	6.39	20.3

Table A-12: CP and Precipitation characteristics at Station Forchheim in Summer

CP	Frequency [HH] (%)	Precipitation Probability (%)	Sum of Precipitation (mm)	Contribution [A] (%)	Wetness Index [A/HH]	Mean (mm)	Standard Deviation (mm)	Max. (mm)
CP01	13.97	60.89	1478.8	16.36	1.17	4.72	5.01	28.2
CP02	9.54	24.79	361.1	3.99	0.42	4.15	5.19	23.2
CP03	3.45	38.58	347.3	3.84	1.11	7.09	11.35	67.6
CP04	9.89	69.78	1967.1	21.76	2.20	7.74	10.16	67.5
CP05	8.29	55.74	802.2	8.87	1.07	4.72	6.08	37.8
CP06	6.41	37.29	435.3	4.82	0.75	4.95	7.55	44.7
CP07	6.49	64.44	1105.6	12.23	1.88	7.18	8.47	59.6
CP08	5.38	49.49	496.0	5.49	1.02	5.06	7.01	40.0
CP09	11.60	28.10	442.3	4.89	0.42	3.69	5.10	25.5
CP10	8.32	43.14	631.4	6.98	0.84	4.78	7.44	64.2
CP11	7.09	35.63	280.0	3.10	0.44	3.01	3.35	18.5
CP12	8.67	32.29	625.7	6.92	0.80	6.07	10.14	65.9
CP99	0.90	39.39	67.0	0.74	0.83	5.15	6.20	22.6

Table A-13: CP and Precipitation characteristics at Station Grünhainichen in Summer

CP	Frequency [HH] (%)	Precipitation Probability (%)	Sum of Precipitation (mm)	Contribution [A] (%)	Wetness Index [A/HH]	Mean (mm)	Standard Deviation (mm)	Max. (mm)
CP01	13.97	62.89	1668.7	17.46	1.25	5.18	5.99	54.4
CP02	9.53	23.50	417.6	4.37	0.46	5.09	6.82	36.6
CP03	3.47	42.52	353.5	3.70	1.07	6.55	11.45	71.1
CP04	9.83	73.06	1979.1	20.71	2.11	7.53	10.17	63.6
CP05	8.32	55.08	869.7	9.10	1.09	5.18	6.41	38.3
CP06	6.41	39.57	406.6	4.26	0.66	4.37	6.60	45.9
CP07	6.52	64.02	1212.0	12.68	1.94	7.92	9.44	67.9
CP08	5.32	48.21	534.5	5.59	1.05	5.69	7.56	45.4
CP09	11.65	27.40	468.9	4.91	0.42	4.01	5.04	23.4
CP10	8.32	45.25	778.2	8.14	0.98	5.64	8.62	70.5
CP11	7.04	34.50	261.3	2.73	0.39	2.94	2.97	13.9
CP12	8.71	31.66	526.2	5.51	0.63	5.21	6.96	38.8
CP99	0.90	42.42	79.2	0.83	0.92	5.66	6.87	24.5

Table A-14: CP and Precipitation characteristics at Station Burgstädt in Summer

CP	Frequency [HH] (%)	Precipitation Probability (%)	Sum of Precipitation (mm)	Contribution [A] (%)	Wetness Index [A/HH]	Mean (mm)	Standard Deviation (mm)	Max. (mm)
CP01	13.97	58.17	1371.6	17.19	1.23	4.59	5.36	45.3
CP02	9.54	19.66	356.0	4.46	0.47	5.16	8.75	62.2
CP03	3.45	41.73	333.2	4.18	1.21	6.29	13.15	75.8
CP04	9.89	69.78	1618.4	20.29	2.05	6.37	7.77	50.0
CP05	8.29	55.74	809.8	10.15	1.22	4.76	7.60	73.7
CP06	6.41	33.47	295.0	3.70	0.58	3.73	5.61	38.5
CP07	6.49	61.92	950.7	11.92	1.83	6.42	7.44	50.0
CP08	5.38	50.00	478.6	6.00	1.11	4.83	9.62	77.0
CP09	11.60	25.06	374.3	4.69	0.40	3.5	4.98	29.0
CP10	8.32	43.79	605.1	7.58	0.91	4.52	6.19	47.3
CP11	7.09	29.12	206.7	2.59	0.37	2.72	3.11	14.0
CP12	8.67	31.66	518.3	6.50	0.75	5.13	6.61	33.0
CP99	0.90	36.36	60.2	0.75	0.84	5.02	5.82	19.3

Table A-15: CP and Precipitation characteristics at Station Rittersgrün in Summer

CP	Frequency [HH] (%)	Precipitation Probability (%)	Sum of Precipitation (mm)	Contribution [A] (%)	Wetness Index [A/HH]	Mean (mm)	Standard Deviation (mm)	Max. (mm)
CP01	13.97	67.70	1664.8	15.34	1.10	4.78	5.02	28.2
CP02	9.54	28.21	408.6	3.76	0.39	4.13	5.75	35.2
CP03	3.45	48.82	352.7	3.25	0.94	5.69	9.19	40.5
CP04	9.89	79.67	2298.3	21.18	2.14	7.93	9.68	67.3
CP05	8.29	61.97	961.4	8.86	1.07	5.09	6.29	49.0
CP06	6.41	44.49	504.0	4.64	0.72	4.80	10.8	89.8
CP07	6.49	73.64	1396.9	12.87	1.98	7.94	10.02	61.0
CP08	5.38	61.11	706.5	6.51	1.21	5.84	8.93	53.5
CP09	11.60	34.43	561.6	5.17	0.45	3.82	4.72	23.0
CP10	8.32	50.65	788.8	7.27	0.87	5.09	8.30	54.7
CP11	7.09	44.83	421.5	3.88	0.55	3.60	5.24	33.5
CP12	8.67	36.36	696.9	6.42	0.74	6.01	8.83	47.0
CP99	0.90	51.52	91.2	0.84	0.94	5.36	8.00	33.5

Table A-16: CP and Precipitation characteristics at Station Bräunsdorf, Krs. Chemnitz in Summer

CP	Frequency [HH] (%)	Precipitation Probability (%)	Sum of Precipitation (mm)	Contribution [A] (%)	Wetness Index [A/HH]	Mean (mm)	Standard Deviation (mm)	Max. (mm)
CP01	13.97	60.12	1312.0	16.24	1.16	4.25	4.85	38.8
CP02	9.54	20.80	363.8	4.50	0.47	4.98	6.66	34.2
CP03	3.45	40.94	319.1	3.95	1.14	6.14	10.89	63.9
CP04	9.89	71.98	1702.8	21.08	2.13	6.50	8.17	57.5
CP05	8.29	53.77	779.7	9.65	1.16	4.75	6.95	57.4
CP06	6.41	33.05	330.7	4.09	0.64	4.24	5.34	36.6
CP07	6.49	68.62	1040.4	12.88	1.98	6.34	8.44	74.4
CP08	5.38	49.49	422.8	5.23	0.97	4.31	6.27	33.8
CP09	11.60	26.46	415.8	5.15	0.44	3.68	5.15	31.1
CP10	8.32	46.08	674.4	8.35	1.00	4.78	6.52	48.9
CP11	7.09	29.50	168.3	2.08	0.29	2.19	2.51	13.5
CP12	8.67	31.03	476.6	5.90	0.68	4.81	6.06	22.8
CP99	0.90	39.39	73.1	0.90	1.01	5.62	5.85	15.8

Table A-17: CP and Precipitation characteristics at Station Pleissa in Summer

CP	Frequency [HH] (%)	Precipitation Probability (%)	Sum of Precipitation (mm)	Contribution [A] (%)	Wetness Index [A/HH]	Mean (mm)	Standard Deviation (mm)	Max. (mm)
CP01	13.97	61.09	1173.8	16.89	1.21	3.74	4.16	30.6
CP02	9.54	21.37	327.3	4.71	0.49	4.36	5.27	23.4
CP03	3.45	36.22	280.8	4.04	1.17	6.10	13.07	78.6
CP04	9.89	66.76	1448.1	20.84	2.11	5.96	7.26	44.4
CP05	8.29	50.82	620.1	8.92	1.08	4.00	6.45	55.6
CP06	6.41	35.59	298.7	4.30	0.67	3.56	5.30	30.7
CP07	6.49	65.27	779.9	11.22	1.73	5.00	6.11	33.8
CP08	5.38	47.47	399.9	5.75	1.07	4.25	5.86	33.1
CP09	11.60	24.59	387.4	5.57	0.48	3.69	5.09	26.0
CP10	8.32	47.06	570.1	8.20	0.99	3.96	6.36	58.0
CP11	7.09	31.03	170.6	2.45	0.35	2.11	2.93	14.1
CP12	8.67	30.41	430.9	6.20	0.72	4.44	5.97	27.2
CP99	0.90	33.33	62.6	0.90	1.00	5.69	6.54	24.2

Table A-18: CP and Precipitation characteristics at Station Colditz in Summer

CP	Frequency [HH] (%)	Precipitation Probability (%)	Sum of Precipitation (mm)	Contribution [A] (%)	Wetness Index [A/HH]	Mean (mm)	Standard Deviation (mm)	Max. (mm)
CP01	13.97	57.78	1549.6	16.8	1.20	5.22	5.45	49.1
CP02	9.54	18.52	351.0	3.80	0.40	5.4	5.75	26.5
CP03	3.45	36.22	343.8	3.73	1.08	7.47	11.87	62.3
CP04	9.89	68.41	1955.6	21.20	2.14	7.85	8.82	51.8
CP05	8.29	53.44	827.7	8.97	1.08	5.08	7.29	69.6
CP06	6.41	33.05	364.5	3.95	0.62	4.67	5.77	39.5
CP07	6.49	61.92	1121.0	12.15	1.87	7.57	8.93	62.2
CP08	5.38	46.97	552.0	5.98	1.11	5.94	8.65	56.8
CP09	11.60	22.95	490.7	5.32	0.46	5.01	6.24	30.4
CP10	8.32	43.79	754.1	8.17	0.98	5.63	6.91	51.2
CP11	7.09	26.05	214.8	2.33	0.33	3.16	3.88	24.6
CP12	8.67	29.15	601.4	6.52	0.75	6.47	7.53	33.7
CP99	0.90	33.33	99.6	1.08	1.20	9.05	8.39	28.2

Table A-19: CP and Precipitation characteristics at Station Einsiedel (TS) in Summer

CP	Frequency [HH] (%)	Precipitation Probability (%)	Sum of Precipitation (mm)	Contribution [A] (%)	Wetness Index [A/HH]	Mean (mm)	Standard Deviation (mm)	Max. (mm)
CP01	14.06	61.49	1449	15.98	1.14	4.63	5.22	33.2
CP02	9.45	23.68	449.5	4.96	0.52	5.55	9.14	65.8
CP03	3.45	38.40	367.0	4.05	1.17	7.65	15.63	100.0
CP04	9.75	71.39	1953	21.54	2.21	7.75	9.98	70.0
CP05	8.40	53.95	840.0	9.27	1.10	5.12	7.89	61.4
CP06	6.46	39.74	401.3	4.43	0.68	4.32	6.07	32.5
CP07	6.49	67.66	1170.5	12.91	1.99	7.36	9.40	68.2
CP08	5.39	50.26	459.9	5.07	0.94	4.69	6.63	42.7
CP09	11.57	26.73	419.4	4.63	0.40	3.74	4.23	22.2
CP10	8.45	46.08	685.1	7.56	0.89	4.86	8.14	62.2
CP11	7.02	33.46	223.8	2.47	0.35	2.63	3.55	22.4
CP12	8.59	30.87	565.3	6.24	0.73	5.89	7.90	40.7
CP99	0.91	42.42	81.4	0.90	0.99	5.81	7.95	27.4

Table A-20: CP and Precipitation characteristics at Station Gablenz in Summer

CP	Frequency [HH] (%)	Precipitation Probability (%)	Sum of Precipitation (mm)	Contribution [A] (%)	Wetness Index [A/HH]	Mean (mm)	Standard Deviation (mm)	Max. (mm)
CP01	13.97	58.17	1503.3	16.61	1.19	5.03	4.97	28.7
CP02	9.54	23.65	438.6	4.85	0.51	5.28	8.69	58.9
CP03	3.45	41.73	298.9	3.30..	0.96	5.64	7.66	37.7
CP04	9.89	72.53	1904.7	21.04	2.13	7.21	8.54	53.9
CP05	8.26	53.29	766.4	8.47	1.02	4.73	6.08	43.6
CP06	6.41	39.41	358.4	3.96	0.62	3.85	5.94	40.0
CP07	6.50	68.20	1178.6	13.02	2.00	7.23	9.89	71.2
CP08	5.38	52.02	518.7	5.73	1.06	5.04	7.71	51.4
CP09	11.61	28.34	450.4	4.98	0.43	3.72	4.83	23.0
CP10	8.32	46.08	702.2	7.76	0.93	4.98	6.53	39.3
CP11	7.09	31.80	263.4	2.91	0.41	3.17	4.27	26.3
CP12	8.67	30.72	577.9	6.38	0.74	5.90	7.75	37.8
CP99	0.90	45.45	90.6	1.00	1.12	6.04	8.65	28.1

Table A-21: CP and Precipitation characteristics at Station Chemnitz (WST) in Summer

CP	Frequency [HH] (%)	Precipitation Probability (%)	Sum of Precipitation (mm)	Contribution [A] (%)	Wetness Index [A/HH]	Mean (mm)	Standard Deviation (mm)	Max. (mm)
CP01	13.97	62.84	1407.3	16.45	1.18	4.36	5.03	35.3
CP02	9.54	21.08	378.0	4.42	0.46	5.11	6.47	36.4
CP03	3.45	41.73	311.8	3.65	1.06	5.88	11.15	64.6
CP04	9.89	71.70	1856.0	21.70	2.19	7.11	8.69	48.8
CP05	8.29	56.07	794.5	9.29	1.12	4.65	7.25	64.2
CP06	6.41	34.32	327.8	3.83	0.60	4.05	6.14	37.0
CP07	6.49	66.53	1064.4	12.45	1.92	6.69	8.96	58.0
CP08	5.38	49.49	491.2	5.74	1.07	5.01	7.59	54.3
CP09	11.60	28.81	411.9	4.82	0.42	3.35	4.26	22.6
CP10	8.32	44.12	675.4	7.90	0.95	5.00	6.65	40.8
CP11	7.09	33.33	209.9	2.45	0.35	2.41	2.98	18.1
CP12	8.67	30.09	537.3	6.28	0.72	5.60	7.93	43.8
CP99	0.90	42.42	87.0	1.02	1.13	6.21	7.26	26.0

Table A-22: CP and Precipitation characteristics at Station Grosshartmannsdorf in Summer

CP	Frequency [HH] (%)	Precipitation Probability (%)	Sum of Precipitation (mm)	Contribution [A] (%)	Wetness Index [A/HH]	Mean (mm)	Standard Deviation (mm)	Max. (mm)
CP01	14.02	62.9	1516.1	17.66	1.26	4.78	5.65	45.6
CP02	9.71	25.21	369.2	4.30	0.44	4.20	5.21	25.0
CP03	3.45	45.16	289.7	3.38	0.98	5.17	10.69	70.8
CP04	9.63	73.70	1950.8	22.73	2.36	7.65	9.83	61.5
CP05	8.21	58.31	716.3	8.35	1.02	4.16	4.89	25.5
CP06	6.51	35.04	329.5	3.84	0.59	4.02	6.38	38.8
CP07	6.40	64.35	1025.7	11.95	1.87	6.93	8.25	42.6
CP08	5.40	50.52	491.5	5.73	1.06	5.02	6.29	35.0
CP09	11.69	27.62	478.0	5.57	0.48	4.12	6.27	38.8
CP10	8.38	48.17	618.0	7.20	0.86	4.26	7.77	76.0
CP11	7.18	35.66	227.7	2.65	0.37	2.48	2.72	14.4
CP12	8.51	31.37	505.4	5.89	0.69	5.26	7.63	39.2
CP99	0.92	39.39	65.0	0.76	0.82	5.00	4.47	19.0

Table A-23: CP and Precipitation characteristics at Station Oberbobritzsch in Summer

CP	Frequency [HH] (%)	Precipitation Probability (%)	Sum of Precipitation (mm)	Contribution [A] (%)	Wetness Index [A/HH]	Mean (mm)	Standard Deviation (mm)	Max. (mm)
CP01	14.00	65.75	1558.1	17.77	1.27	4.64	5.43	31.5
CP02	9.56	28.08	431.8	4.92	0.52	4.41	6.32	28.2
CP03	3.48	49.61	365.5	4.17	1.20	5.80	11.06	64.5
CP04	9.92	76.80	1865.4	21.28	2.15	6.71	9.77	69.6
CP05	8.33	60.20	792.3	9.04	1.08	4.33	5.53	33.2
CP06	6.38	44.21	372.1	4.24	0.66	3.61	5.84	38.8
CP07	6.47	69.07	1034.4	11.80	1.82	6.35	8.00	55.0
CP08	5.37	55.10	452.5	5.16	0.96	4.19	6.41	49.6
CP09	11.62	30.66	444.9	5.07	0.44	3.42	4.51	23.8
CP10	8.36	48.52	614.7	7.01	0.84	4.15	7.60	75.3
CP11	7.04	39.69	247.5	2.82	0.40	2.43	3.13	16.6
CP12	8.60	33.12	546.4	6.23	0.72	5.25	8.38	50.1
CP99	0.88	34.38	42.1	0.48	0.55	3.83	2.09	7.1

Table A-24: CP and Precipitation characteristics at Station St. Michaelis in Summer

CP	Frequency [HH] (%)	Precipitation Probability (%)	Sum of Precipitation (mm)	Contribution [A] (%)	Wetness Index [A/HH]	Mean (mm)	Standard Deviation (mm)	Max. (mm)
CP01	13.97	63.04	1669.9	17.73	1.27	5.15	5.68	35.0
CP02	9.54	22.51	386.1	4.10	0.43	4.89	5.79	24.3
CP03	3.45	42.52	396.5	4.21	1.22	7.34	13.46	79.3
CP04	9.89	75.27	1991	21.14	2.14	7.27	9.46	72.8
CP05	8.29	56.72	787.1	8.36	1.01	4.55	5.31	26.3
CP06	6.41	38.14	395.2	4.20	0.65	4.39	6.07	36.8
CP07	6.49	66.95	1061.2	11.27	1.74	6.63	7.94	38.0
CP08	5.38	51.52	585.8	6.22	1.16	5.74	7.96	42.6
CP09	11.60	29.74	501.7	5.33	0.46	3.95	4.90	20.4
CP10	8.32	46.41	729.7	7.75	0.93	5.14	9.45	95.6
CP11	7.09	35.63	258.3	2.74	0.39	2.78	3.09	19.7
CP12	8.67	31.03	574.0	6.10	0.70	5.80	8.75	43.2
CP99	0.90	36.36	80.9	0.86	0.96	6.74	6.88	28.3

Table A-25: CP and Precipitation characteristics at Station Bräunsdorf, Krs. Freiberg in Summer

CP	Frequency [HH] (%)	Precipitation Probability (%)	Sum of Precipitation (mm)	Contribution [A] (%)	Wetness Index [A/HH]	Mean (mm)	Standard Deviation (mm)	Max. (mm)
CP01	13.97	63.04	1505.2	17.32	1.24	4.65	6.30	55.3
CP02	9.54	23.08	325.4	3.74	0.39	4.02	5.05	21.9
CP03	3.45	44.09	314.2	3.62	1.05	5.61	11.53	71.7
CP04	9.89	70.60	2014.5	23.18	2.34	7.84	10.56	92.6
CP05	8.29	58.03	814.4	9.37	1.13	4.60	6.93	57.5
CP06	6.41	35.59	382.4	4.40	0.69	4.55	6.97	37.6
CP07	6.49	64.44	940.6	10.82	1.67	6.11	7.04	33.5
CP08	5.38	53.03	468.1	5.39	1.00	4.46	6.83	51.8
CP09	11.60	27.63	442.3	5.09	0.44	3.75	4.69	21.6
CP10	8.32	47.06	628.5	7.23	0.87	4.36	6.42	56.1
CP11	7.09	34.10	201.5	2.32	0.33	2.26	2.90	15.5
CP12	8.67	31.35	590.8	6.80	0.78	5.91	9.18	46.2
CP99	0.90	36.36	62.9	0.72	0.81	5.24	5.05	17.1

Table A-26: CP and Precipitation characteristics at Station Drebach in Summer

CP	Frequency [HH] (%)	Precipitation Probability (%)	Sum of Precipitation (mm)	Contribution [A] (%)	Wetness Index [A/HH]	Mean (mm)	Standard Deviation (mm)	Max. (mm)
CP01	14.00	63.41	1725.7	17.64	1.26	5.33	6.54	45.8
CP02	9.48	26.01	333.0	3.40	0.36	3.70	4.53	22.5
CP03	3.48	44.09	403.3	4.12	1.18	7.20	12.89	72.2
CP04	9.92	76.24	2138.1	21.85	2.20	7.75	10.13	63.5
CP05	8.33	57.24	805.8	8.24	0.99	4.63	6.01	44.3
CP06	6.44	37.45	451.8	4.62	0.72	5.13	7.50	41.0
CP07	6.52	71.01	1155.6	11.81	1.81	6.84	8.43	53.4
CP08	5.34	50.26	631.2	6.45	1.21	6.44	9.18	51.3
CP09	11.62	28.07	455.2	4.65	0.40	3.83	5.02	27.5
CP10	8.39	47.06	712.8	7.29	0.87	4.95	7.38	57.7
CP11	6.99	38.82	323.3	3.30	0.47	3.27	4.72	33.4
CP12	8.69	34.38	575.2	5.88	0.68	5.28	7.57	47.0
CP99	0.79	41.38	73.0	0.75	0.94	6.08	5.96	19.7

Table A-27: CP and Precipitation characteristics at Station Augustusburg in Summer

CP	Frequency [HH] (%)	Precipitation Probability (%)	Sum of Precipitation (mm)	Contribution [A] (%)	Wetness Index [A/HH]	Mean (mm)	Standard Deviation (mm)	Max. (mm)
CP01	13.91	61.92	1526.8	17.50	1.26	4.94	5.62	35.6
CP02	9.64	21.97	332.4	3.81	0.40	4.37	4.80	22.0
CP03	3.40	35.25	288.7	3.31	0.97	6.71	12.14	70.6
CP04	9.84	70.54	1836.2	21.04	2.14	7.37	9.54	65.3
CP05	8.17	57.68	779.6	8.93	1.09	4.61	6.54	45.5
CP06	6.49	36.91	358.6	4.11	0.63	4.17	6.00	40.2
CP07	6.52	63.25	1065.6	12.21	1.87	7.20	8.37	50.3
CP08	5.43	49.23	538.6	6.17	1.14	5.61	7.91	53.6
CP09	11.57	25.06	423.5	4.85	0.42	4.07	5.05	31.8
CP10	8.22	45.76	700.6	8.03	0.98	5.19	7.50	56.6
CP11	7.11	32.94	210.8	2.42	0.34	2.51	2.49	11.7
CP12	8.81	31.96	583.9	6.69	0.76	5.78	10.16	70.6
CP99	0.89	40.63	80.1	0.92	1.03	6.16	6.68	27.6

Table A-28: CP and Precipitation characteristics at Station Flöha in Summer

CP	Frequency [HH] (%)	Precipitation Probability (%)	Sum of Precipitation (mm)	Contribution [A] (%)	Wetness Index [A/HH]	Mean (mm)	Standard Deviation (mm)	Max. (mm)
CP01	13.97	54.47	1537.5	17.47	1.25	5.49	6.15	45.2
CP02	9.54	17.95	293.0	3.33	0.35	4.65	5.22	22.5
CP03	3.45	34.65	291.8	3.31	0.96	6.63	12.87	71.8
CP04	9.89	67.03	1745.8	19.83	2.01	7.15	8.56	55.0
CP05	8.29	55.41	947.3	10.76	1.30	5.61	8.38	69.3
CP06	6.41	31.78	401.7	4.56	0.71	5.36	7.62	46.2
CP07	6.49	58.58	1093.4	12.42	1.91	7.81	9.90	68.8
CP08	5.38	46.46	478.2	5.43	1.01	5.20	7.25	49.6
CP09	11.60	22.01	470.1	5.34	0.46	5.00	5.90	38.2
CP10	8.32	41.18	697.5	7.92	0.95	5.54	8.38	58.3
CP11	7.09	27.20	196.4	2.23	0.31	2.77	2.52	13.3
CP12	8.67	27.90	565.6	6.43	0.74	6.36	8.65	44.7
CP99	0.90	39.39	84.5	0.96	1.07	6.50	5.67	21.0

Table A-29: CP and Precipitation characteristics at Station Reinersdorf in Summer

CP	Frequency [HH] (%)	Precipitation Probability (%)	Sum of Precipitation (mm)	Contribution [A] (%)	Wetness Index [A/HH]	Mean (mm)	Standard Deviation (mm)	Max. (mm)
CP01	13.97	51.75	1161.4	17.13	1.23	4.37	4.44	24.8
CP02	9.54	18.23	285.8	4.21	0.44	4.47	5.98	29.2
CP03	3.45	37.01	235.0	3.47	1.00	5.00	8.97	46.3
CP04	9.89	60.71	1401.3	20.66	2.09	6.34	8.20	51.5
CP05	8.29	41.31	594.5	8.77	1.06	4.72	5.56	32.8
CP06	6.41	30.08	302.0	4.45	0.69	4.25	4.92	26.3
CP07	6.49	59.00	835.7	12.32	1.90	5.93	6.25	37.1
CP08	5.38	42.42	334.8	4.94	0.92	3.99	5.07	27.2
CP09	11.60	22.95	357.9	5.28	0.45	3.65	4.34	24.8
CP10	8.32	38.56	561.1	8.27	0.99	4.76	10.16	99.3
CP11	7.09	22.99	164.0	2.42	0.34	2.73	2.63	11.2
CP12	8.67	23.51	506.2	7.46	0.86	6.75	12,24	64.0
CP99	0.90	30.30	42.1	0.62	0.69	4.21	4.67	17.0

Table A-30: CP and Precipitation characteristics at Station Kadan, Tuimice in Summer

CP	Frequency [HH] (%)	Precipitation Probability (%)	Sum of Precipitation (mm)	Contribution [A] (%)	Wetness Index [A/HH]	Mean (mm)	Standard Deviation (mm)	Max. (mm)
CP01	13.97	54.47	757.4	13.98	1.00	2.70	3.85	24.3
CP02	9.54	26.21	236.2	4.36	0.46	2.57	4.18	19.9
CP03	3.45	38.58	220.7	4.07	1.18	4.50	7.46	35.7
CP04	9.89	62.09	842.4	15.55	1.57	3.73	5.45	29.5
CP05	8.29	53.11	553.4	10.21	1.23	3.42	5.13	33.8
CP06	6.41	32.63	263.0	4.85	0.76	3.42	7.49	45.8
CP07	6.49	66.53	855.8	15.80	2.43	5.38	6.79	40.2
CP08	5.38	45.45	316.6	5.84	1.09	3.52	4.75	18.0
CP09	11.60	26.46	295.2	5.45	0.47	2.61	4.75	30.0
CP10	8.32	46.73	404.2	7.46	0.90	2.83	3.81	24.7
CP11	7.09	27.59	151.2	2.79	0.39	2.10	4.35	31.1
CP12	8.67	32.92	493.9	9.12	1.05	4.70	7.45	46.3
CP99	0.90	39.39	27.9	0.51	0.57	2.15	3.38	13.0

Table A-31: CP and Precipitation characteristics at Station Kopisty in Summer

CP	Frequency [HH] (%)	Precipitation Probability (%)	Sum of Precipitation (mm)	Contribution [A] (%)	Wetness Index [A/HH]	Mean (mm)	Standard Deviation (mm)	Max. (mm)
CP01	13.97	52.72	806.2	14.83	1.06	2.97	3.63	20.1
CP02	9.54	23.65	216.2	3.98	0.42	2.60	3.77	17.5
CP03	3.45	33.86	176.2	3.24	0.94	4.10	5.83	26.3
CP04	9.89	57.42	875.3	16.10	1.63	4.19	5.75	36.1
CP05	8.29	48.52	564.5	10.39	1.25	3.81	5.08	28.9
CP06	6.41	29.24	217.6	4.00	0.62	3.15	5.93	27.4
CP07	6.49	59.00	824.7	15.17	2.34	5.85	7.33	38.4
CP08	5.38	39.90	318.8	5.87	1.09	4.04	5.28	22.7
CP09	11.60	27.17	311.5	5.73	0.49	2.69	4.08	21.7
CP10	8.32	44.12	442.1	8.13	0.98	3.27	4.55	32.7
CP11	7.09	24.14	140.7	2.59	0.37	2.23	3.67	20.7
CP12	8.67	29.78	493.0	9.07	1.05	5.19	8.24	57.0
CP99	0.90	42.42	48.3	0.89	0.99	3.45	6.43	25.1

Table A-32: CP and Precipitation characteristics at Station Hartmannsdorf (LehnmühleTS) in Winter

CP	Frequency [HH] (%)	Precipitation Probability (%)	Sum of Precipitation (mm)	Contribution [A] (%)	Wetness Index [A/HH]	Mean (mm)	Standard Deviation (mm)	Max. (mm)
CP01	15.94	73.47	2074.3	26.29	1.65	4.93	6.26	44.8
CP02	7.51	36.30	221.7	2.81	0.37	2.26	3.00	17.5
CP03	3.51	72.22	350.2	4.44	1.27	3.85	5.19	27.7
CP04	7.65	88.36	1614.5	20.46	2.67	6.64	7.13	61.2
CP05	7.40	46.24	358.4	4.54	0.61	2.91	4.29	35.1
CP06	5.82	46.89	225.2	2.85	0.49	2.30	3.01	19.0
CP07	6.29	74.34	889.6	11.27	1.79	5.30	6.40	27.0
CP08	5.18	54.30	327.8	4.15	0.80	3.25	2.87	12.5
CP09	14.97	38.10	479.9	6.08	0.41	2.34	2.75	17.2
CP10	8.93	53.89	629.8	7.98	0.89	3.64	4.22	24.4
CP11	5.84	56.19	348.0	4.41	0.75	2.95	3.96	22.4
CP12	9.65	38.90	305.2	3.87	0.40	2.26	3.19	17.4
CP99	1.31	48.94	65.8	0.83	0.64	2.86	3.8	14.2

Table A-33: CP and Precipitation characteristics at Station Klingenberg (TS) in Winter

CP	Frequency [HH] (%)	Precipitation Probability (%)	Sum of Precipitation (mm)	Contribution [A] (%)	Wetness Index [A/HH]	Mean (mm)	Standard Deviation (mm)	Max. (mm)
CP01	15.79	71.88	1636.4	25.45	1.61	4.19	5.52	36.7
CP02	7.46	35.41	182.6	2.84	0.38	2.01	2.66	14.2
CP03	3.51	73.55	269.4	4.19	1.19	3.03	4.07	25.7
CP04	7.57	90.42	1306	20.31	2.68	5.53	5.92	50.0
CP05	7.37	48.43	311.7	4.85	0.66	2.53	3.55	22.5
CP06	5.89	50.74	184.3	2.87	0.49	1.79	2.40	15.4
CP07	6.36	74.43	819.8	12.75	2.01	5.03	6.11	34.2
CP08	5.22	57.22	299.9	4.66	0.89	2.91	3.23	15.6
CP09	14.65	36.04	360.9	5.61	0.38	1.98	2.3	12.1
CP10	9.29	54.69	490.9	7.64	0.82	2.81	3.68	26.4
CP11	5.86	58.42	269.0	4.18	0.71	2.28	3.49	21.0
CP12	9.84	38.35	246.0	3.83	0.39	1.89	2.63	14.4
CP99	1.19	53.66	51.9	0.81	0.68	2.36	3.26	13.5

Table A-34: CP and Precipitation characteristics at Station Triebischthal OT Munzig in Winter

CP	Frequency [HH] (%)	Precipitation Probability (%)	Sum of Precipitation (mm)	Contribution [A] (%)	Wetness Index [A/HH]	Mean (mm)	Standard Deviation (mm)	Max. (mm)
CP01	16.18	60.14	1594.3	27.40	1.69	4.68	5.42	43.2
CP02	7.70	24.81	178.2	3.06	0.40	2.66	2.94	15.0
CP03	3.34	60.68	221.2	3.80	1.14	3.12	4.32	34.1
CP04	7.53	78.03	981.6	16.87	2.24	4.77	4.97	38.5
CP05	7.16	35.06	262.9	4.52	0.63	2.99	3.76	28.6
CP06	5.91	36.23	158.8	2.73	0.46	2.12	2.11	11.4
CP07	6.08	63.38	715.1	12.29	2.02	5.30	6.45	37.8
CP08	5.25	47.83	291.6	5.01	0.95	3.31	3.20	16.6
CP09	15.06	25.76	323.4	5.56	0.37	2.38	2.51	14.8
CP10	8.84	43.23	522.2	8.98	1.01	3.90	3.83	20.7
CP11	5.99	44.76	253.3	4.35	0.73	2.69	3.44	19.0
CP12	9.61	26.41	258.7	4.45	0.46	2.91	3.23	18.2
CP99	1.34	48.94	56.6	0.97	0.73	2.46	2.89	13.8

Table A-35: CP and Precipitation characteristics at Station Obersteina in Winter

CP	Frequency [HH] (%)	Precipitation Probability (%)	Sum of Precipitation (mm)	Contribution [A] (%)	Wetness Index [A/HH]	Mean (mm)	Standard Deviation (mm)	Max. (mm)
CP01	16.08	65.87	1596.5	28.00	1.74	4.16	4.81	33.2
CP02	7.50	25.00	140.0	2.46	0.33	2.06	2.75	15.1
CP03	3.48	55.56	159.1	2.79	0.80	2.27	3.01	16.2
CP04	7.59	84.00	998.8	17.52	2.31	4.32	4.70	30.3
CP05	7.37	43.82	304.0	5.33	0.72	2.60	3.13	24.2
CP06	5.79	40.48	154.8	2.72	0.47	1.82	2.44	16.6
CP07	6.23	68.14	736.3	12.92	2.07	4.78	6.64	39.0
CP08	5.13	51.61	261.6	4.59	0.89	2.72	2.84	13.3
CP09	14.90	30.19	308.5	5.41	0.36	1.89	2.36	13.6
CP10	9.13	51.06	588.9	10.33	1.13	3.48	3.67	21.4
CP11	5.85	43.40	165.6	2.90	0.50	1.80	2.11	9.7
CP12	9.66	31.71	238.6	4.19	0.43	2.15	2.59	10.8
CP99	1.30	53.19	48.2	0.85	0.65	1.93	3.67	18.3

Table A-36: CP and Precipitation characteristics at Station Ostrau in Winter

CP	Frequency [HH] (%)	Precipitation Probability (%)	Sum of Precipitation (mm)	Contribution [A] (%)	Wetness Index [A/HH]	Mean (mm)	Standard Deviation (mm)	Max. (mm)
CP01	16.08	67.07	1952.7	27.83	1.73	4.99	6.07	42.6
CP02	7.50	25.74	171.6	2.45	0.33	2.45	2.98	15.6
CP03	3.48	63.49	222.6	3.17	0.91	2.78	4.16	21.9
CP04	7.59	84.73	1320.1	18.81	2.48	5.67	6.18	50.1
CP05	7.37	41.95	339.8	4.84	0.66	3.03	4.06	32.8
CP06	5.79	41.90	202.3	2.88	0.50	2.30	2.93	19.3
CP07	6.23	65.93	862.8	12.29	1.97	5.79	7.41	42.4
CP08	5.13	53.23	330.3	4.71	0.92	3.34	3.12	13.5
CP09	14.90	28.52	374.8	5.34	0.36	2.43	2.79	15.7
CP10	9.13	51.36	677.9	9.66	1.06	3.99	4.34	24.5
CP11	5.85	45.28	234.9	3.35	0.57	2.45	3.30	18.7
CP12	9.66	30.86	271.2	3.86	0.40	2.51	2.83	12.1
CP99	1.30	46.81	56.5	0.81	0.62	2.57	4.97	23.5

Table A-37: CP and Precipitation characteristics at Station Höfchen(Kriebstein-TS) in Winter

CP	Frequency [HH] (%)	Precipitation Probability (%)	Sum of Precipitation (mm)	Contribution [A] (%)	Wetness Index [A/HH]	Mean (mm)	Standard Deviation (mm)	Max. (mm)
CP01	16.08	65.69	1550.6	29.03	1.80	4.05	5.01	34.5
CP02	7.50	25.37	119.8	2.24	0.30	1.74	2.33	14.9
CP03	3.48	54.76	155.9	2.92	0.84	2.26	2.81	15.0
CP04	7.59	78.55	914.4	17.12	2.26	4.23	4.90	32.5
CP05	7.37	42.70	281.4	5.27	0.72	2.47	3.30	25.5
CP06	5.79	36.19	157.6	2.95	0.51	2.07	2.67	18.0
CP07	6.23	63.72	708.0	13.25	2.13	4.92	6.90	43.9
CP08	5.13	51.61	229.6	4.30	0.84	2.39	2.30	9.1
CP09	14.90	28.33	281.7	5.27	0.35	1.84	2.42	15.3
CP10	9.13	49.24	540.2	10.11	1.11	3.31	3.53	22.7
CP11	5.85	41.04	136.5	2.56	0.44	1.57	1.95	9.6
CP12	9.66	28.00	225.9	4.23	0.44	2.31	2.56	10.5
CP99	1.30	44.68	40.4	0.76	0.58	1.92	4.03	19.0

Table A-38: CP and Precipitation characteristics at Station Jöhstadt in Winter

CP	Frequency [HH] (%)	Precipitation Probability (%)	Sum of Precipitation (mm)	Contribution [A] (%)	Wetness Index [A/HH]	Mean (mm)	Standard Deviation (mm)	Max. (mm)
CP01	16.08	73.58	1960.0	25.36	1.58	4.57	5.13	32.6
CP02	7.50	37.50	209.9	2.72	0.36	2.06	2.48	15.2
CP03	3.48	69.84	286.6	3.71	1.07	3.26	2.98	11.5
CP04	7.59	89.82	1541.7	19.95	2.63	6.24	6.21	40.7
CP05	7.37	44.94	343.0	4.44	0.60	2.86	3.77	31.5
CP06	5.79	48.10	211.0	2.73	0.47	2.09	2.56	11.8
CP07	6.23	72.12	896.4	11.60	1.86	5.50	6.16	35.2
CP08	5.13	55.38	364.3	4.71	0.92	3.54	3.12	12.0
CP09	14.90	35.74	442.1	5.72	0.38	2.29	2.41	11.2
CP10	9.13	58.61	665.3	8.61	0.94	3.43	4.11	26.8
CP11	5.85	56.13	329.0	4.26	0.73	2.76	3.52	21.3
CP12	9.66	41.14	434.5	5.62	0.58	3.02	4.43	33.1
CP99	1.30	44.68	45.5	0.59	0.45	2.17	2.32	7.8

Table A-39: CP and Precipitation characteristics at Station Weissbach in Winter

CP	Frequency [HH] (%)	Precipitation Probability (%)	Sum of Precipitation (mm)	Contribution [A] (%)	Wetness Index [A/HH]	Mean (mm)	Standard Deviation (mm)	Max. (mm)
CP01	16.02	71.53	2050.4	27.58	1.72	4.98	6.28	46.0
CP02	7.54	33.95	174.4	2.35	0.31	1.90	2.35	14.2
CP03	3.50	68.25	264.9	3.56	1.02	3.08	3.35	16.0
CP04	7.62	88.32	1595.5	21.46	2.82	6.59	7.07	53.4
CP05	7.29	41.98	342.8	4.61	0.63	3.12	3.75	26.0
CP06	5.76	45.89	197.7	2.66	0.46	2.08	2.26	12.5
CP07	6.29	70.80	844.8	11.36	1.81	5.28	6.54	35.0
CP08	5.17	55.91	350.5	4.71	0.91	3.37	3.10	15.0
CP09	14.94	35.94	401.2	5.40	0.36	2.08	2.57	14.6
CP10	9.12	54.88	612.1	8.23	0.90	3.40	4.13	19.2
CP11	5.81	55.98	277.8	3.74	0.64	2.37	3.16	16.7
CP12	9.62	34.10	272.0	3.66	0.38	2.31	2.88	12.9
CP99	1.31	51.06	50.5	0.68	0.52	2.10	3.16	14.6

Table A-40: CP and Precipitation characteristics at Station Neuhausen in Winter

CP	Frequency [HH] (%)	Precipitation Probability (%)	Sum of Precipitation (mm)	Contribution [A] (%)	Wetness Index [A/HH]	Mean (mm)	Standard Deviation (mm)	Max. (mm)
CP01	16.08	76.84	2230.2	26.63	1.66	4.98	6.29	44.8
CP02	7.50	42.28	221.5	2.64	0.35	1.93	2.88	17.8
CP03	3.48	75.40	310.4	3.71	1.07	3.27	3.85	20.4
CP04	7.59	90.18	1779.2	21.24	2.80	7.17	7.52	54.3
CP05	7.37	46.82	339.1	4.05	0.55	2.71	3.65	27.5
CP06	5.79	50.95	240.8	2.87	0.50	2.25	2.50	12.8
CP07	6.23	75.66	914.5	10.92	1.75	5.35	6.32	29.0
CP08	5.13	58.06	345.5	4.12	0.80	3.20	3.16	16.6
CP09	14.90	41.85	520.4	6.21	0.42	2.30	2.87	17.3
CP10	9.13	60.42	690.3	8.24	0.90	3.45	4.19	27.5
CP11	5.85	61.79	364.6	4.35	0.74	2.78	3.98	28.3
CP12	9.66	40.00	369.8	4.41	0.46	2.64	3.74	28.0
CP99	1.30	48.94	49.7	0.59	0.46	2.16	2.70	10.3

Table A-41: CP and Precipitation characteristics at Station Pockau in Winter

CP	Frequency [HH] (%)	Precipitation Probability (%)	Sum of Precipitation (mm)	Contribution [A] (%)	Wetness Index [A/HH]	Mean (mm)	Standard Deviation (mm)	Max. (mm)
CP01	16.08	70.84	2108.1	27.32	1.70	5.10	6.25	41.2
CP02	7.50	31.25	176.9	2.29	0.31	2.08	2.34	10.8
CP03	3.48	70.63	283.4	3.67	1.06	3.18	3.92	26.8
CP04	7.59	85.09	1634.7	21.18	2.79	6.99	7.24	55.9
CP05	7.37	45.32	357.6	4.63	0.63	2.96	3.78	27.7
CP06	5.79	43.81	207.5	2.69	0.46	2.26	2.33	13.1
CP07	6.23	68.58	888.9	11.52	1.85	5.73	7.07	40.9
CP08	5.13	53.76	332.8	4.31	0.84	3.33	3.00	17.5
CP09	14.90	32.41	416.7	5.40	0.36	2.38	2.77	13.5
CP10	9.13	54.68	676.5	8.77	0.96	3.74	4.02	18.1
CP11	5.85	45.28	287.3	3.72	0.64	2.99	3.63	21.3
CP12	9.66	32.86	296.3	3.84	0.40	2.58	3.02	15.4
CP99	1.30	46.81	50.1	0.65	0.50	2.28	3.27	14.5

Table A-42: CP and Precipitation characteristics at Station Reifland (Saidenbach-TS) in Winter

CP	Frequency [HH] (%)	Precipitation Probability (%)	Sum of Precipitation (mm)	Contribution [A] (%)	Wetness Index [A/HH]	Mean (mm)	Standard Deviation (mm)	Max. (mm)
CP01	16.08	72.90	2044.1	27.45	1.71	4.81	5.93	39.3
CP02	7.50	36.76	173.7	2.33	0.31	1.74	2.26	12.0
CP03	3.48	74.60	279.8	3.76	1.08	2.98	3.34	17.5
CP04	7.59	88.36	1524.4	20.47	2.70	6.27	6.66	49.3
CP05	7.37	45.69	347.0	4.66	0.63	2.84	3.52	25.1
CP06	5.79	48.57	208.9	2.81	0.48	2.05	2.35	13.4
CP07	6.23	73.45	857.9	11.52	1.85	5.17	6.24	32.8
CP08	5.13	55.91	330.2	4.43	0.86	3.18	2.84	16.4
CP09	14.90	37.78	450.0	6.04	0.41	2.21	2.85	19.5
CP10	9.13	56.50	628.8	8.44	0.92	3.36	3.94	22.2
CP11	5.85	53.30	287.2	3.86	0.66	2.54	3.11	19.4
CP12	9.66	35.43	265.9	3.57	0.37	2.14	2.57	13.8
CP99	1.30	48.94	48.2	0.65	0.50	2.10	2.80	12.3

Table A-43: CP and Precipitation characteristics at Station Forchheim in Winter

CP	Frequency [HH] (%)	Precipitation Probability (%)	Sum of Precipitation (mm)	Contribution [A] (%)	Wetness Index [A/HH]	Mean (mm)	Standard Deviation (mm)	Max. (mm)
CP01	16.08	70.67	1964.4	26.26	1.63	4.77	5.90	39.4
CP02	7.50	33.46	172.8	2.31	0.31	1.90	2.24	9.3
CP03	3.48	69.05	294.6	3.94	1.13	3.39	3.45	17.9
CP04	7.59	87.27	1592.0	21.28	2.81	6.63	6.31	42.6
CP05	7.37	41.57	352.5	4.71	0.64	3.18	5.18	49.5
CP06	5.79	43.33	222.7	2.98	0.51	2.45	2.74	14.3
CP07	6.23	67.26	861.2	11.51	1.85	5.67	6.38	30.3
CP08	5.13	53.76	326.0	4.36	0.85	3.26	2.73	17.2
CP09	14.90	34.07	441.3	5.90	0.40	2.40	2.72	14.7
CP10	9.13	53.78	618.2	8.26	0.91	3.47	3.94	19.6
CP11	5.85	52.83	302.5	4.04	0.69	2.70	3.47	19.4
CP12	9.66	35.43	281.7	3.77	0.39	2.27	2.51	11.9
CP99	1.30	36.17	50.5	0.68	0.52	2.97	2.67	9.7

Table A-44: CP and Precipitation characteristics at Station Grünhainichen in Winter

CP	Frequency [HH] (%)	Precipitation Probability (%)	Sum of Precipitation (mm)	Contribution [A] (%)	Wetness Index [A/HH]	Mean (mm)	Standard Deviation (mm)	Max. (mm)
CP01	16.09	72.23	2037.7	26.78	1.66	4.96	6.15	38.0
CP02	7.58	33.96	172.6	2.27	0.30	1.90	2.22	11.1
CP03	3.39	69.17	272.3	3.58	1.05	3.28	3.55	17.1
CP04	7.44	86.31	1604.1	21.08	2.83	7.07	7.06	46.3
CP05	7.41	43.51	327.8	4.31	0.58	2.88	3.15	17.9
CP06	5.63	44.72	195.0	2.56	0.46	2.19	2.47	14.2
CP07	6.36	70.67	898.4	11.81	1.86	5.65	6.56	29.4
CP08	5.20	52.72	342.3	4.50	0.86	3.53	2.85	13.5
CP09	14.76	35.06	438.6	5.76	0.39	2.40	2.85	16.2
CP10	9.25	52.60	666.2	8.76	0.95	3.87	4.56	26.4
CP11	5.80	50.73	313.7	4.12	0.71	3.02	3.86	21.3
CP12	9.81	34.58	286.7	3.77	0.38	2.39	2.81	12.5
CP99	1.27	48.89	53.6	0.70	0.55	2.44	3.19	14.3

Table A-45: CP and Precipitation characteristics at Station Burgstädt in Winter

CP	Frequency [HH] (%)	Precipitation Probability (%)	Sum of Precipitation (mm)	Contribution [A] (%)	Wetness Index [A/HH]	Mean (mm)	Standard Deviation (mm)	Max. (mm)
CP01	16.08	67.41	1598.9	27.64	1.72	4.07	5.24	35.4
CP02	7.50	28.68	144.3	2.49	0.33	1.85	2.54	13.3
CP03	3.48	54.76	175.1	3.03	0.87	2.54	2.70	10.5
CP04	7.59	81.09	1070.7	18.51	2.44	4.80	5.26	37.8
CP05	7.37	39.70	291.4	5.04	0.68	2.75	3.77	26.2
CP06	5.79	42.38	136.6	2.36	0.41	1.53	1.82	9.7
CP07	6.23	66.37	668.7	11.56	1.85	4.46	6.08	36.4
CP08	5.13	52.69	290.5	5.02	0.98	2.96	3.13	16.2
CP09	14.90	27.78	297.2	5.14	0.34	1.98	2.29	11.9
CP10	9.13	51.06	559.0	9.66	1.06	3.31	3.94	21.0
CP11	5.85	48.11	229.2	3.96	0.68	2.25	2.93	13.8
CP12	9.66	30.57	275.9	4.77	0.49	2.58	3.30	13.5
CP99	1.30	36.17	46.9	0.81	0.63	2.76	3.73	16.2

Table A-46: CP and Precipitation characteristics at Station Rittersgrün in Winter

CP	Frequency [HH] (%)	Precipitation Probability (%)	Sum of Precipitation (mm)	Contribution [A] (%)	Wetness Index [A/HH]	Mean (mm)	Standard Deviation (mm)	Max. (mm)
CP01	16.08	77.53	2563.1	27.15	1.69	5.67	6.22	43.5
CP02	7.50	39.34	241.0	2.55	0.34	2.25	2.51	12.0
CP03	3.48	72.22	361.1	3.82	1.10	3.97	4.08	16.5
CP04	7.59	91.27	1891	20.03	2.64	7.53	6.79	42.3
CP05	7.37	52.81	510.4	5.41	0.73	3.62	4.60	34.1
CP06	5.79	51.90	282.0	2.99	0.52	2.59	3.45	18.0
CP07	6.23	77.88	943.3	9.99	1.60	5.36	6.72	46.8
CP08	5.13	60.75	474.2	5.02	0.98	4.20	4.38	24.3
CP09	14.90	38.70	523.2	5.54	0.37	2.50	2.78	17.8
CP10	9.13	64.65	884.9	9.37	1.03	4.14	4.70	31.5
CP11	5.85	59.91	391.2	4.14	0.71	3.08	4.13	28.1
CP12	9.66	35.14	303.2	3.21	0.33	2.47	2.99	13.8
CP99	1.30	51.06	73.5	0.78	0.60	3.06	3.31	14.8

Table A-47: CP and Precipitation characteristics at Station Bräunsdorf, Krs. Chemnitz in Winter

CP	Frequency [HH] (%)	Precipitation Probability (%)	Sum of Precipitation (mm)	Contribution [A] (%)	Wetness Index [A/HH]	Mean (mm)	Standard Deviation (mm)	Max. (mm)
CP01	16.08	67.58	1475.6	25.11	1.56	3.75	4.59	30.6
CP02	7.50	29.41	161.3	2.74	0.37	2.02	2.35	11.7
CP03	3.48	65.87	197.3	3.36	0.97	2.38	2.82	15.3
CP04	7.59	85.82	1057.5	18.00	2.37	4.48	4.93	42.7
CP05	7.37	44.57	332.0	5.65	0.77	2.79	3.23	19.3
CP06	5.79	41.43	154.1	2.62	0.45	1.77	1.97	11.9
CP07	6.23	71.24	733.9	12.49	2.00	4.56	5.92	31.5
CP08	5.13	54.30	284.6	4.84	0.94	2.82	2.72	12.8
CP09	14.90	33.89	354.8	6.04	0.41	1.94	2.20	11.2
CP10	9.13	53.17	554.5	9.44	1.03	3.15	3.73	23.6
CP11	5.85	51.89	234.7	3.99	0.68	2.13	2.72	15.1
CP12	9.66	32.86	285.8	4.86	0.50	2.49	3.22	14.4
CP99	1.30	44.68	50.3	0.86	0.66	2.40	2.99	13.8

Table A-48: CP and Precipitation characteristics at Station Pleissa in Winter

CP	Frequency [HH] (%)	Precipitation Probability (%)	Sum of Precipitation (mm)	Contribution [A] (%)	Wetness Index [A/HH]	Mean (mm)	Standard Deviation (mm)	Max. (mm)
CP01	16.08	67.24	1525	27.08	1.68	3.89	4.92	43.1
CP02	7.50	30.88	151.6	2.69	0.36	1.80	2.59	14.8
CP03	3.48	61.11	159.0	2.82	0.81	2.06	2.92	14.1
CP04	7.59	82.91	1016.5	18.05	2.38	4.46	5.07	34.7
CP05	7.37	46.82	310.0	5.51	0.75	2.48	3.11	19.3
CP06	5.79	40.48	161.1	2.86	0.49	1.90	2.22	11.4
CP07	6.23	69.47	697.9	12.39	1.99	4.45	6.52	49.3
CP08	5.13	55.38	252.2	4.48	0.87	2.45	2.69	12.8
CP09	14.90	31.85	313.4	5.57	0.37	1.82	2.35	11.2
CP10	9.13	52.87	564.1	10.02	1.10	3.22	3.83	21.2
CP11	5.85	47.64	188.6	3.35	0.57	1.87	2.52	13.5
CP12	9.66	31.71	241.0	4.28	0.44	2.17	2.94	13.8
CP99	1.30	48.94	50.3	0.89	0.69	2.19	3.96	18.9

Table A-49: CP and Precipitation characteristics at Station Colditz in Winter

CP	Frequency [HH] (%)	Precipitation Probability (%)	Sum of Precipitation (mm)	Contribution [A] (%)	Wetness Index [A/HH]	Mean (mm)	Standard Deviation (mm)	Max. (mm)
CP01	16.08	63.98	1807.6	26.26	1.63	4.85	5.60	37.2
CP02	7.500	25.74	175.5	2.55	0.34	2.51	2.71	14.6
CP03	3.48	56.35	226.5	3.29	0.95	3.19	3.57	15.8
CP04	7.59	79.64	1307.9	19.00	2.50	5.97	5.50	47.5
CP05	7.37	37.83	378.5	5.50	0.75	3.75	4.10	25.3
CP06	5.79	37.14	187.7	2.73	0.47	2.41	2.41	12.7
CP07	6.23	61.50	800.9	11.64	1.87	5.76	6.79	32.2
CP08	5.13	47.31	372.5	5.41	1.05	4.23	3.69	21.3
CP09	14.90	27.22	373.5	5.43	0.36	2.54	2.64	14.0
CP10	9.13	48.04	606.0	8.80	0.96	3.81	3.95	27.4
CP11	5.85	45.28	271.8	3.95	0.68	2.83	3.29	20.6
CP12	9.66	26.29	308.9	4.49	0.46	3.36	3.62	15.3
CP99	1.30	44.68	65.2	0.95	0.73	3.10	3.71	17.2

Table A-50: CP and Precipitation characteristics at Station Einsiedel (TS) in Winter

CP	Frequency [HH] (%)	Precipitation Probability (%)	Sum of Precipitation (mm)	Contribution [A] (%)	Wetness Index [A/HH]	Mean (mm)	Standard Deviation (mm)	Max. (mm)
CP01	16.09	71.43	1849.9	26.02	1.62	4.51	5.58	40.0
CP02	7.51	30.22	165.1	2.32	0.31	2.04	2.14	11.8
CP03	3.53	64.29	300.7	4.23	1.20	3.71	4.28	17.5
CP04	7.57	86.67	1411.1	19.85	2.62	6.03	6.85	64.3
CP05	7.26	41.31	359.9	5.06	0.70	3.36	4.25	33.2
CP06	5.83	43.75	186.4	2.62	0.45	2.05	2.26	10.3
CP07	6.28	70.09	886.0	12.46	1.99	5.64	7.00	37.8
CP08	5.13	54.10	376.1	5.29	1.03	3.80	3.80	19.0
CP09	15.02	33.40	399.6	5.62	0.37	2.23	2.58	13.6
CP10	9.11	50.46	586.3	8.25	0.91	3.58	4.41	26.8
CP11	5.94	51.42	274.4	3.86	0.65	2.52	3.20	17.7
CP12	9.42	33.63	254.9	3.59	0.38	2.26	2.83	12.5
CP99	1.32	51.06	58.5	0.82	0.62	2.44	3.12	15.2

Table A-51: CP and Precipitation characteristics at Station Gablenz in Winter

CP	Frequency [HH] (%)	Precipitation Probability (%)	Sum of Precipitation (mm)	Contribution [A] (%)	Wetness Index [A/HH]	Mean (mm)	Standard Deviation (mm)	Max. (mm)
CP01	16.16	69.54	1794.0	26.74	1.66	4.44	5.69	44.1
CP02	7.54	30.26	127.8	1.91	0.25	1.56	1.90	11.0
CP03	3.48	70.40	250.4	3.73	1.07	2.85	2.77	11.4
CP04	7.51	87.41	1334.9	19.90	2.65	5.66	5.92	35.2
CP05	7.34	41.29	309.6	4.62	0.63	2.84	3.13	17.2
CP06	5.78	40.38	193.7	2.89	0.50	2.31	2.54	16.7
CP07	6.26	68.00	763.8	11.39	1.82	4.99	6.27	39.3
CP08	5.12	53.26	336.9	5.02	0.98	3.44	3.67	29.2
CP09	15.02	35.74	416.7	6.21	0.41	2.16	2.49	13.9
CP10	9.04	52.92	568.0	8.47	0.94	3.30	3.93	20.8
CP11	5.78	50.48	266.0	3.97	0.69	2.53	3.78	26.7
CP12	9.68	33.62	295.7	4.41	0.46	2.53	3.14	16.5
CP99	1.31	44.68	50.3	0.75	0.57	2.40	2.70	10.0

Table A-52: CP and Precipitation characteristics at Station Chemnitz (WST) in Winter

CP	Frequency [HH] (%)	Precipitation Probability (%)	Sum of Precipitation (mm)	Contribution [A] (%)	Wetness Index [A/HH]	Mean (mm)	Standard Deviation (mm)	Max. (mm)
CP01	16.08	69.47	1622.5	29.97	1.86	4.01	5.21	35.5
CP02	7.50	33.09	124.3	2.30	0.31	1.38	2.10	10.8
CP03	3.48	65.08	149.1	2.75	0.79	1.82	2.03	9.8
CP04	7.59	87.64	1017.9	18.8	2.48	4.22	4.76	28.6
CP05	7.37	43.82	281.4	5.20	0.71	2.41	3.52	27.0
CP06	5.79	43.81	128.8	2.38	0.41	1.40	1.72	9.7
CP07	6.23	66.81	576.3	10.65	1.71	3.82	5.15	40.2
CP08	5.13	53.76	245.8	4.54	0.88	2.46	2.56	12.7
CP09	14.90	34.26	301.9	5.58	0.37	1.63	1.97	9.7
CP10	9.13	52.57	487.7	9.01	0.99	2.80	3.50	19.8
CP11	5.85	48.58	203.2	3.75	0.64	1.97	2.69	13.7
CP12	9.66	31.43	237.0	4.38	0.45	2.15	2.57	12.7
CP99	1.30	42.55	37.2	0.69	0.53	1.86	2.90	13.2

Table A-53: CP and Precipitation characteristics at Station Grosshartmannsdorf in Winter

CP	Frequency [HH] (%)	Precipitation Probability (%)	Sum of Precipitation (mm)	Contribution [A] (%)	Wetness Index [A/HH]	Mean (mm)	Standard Deviation (mm)	Max. (mm)
CP01	16.08	73.07	1909.8	28.10	1.75	4.48	5.77	44.3
CP02	7.50	35.29	154.5	2.27	0.30	1.61	1.88	9.8
CP03	3.48	73.02	234.8	3.45	0.99	2.55	2.93	16.1
CP04	7.59	89.09	1372.8	20.20	2.66	5.60	6.27	42.5
CP05	7.37	43.82	304.2	4.48	0.61	2.60	3.04	19.2
CP06	5.79	48.10	197.9	2.91	0.5	1.96	2.37	12.8
CP07	6.23	71.68	779.0	11.46	1.84	4.81	6.12	33.8
CP08	5.13	56.45	279.9	4.12	0.80	2.67	2.50	11.1
CP09	14.90	36.30	415.1	6.11	0.41	2.12	2.57	14.8
CP10	9.13	54.08	548.2	8.07	0.88	3.06	3.59	21.3
CP11	5.85	56.13	302.7	4.45	0.76	2.54	3.43	20.4
CP12	9.66	36.86	246.2	3.62	0.38	1.91	2.46	15.2
CP99	1.30	51.06	50.9	0.75	0.58	2.12	2.36	9.4

Table A-54: CP and Precipitation characteristics at Station Oberbobritzsch in Winter

CP	Frequency [HH] (%)	Precipitation Probability (%)	Sum of Precipitation (mm)	Contribution [A] (%)	Wetness Index [A/HH]	Mean (mm)	Standard Deviation (mm)	Max. (mm)
CP01	15.98	76.25	1860.4	27.35	1.71	4.36	5.46	36.1
CP02	7.65	36.94	176.4	2.59	0.34	1.78	2.46	13.4
CP03	3.37	72.03	238.4	3.50	1.04	2.80	3.28	15.9
CP04	7.67	89.22	1276.5	18.76	2.44	5.32	5.71	52.4
CP05	7.28	49.80	333.7	4.91	0.67	2.63	3.98	34.6
CP06	5.76	50.50	202.9	2.98	0.52	1.99	2.38	12.6
CP07	6.22	75.69	806.5	11.86	1.91	4.89	5.75	22.8
CP08	5.02	58.52	330.5	4.86	0.97	3.21	3.52	19.4
CP09	15.24	39.33	404.4	5.94	0.39	1.93	2.54	16.4
CP10	8.96	57.96	606.9	8.92	1.00	3.33	3.88	22.0
CP11	5.79	58.13	249.9	3.67	0.63	2.12	3.23	20.2
CP12	9.73	38.71	258.6	3.80	0.39	1.96	2.57	13.5
CP99	1.34	61.70	57.9	0.85	0.63	2.00	3.11	15.8

Table A-55: CP and Precipitation characteristics at Station St. Michaelis in Winter

CP	Frequency [HH] (%)	Precipitation Probability (%)	Sum of Precipitation (mm)	Contribution [A] (%)	Wetness Index [A/HH]	Mean (mm)	Standard Deviation (mm)	Max. (mm)
CP01	16.08	75.47	2338.0	26.96	1.68	5.31	6.43	49.3
CP02	7.50	32.72	220.7	2.55	0.34	2.48	3.07	14.1
CP03	3.48	69.05	326.6	3.77	1.08	3.75	4.10	21.1
CP04	7.59	86.91	1728.7	19.93	2.63	7.23	7.11	59.9
CP05	7.37	47.57	396.1	4.57	0.62	3.12	3.61	24.3
CP06	5.79	50.48	263.4	3.04	0.52	2.48	2.61	13.5
CP07	6.23	74.34	1018.2	11.74	1.88	6.06	7.67	51.6
CP08	5.13	54.84	426.5	4.92	0.96	4.18	3.98	24.5
CP09	14.90	36.30	494.6	5.70	0.38	2.52	2.98	21.6
CP10	9.13	57.10	770.7	8.89	0.97	4.08	4.41	24.5
CP11	5.85	51.89	317.7	3.66	0.63	2.89	3.18	18.3
CP12	9.66	34.00	300.0	3.46	0.36	2.52	2.87	12.8
CP99	1.30	48.94	70.5	0.81	0.63	3.07	4.31	19.0

Table A-56: CP and Precipitation characteristics at Station Bräunsdorf, Krs. Freiberg in Winter

CP	Frequency [HH] (%)	Precipitation Probability (%)	Sum of Precipitation (mm)	Contribution [A] (%)	Wetness Index [A/HH]	Mean (mm)	Standard Deviation (mm)	Max. (mm)
CP01	16.08	72.38	1842.3	27.81	1.73	4.37	5.34	37.1
CP02	7.50	31.62	169.3	2.56	0.34	1.97	2.71	13.5
CP03	3.48	66.67	242.1	3.65	1.05	2.88	3.62	15.7
CP04	7.59	85.82	1194.4	18.03	2.38	5.06	5.59	48.4
CP05	7.37	47.57	343.8	5.19	0.70	2.71	3.37	26.8
CP06	5.79	46.19	196.0	2.96	0.51	2.02	2.45	12.4
CP07	6.23	70.35	789.5	11.92	1.91	4.97	6.39	39.0
CP08	5.13	54.30	351.0	5.30	1.03	3.48	3.99	23.6
CP09	14.90	35.00	339.5	5.13	0.34	1.80	2.11	12.4
CP10	9.13	51.66	635.4	9.59	1.05	3.72	4.18	24.2
CP11	5.85	49.53	225.0	3.40	0.58	2.14	2.88	14.2
CP12	9.66	35.14	252.7	3.81	0.40	2.05	2.60	11.0
CP99	1.30	46.81	43.1	0.65	0.50	1.96	3.11	14.9

Table A-57: CP and Precipitation characteristics at Station Drebach in Winter

CP	Frequency [HH] (%)	Precipitation Probability (%)	Sum of Precipitation (mm)	Contribution [A] (%)	Wetness Index [A/HH]	Mean (mm)	Standard Deviation (mm)	Max. (mm)
CP01	15.49	74.40	2520.2	29.36	1.90	6.24	8.00	71.0
CP02	7.53	34.47	170.1	1.98	0.26	1.87	2.53	16.6
CP03	3.59	69.05	307.8	3.59	1.00	3.54	4.02	21.5
CP04	7.79	88.64	1856.6	21.63	2.78	7.67	9.13	65.4
CP05	7.33	50.58	419.9	4.89	0.67	3.23	4.81	39.8
CP06	5.88	45.63	234.9	2.74	0.47	2.50	3.33	19.2
CP07	6.33	72.97	880.4	10.26	1.62	5.43	7.13	44.0
CP08	5.28	57.30	406.3	4.73	0.90	3.83	3.94	28.3
CP09	14.55	37.45	433.5	5.05	0.35	2.27	2.61	14.6
CP10	9.07	55.66	661.1	7.70	0.85	3.74	4.61	26.0
CP11	5.96	59.33	310.1	3.61	0.61	2.50	3.51	21.0
CP12	9.84	36.52	323.9	3.77	0.38	2.57	3.41	15.8
CP99	1.34	51.06	58.8	0.69	0.51	2.45	3.17	13.6

Table A-58: CP and Precipitation characteristics at Station Augustusburg in Winter

CP	Frequency [HH] (%)	Precipitation Probability (%)	Sum of Precipitation (mm)	Contribution [A] (%)	Wetness Index [A/HH]	Mean (mm)	Standard Deviation (mm)	Max. (mm)
CP01	15.8	67.96	1865.9	26.45	1.67	4.83	5.85	37.2
CP02	7.57	31.62	179.6	2.55	0.34	2.09	2.46	13.0
CP03	3.42	63.41	234.9	3.33	0.97	3.01	2.95	12.3
CP04	7.59	83.88	1367.0	19.38	2.55	5.97	5.68	39.8
CP05	7.40	42.11	346.4	4.91	0.66	3.09	3.36	23.0
CP06	5.84	43.81	218.6	3.10	0.53	2.38	2.52	12.4
CP07	6.29	69.91	868.0	12.30	1.96	5.49	6.29	28.7
CP08	5.17	51.08	350.5	4.97	0.96	3.69	3.36	21.0
CP09	14.85	32.77	390.4	5.53	0.37	2.23	2.57	15.6
CP10	9.21	51.66	652.5	9.25	1.00	3.82	4.17	23.0
CP11	5.81	50.72	243.1	3.45	0.59	2.29	2.81	15.3
CP12	9.74	31.43	285.9	4.05	0.42	2.60	2.70	11.6
CP99	1.31	44.68	52.3	0.74	0.57	2.49	3.26	14.4

Table A-59: CP and Precipitation characteristics at Station Flöha in Winter

CP	Frequency [HH] (%)	Precipitation Probability (%)	Sum of Precipitation (mm)	Contribution [A] (%)	Wetness Index [A/HH]	Mean (mm)	Standard Deviation (mm)	Max. (mm)
CP01	15.99	64.32	1712.5	27.47	1.72	4.80	5.69	38.5
CP02	7.60	25.00	151.2	2.43	0.32	2.29	2.57	11.4
CP03	3.37	61.54	193.0	3.10	0.92	2.68	3.05	15.3
CP04	7.55	82.82	1217.4	19.53	2.59	5.61	5.37	35.2
CP05	7.20	40.00	306.1	4.91	0.68	3.06	3.89	31.7
CP06	5.90	39.02	165.6	2.66	0.45	2.07	2.23	10.2
CP07	6.34	59.55	734.7	11.78	1.86	5.61	5.99	31.0
CP08	5.21	50.83	354.6	5.69	1.09	3.85	3.62	22.7
CP09	14.86	26.16	316.4	5.07	0.34	2.34	2.56	13.1
CP10	9.13	47.95	573.0	9.19	1.01	3.77	3.80	24.3
CP11	5.90	41.95	232.9	3.74	0.63	2.71	3.24	18.2
CP12	9.68	26.19	242.1	3.88	0.40	2.75	2.56	10.9
CP99	1.27	40.91	35.5	0.57	0.45	1.97	1.89	5.6

Table A-60: CP and Precipitation characteristics at Station Reinersdorf in Winter

CP	Frequency [HH] (%)	Precipitation Probability (%)	Sum of Precipitation (mm)	Contribution [A] (%)	Wetness Index [A/HH]	Mean (mm)	Standard Deviation (mm)	Max. (mm)
CP01	16.18	61.86	1468.7	28.13	1.74	4.08	5.14	34.5
CP02	7.56	25.37	132.6	2.54	0.34	1.92	2.39	13.8
CP03	3.48	51.20	179.4	3.44	0.99	2.8	3.13	17.0
CP04	7.65	72.36	803.4	15.38	2.01	4.04	4.21	29.1
CP05	7.23	37.69	249.4	4.78	0.66	2.54	3.59	29.2
CP06	5.81	35.89	126.6	2.42	0.42	1.69	1.83	7.7
CP07	6.26	64.89	695.3	13.31	2.13	4.76	6.41	46.7
CP08	5.17	46.77	229.9	4.40	0.85	2.64	2.41	10.2
CP09	14.79	28.20	319.7	6.12	0.41	2.13	2.44	14.5
CP10	9.04	46.46	561.1	10.74	1.19	3.72	3.59	18.3
CP11	5.89	41.04	172.9	3.31	0.56	1.99	1.97	10.3
CP12	9.65	28.53	238.0	4.56	0.47	2.40	2.42	12.0
CP99	1.31	46.81	45.0	0.86	0.66	2.05	3.77	18.3

Table A-61: CP and Precipitation characteristics at Station Kadan, Tuimice in Winter

CP	Frequency [HH] (%)	Precipitation Probability (%)	Sum of Precipitation (mm)	Contribution [A] (%)	Wetness Index [A/HH]	Mean (mm)	Standard Deviation (mm)	Max. (mm)
CP01	16.08	55.57	715.2	24.68	1.53	2.21	2.86	18.2
CP02	7.50	24.26	105.1	3.63	0.48	1.59	2.67	15.4
CP03	3.48	40.48	84.2	2.91	0.84	1.65	3.18	15.1
CP04	7.59	68.73	352.0	12.15	1.60	1.86	2.34	15.6
CP05	7.37	46.07	190.7	6.58	0.89	1.55	2.61	16.1
CP06	5.79	28.57	48.2	1.66	0.29	0.80	1.07	5.4
CP07	6.23	63.72	430.1	14.84	2.38	2.99	4.28	21.7
CP08	5.13	43.55	110.5	3.81	0.74	1.36	2.19	14.1
CP09	14.90	20.00	86.7	2.99	0.20	0.80	1.16	7.1
CP10	9.13	51.96	401.3	13.85	1.52	2.33	2.66	14.2
CP11	5.85	29.72	91.3	3.15	0.54	1.45	2.43	12.2
CP12	9.66	39.43	257.8	8.90	0.92	1.87	2.39	11.9
CP99	1.30	40.43	24.4	0.84	0.65	1.28	2.50	10.9

Table A-62: CP and Precipitation characteristics at Station Kopisty in Winter

CP	Frequency [HH] (%)	Precipitation Probability (%)	Sum of Precipitation (mm)	Contribution [A] (%)	Wetness Index [A/HH]	Mean (mm)	Standard Deviation (mm)	Max. (mm)
CP01	16.08	60.72	818.7	26.12	1.62	2.31	3.03	19.2
CP02	7.50	24.63	87.2	2.78	0.37	1.30	2.11	11.4
CP03	3.48	46.03	56.4	1.80	0.52	0.97	1.84	11.7
CP04	7.59	71.64	435.1	13.88	1.83	2.21	2.57	15.8
CP05	7.37	37.83	186.8	5.96	0.81	1.85	2.38	12.0
CP06	5.79	32.38	57.0	1.82	0.31	0.84	1.08	4.2
CP07	6.23	64.16	450.0	14.35	2.30	3.10	4.53	29.8
CP08	5.13	39.78	126.1	4.02	0.78	1.70	2.43	13.4
CP09	14.90	23.33	103.4	3.30	0.22	0.82	1.14	6.0
CP10	9.13	53.78	451.2	14.39	1.58	2.53	3.14	17.4
CP11	5.85	33.02	88.8	2.83	0.48	1.27	1.87	9.5
CP12	9.66	35.71	253.6	8.09	0.84	2.03	2.82	20.0
CP99	1.30	31.91	20.6	0.66	0.51	1.37	2.01	8.1

APPENDIX B

SAMPLE CALCULATION OF VARIOGRAMM, ORDINARY KRIGING AND EXTERNAL DRIFT KRIGING

1. Sample calculation of Variogram.

Variogram calculation is shown by an example here. The following figure presents a set of measurements of a rainfall on a regular grid of 1 m cell size. Fields marked with "*x*" are points without measurements:

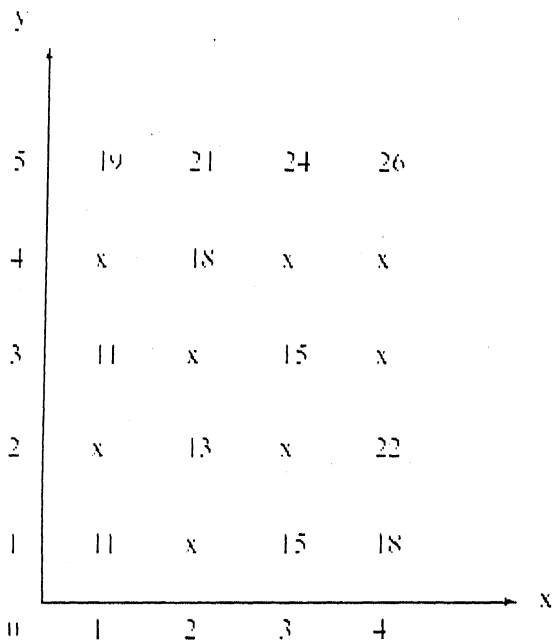

The general formula for the variogram - for a specific distance or vector h is:

$$\gamma(\hat{h},\hat{\theta}) = \frac{1}{2N(h)} \sum_{i=1}^{N(h)} [z(u_i + h,\hat{\theta}) - z(u_i,\hat{\theta})]^2$$

where $N(h)$ is the number of pairs separated by the vector (or distance) h. Applying the formula gives:

1. For the horizontal direction (x) and distance 1m, 4 pairs of the matrix:

$$\gamma(1hor) = 1/2 \times 4\ [(19\text{-}21)^2 + (21\text{-}24)^2 + (24\text{-}26)^2 + (15\text{-}18)^2]$$

γ (1*hor*) =1/2×4 (2^2+3^2+2^2+3^2)

γ (1*hor*) =26/8 = 3.25

2. For the vertical direction (*y*) and distance 1m, 2 pairs of the matrix:

γ (1*ver*) = 1/ 2×2 [(21-18)^2+ (22-18)^2]

γ (1*ver*) =1/2 ×2 (3^2+4^2)

γ (1*ver*) = 25/4 = 6.25

3. For the horizontal direction (*x*) and distance 2m, 5 pairs of the matrix:

γ (2*hor*) = 1/2× 5 [(19-24)^2+ (21-26)^2+ (11-15)^2+ (13-22)^2+ (11-15)^2]

γ (2*hor*) =1/2 ×5 (5^2+5^2+4^2+9^2+4^2)

γ (2*hor*) =163/10 = 16.3

4. For vertical direction (*y*), distance 2m, 5 pairs of the matrix:

γ (2*ver*) =1/2 ×5 [(19-11)^2+ (11-11)^2+ (18-13)^2+ (24-15)^2+ (15-15)^2]

γ (2*ver*) =1/2 ×5 (8^2+0^2+5^2+9^2+0^2)

γ (2*ver*) = 170/10 = 17.0

2. Sample calculation for Ordinary kriging

Considering the same Figure in previous example we calculate the equations of an ordinary kriging system for the point (2,3) using only the directly neighboring points. For the variogram function let us take $\gamma(h) = 4h$.

The kriging equation for ordinary kriging are:

$$\begin{cases} \sum_{j=1}^{n} \lambda_j \gamma(u_i - u_j) + \mu = \gamma(u_i - u) \\ \sum_{j=1}^{n} \lambda_j = 1 \end{cases} \qquad i = 1,\ldots,n$$

with kriging weights λ_i for the measurement at u_i, i=1,....,n. In this case the neighbouring points of (2,3) = u are: (1,3) = u_1, (2,2) = u_2, (2,4) = u_3, (3,3) = u_4. The distances in this configuration are: 1 m (x and y direction) with $\gamma(1)$ = 4, 2 m (x and y direction) with $\gamma(2)$ = 8, 1.41 m (diagonal, ex. (2,2) to (3,3)) with $\gamma(1.41)$ = 5.64.

The kriging system without using the symmetry can then be written as follows:

$$i = 1: \lambda_1.0+\lambda_2.\gamma(1.41)+\lambda_3.\gamma(1.41)+\lambda_4.\gamma(2)+\mu = \gamma(1)$$

$$i = 2: \lambda_1.\gamma(1.41)+\lambda_2.0+\lambda_3.\gamma(2)+\lambda_4.\gamma(1.41)+\mu = \gamma(1)$$

$$i = 3: \lambda_1.\gamma(1.41)+\lambda_2.\gamma(2)+\lambda_3.0+\lambda_4.\gamma(1.41)+\mu = \gamma(1)$$

$$i = 4: \lambda_1.\gamma(2)+\lambda_2.\gamma(1.41)+\lambda_3.\gamma(1.41)+\lambda_4.0+\mu = \gamma(1)$$

$$\lambda_1+\lambda_2+\lambda_3+\lambda_4 = 1$$

and by evaluating the variogram $\gamma(h)$:

$$i = 1: \lambda_1.0+\lambda_2.5.64+\lambda_3.5.64+\lambda_4.8+\mu = 1 \qquad (1)$$

$$i = 2: \lambda_1.5.64+\lambda_2.0+\lambda_3.8+\lambda_4.5.64+\mu = 1 \qquad (2)$$

$$i = 3: \lambda_1.5.64+\lambda_2.8+\lambda_3.0+\lambda_4.5.64+\mu = 1 \qquad (3)$$

$$i = 4: \lambda_1.8+\lambda_2.5.64+\lambda_3.5.64+\lambda_4.0+\mu = 1 \qquad (4)$$

$$\lambda_1+\lambda_2+\lambda_3+\lambda_4 = 1 \qquad (5)$$

Calculating the differences between equation (2)-(3) and (1)-(4) leads to:

(2)-(3) : $\lambda_2 = \lambda_3$

(1)-(4): $\lambda_1 = \lambda_4$

evaluating these results in (1) and (2) and calculating the difference:

(1)-(2): $\lambda_2 = \lambda_1$

with (5): $\lambda_4 = \lambda_3 = \lambda_2 = \lambda_1 = 0.25$

The kriging weights are 0.25 for all points. The estimation is therefore

$Z^*(u) = 14.25.$

3. Sample calculation for External Drift Kriging

The table given below displays measurements of rainfall $Z(u)$ for points u ordered in a straight line. We have to Write down the equations of an external drift Kriging system for an estimation of Z^* of rainfall at the point $u = 2$ assuming that chloride is linearly related to square root of elevation. For the variogram take the function $\gamma(h) = 3/2h$ for a distance h.

Table: Measurements of rainfall $Z(u)$ and Square root of elevation for points u ordered in a straight line

Location (u)	Rainfall (mm)	Square Root of Elevation [m]
0	19.4	20
1	22.2	22
2	_	21
3	23.6	24
4	24.8	25

The equations of external drift kriging are as follows:

$$\sum_{j=1}^{I} \lambda_j \gamma(u_i - u_j) + \mu_1 + \mu_2 Y(u_i) = \gamma(u_i - u) \quad i = 1, \ldots, I$$

$$\sum_{j=1}^{I} \lambda_j = 1$$

$$\sum_{j=1}^{I} \lambda_j Y(u_j) = Y(u)$$

Applying these for the above example problem leads to 6 equations, the locations are: u_1=0, u_2=1, u_3=3, u_4=4 and u=2: The corresponding equations are:

$$i = 1: \lambda_1.\gamma(0) + \lambda_2.\gamma(1) + \lambda_3.\gamma(3) + \lambda_4.\gamma(4) + \mu_1 + \mu_2.Y(0) = \gamma(2)$$

$$i = 2: \lambda_1.\gamma(1) + \lambda_2.\gamma(0) + \lambda_3.\gamma(2) + \lambda_4.\gamma(3) + \mu_1 + \mu_2.Y(1) = \gamma(1)$$

$$i = 3: \lambda_1.\gamma(3) + \lambda_2.\gamma(2) + \lambda_3.\gamma(0) + \lambda_4.\gamma(1) + \mu_1 + \mu_2.Y(3) = \gamma(1)$$

$$i = 4: \lambda_1.\gamma(4) + \lambda_2.\gamma(3) + \lambda_3.\gamma(1) + \lambda_4.\gamma(0) + \mu_1 + \mu_2.Y(4) = \gamma(2)$$

$$\lambda_1 + \lambda_2 + \lambda_3 + \lambda_4 = 1$$

$$\lambda_1.Y(0) + \lambda_2.Y(1) + \lambda_3.Y(3) + \lambda_4.Y(4) = Y(2)$$

Inserting the variogram $\gamma(h) = 3/2h$, and the values of the function Y (square root of elevation) gives:

$$i = 1: \ 1.5.\lambda_2 + 4.5.\lambda_3 + 6.\lambda_4 + \mu_1 + 20.\mu_2 = 3$$

$$i = 2: \ 1.5.\lambda_1 + 3.\lambda_3 + 4.5.\lambda_4 + \mu_1 + 22.\mu_2 = 1.5$$

$$i = 3: \ 4.5.\lambda_1 + 3.\lambda_2 + 1.5.\lambda_4 + \mu_1 + 24.\mu_2 = 1.5$$

$$i = 4: \ 6.\lambda_1 + 4.5.\lambda_2 + 1.5.\lambda_3 + \mu_1 + 25.\mu_2 = 3$$

$$\lambda_1 + \lambda_2 + \lambda_3 + \lambda_4 = 1$$

$$20.\lambda_1 + 22.\lambda_2 + 24.\lambda_3 + 25.\lambda_4 = 21$$

By solving these equations, we can get value of Z*.

APPENDIX C:

Decomposition of $C_i(t^*)C_i^T(t^*)$

The matrix C_i can be obtained from Equation (16) by using the Jecobi method. First the Eigen vectors and Eigen values of the right hand sides have to be fond out. Let G be the right side matrix and

$$\Lambda = \begin{pmatrix} \lambda_1 & 0 & \cdots & 0 \\ \vdots & & \ddots & \\ 0 & 0 & \cdots & \lambda_n \end{pmatrix} \tag{C.1}$$

where $\lambda_1, \ldots, \lambda_n$ are the Eigen values of G. The matrix G can be written in the form

$$G = E^T \begin{pmatrix} \lambda_1 & 0 & \cdots & 0 \\ \vdots & & \ddots & \\ 0 & 0 & \cdots & \lambda_n \end{pmatrix} E \tag{C.2}$$

$$G = E^T \begin{pmatrix} \sqrt{\lambda_1} & 0 & \cdots & 0 \\ \vdots & & \ddots & \\ 0 & 0 & \cdots & \sqrt{\lambda_n} \end{pmatrix} \begin{pmatrix} \sqrt{\lambda_1} & 0 & \cdots & 0 \\ \vdots & & \ddots & \\ 0 & 0 & \cdots & \sqrt{\lambda_n} \end{pmatrix} E \tag{C.3}$$

As the previous step ensures the positive definitions of the covariances matrices, all Eigen values have to be positive, thus the above decomposition can be made for Ci.